FACULTY
OF MECHANICAL
ENGINEERING

Ph.D. Thesis

DYNAMIC MODEL OF TWO SYNCHRONOUS GENERATORS CONNECTED VIA LONG TRANSMISSION LINE

Ing. Le Thi Minh Trang

STUDY PROGRAMME: MECHANICAL ENGINEERING
STUDY FIELD: POWER ENGINEERING

Supervisor:

Prof. Ing. Ivan Uhlíř, DrSc.

PRAHA 6
2018

ABSTRACT

Due to the large desire to utilize transmission networks for more flexible power interchange transactions, the high requirement for power system dynamic analysis has grown significantly in recent years. While dynamics and stability have been studied for years in a long term planning and design environment, there is a recognized need to perform this analysis in a weekly or even daily operation environment.

The dynamic performance of power systems is important to both the system organizations, from an economic viewpoint, and society in general, from a reliability viewpoint. The analysis of power system dynamics and stability is increasing daily in terms of number and frequency of studies, as well as in complexity and size. Dynamic phenomena have been discussed according to basic function, time-scale properties, and problem size.

In a realistic system, electric power system consist of the interconnection of large numbers of synchronous generators operating in parallel. These generators are connected together by transmission lines. In the operation process, the rotor angles of generators swing relatively to another one during transients. Under disturbances the synchronism of machines in system is achieved when maintaining equilibrium between electromagnetic and mechanical torques. In other words, a system is unstable if the angle difference between two interconnected generators is not sufficiently damped in the evaluation time. The instability typically occurs as increasingly swings angle generators leading to some loss of synchronism with other generators.

One of the constraints for long distance AC transmission is the large phase angular difference which is required to transmit a given amount of power. Therefore, in order to gain dynamic behavior characteristics of system when subject to disturbances, this work will focus on modeling two synchronous generators linked by long AC transmission line.

Within the content of this work, for the analysis of system modes, the system is computed based on a detailed model of synchronous machines, transformers, loads and the long transmission line including voltage dynamics and frequency response.

The system power equilibrium equations are derived and linearized for the small disturbance stability analysis and some transient disturbances. These results can serve to define stability margin of a power system. This stability limit would play important role in improving designs of the different system connection conditions.

Keywords: synchronous generators, stability, transient model, long transmission line, synchronization.

ACKNOWLEDGEMENT

The research work has been carried out during the years 2015 and 2018 in the Department of Instrumentation and Control Engineering at Czech Technical University (CTU) in Prague, where I have worked as a research student. The task of writing the dissertation has been performed during the year 2017 at UWE in Bristol, where I work as a research visitor and the year 2018 at CTU in Prague. These years of my working in particular proved to be very valuable, since it gave me a wide view and a new understanding concerning the large application area of power system.

I wish to express my deepest gratitude to Professor Ivan Uhlíř, Head, Division of Electrical Engineering, Department of Instrumentation and Control Engineering, Faculty of Mechanical Engineering, Czech Technical University in Prague and supervisor of my thesis, for his immense support. He is the full of knowledge. His activity, enthusiasm and gift of guiding have been of enormous importance to me. He has encouraged me unceasingly and tirelessly throughout the work.

I would like to thank Hassan Nouri, Power System, Electronics and Control Research Laboratory, UWE in Bristol, UK and for giving me the opportunity to work with for a research project.

Special thanks are due to all my colleagues and especially to my friends in Czech Republic and Viet Nam. It has been and will always be a pleasure to work with them.

The financial support of Electrical Power University in Ha Noi and Viet Nam Electricity are also very gratefully acknowledged.

I am deeply indebted to my family for their guidance and for providing me a good basis for my life. There was a time it has been hard for them, but they succeeded. They deserve my special thanks.

TABLE OF CONTENTS

LIST OF FIGURES

LIST OF TABLES

LIST OF SYMBOLS AND ACRONYMS

Acronyms

AVR	Automatic voltage regulator
PSS	Power system stabilizer
PID	Proportional–Integral–Derivative controller
SG	Synchronous generator
DG	Distributed generator

Symbols

t	Time [s]
s	Laplace factor [-]
v_a, v_b, v_c	Phases a, b and c stator voltages of synchronous machine [V]
i_a, i_b, i_c	Phases a, b and c stator currents of synchronous machine [A]
Ψ_a, Ψ_b, Ψ_c	Phases a, b and c flux linkages [V.s]
r_a, r_b, r_c	Phases a, b and c resistance [Ω]
v_s	Stator winding voltage [V]
v_r	Rotor winding voltage [V]
v_f	d-axis field winding voltage [V]
v_{kd}	d-axis damper winding voltage [V]
v_{kq}	q-axis damper winding voltage [V]
v_g	q-axis field winding voltage [V]
Ψ_s	Stator winding flux linkage [V.s]
Ψ_r	Rotor winding flux linkage [V.s]
Ψ_f	d-axis field winding flux linkage [V.s]
Ψ_g	q-axis field winding flux linkage [V.s]
Ψ_{kd}	d-axis damper winding flux linkage [V.s]
Ψ_{kq}	q-axis damper winding flux linkage [V.s]
i_s	Stator winding current [A]
i_r	Rotor winding current [A]
i_f	d-axis field winding current [A]
i_g	q-axis field winding current [A]
i_{kd}	d-axis damper winding current [A]
i_{kq}	q-axis damper winding current [A]
r_s	Stator winding resistance [Ω]
r_r	Rotor winding resistance [Ω]

r_f	d-axis field winding resistance [Ω]
r_g	q-axis field winding resistance [Ω]
r_{kd}	d-axis damper winding resistance [Ω]
r_{kq}	q-axis damper winding resistance [Ω]
θ_r	Electrical angle [rad]
i_q	q-axis stator current [A]
i_d	d- axis stator current [A]
i_0	0- axis stator current [A]
v_q	q-axis stator voltage [V]
v_d	d- axis stator voltage [V]
v_0	0- axis stator voltage [V]
$P(\theta_r)$	Electrical power of synchronous machine [W]
Ψ_q	q-axis stator windings flux linkage [V.s]
Ψ_d	d- axis stator windings flux linkage [V.s]
Ψ_0	0- axis stator windings flux linkage [V.s]
ω_b	Base angular speed [rad/s]
ω_r	Rotor angular speed [rad/s]
ω_{rm}	Mechanical rotor angular speed [rad/s]
ω_e	Electrical angular speed [rad/s]
x_{ls}	Stator winding per phase reactance [Ω]
r_s	Stator winding per phase resistance [Ω]
Ψ'_{kd}	d-axis damper winding flux linkage referred to stator [V.s]
Ψ'_{kq}	q-axis damper winding flux linkage referred to stator [V.s]
Ψ_{mq}	q-axis mutual flux linkage [V.s]
Ψ_{md}	d-axis mutual flux linkage [V.s]
Ψ_f	d-axis exciting winding flux linkage referred to stator [V.s]
r'_{kd}	d-axis damper winding resistance referred to stator [Ω]
x'_{lkd}	d-axis damper winding reactance referred to stator [Ω]
r'_{kq}	q-axis damper winding resistance referred to stator [Ω]
x'_{lkq}	q-axis damper winding reactance referred to stator [Ω]
r'_f	d-axis exciting winding resistance referred to stator [Ω]
v'_f	d-axis exciting winding voltage referred to stator [Ω]
x_{md}	d-axis mutual reactance referred to stator [Ω]
x'_{lf}	d-axis exciting winding reactance referred to stator [Ω]

E_f	Field voltage referred to stator [V]
i'_{kd}	d-axis damper winding current referred to stator [A]
i'_{kq}	q-axis damper winding current referred to stator [A]
i'_f	d-axis exciting winding current referred to stator [A]
v_q^s	Stationary q-axis stator voltage [V]
v_d^s	Stationary d-axis stator voltage [V]
i_q^s	Stationary q-axis stator current [A]
i_d^s	Stationary d-axis stator current [A]
P_{in}	Total input power [W]
P_{em}	Electromechanical power [W]
P_{gen}	Power of synchronous machine [W]
T_{em}	Electromechanical torque [N.m]
p	Poles number [-]
T_{mech}	Mechanical torque [N.m]
T_{damp}	Damping torque [N.m]
J	Moment of inertia [$kg.m^2$]
V	Line voltage [V]
V_b	Base voltage [V]
I_b	Base current [A]
Z_b	Base impedance [Ω]
S_b	Base apparent power [VA]
T_b	Base torque [N.m]
ω_{bm}	Base mechanical angular speed [rad/s]
H	Inertia constant [sW/VA]
J	Moment of inertia [$kg.m^2$]
Ψ_b	Base flux linkage [V.s]
H_b	Base inertia constant [sW/VA]
D	Damping coefficient [-]
x_d	d-axis reactance [Ω]
x_q	q-axis reactance [Ω]
x'_d	d-axis transient reactance [Ω]
x'_q	q-axis transient reactance [Ω]
x''_d	d-axis subtransient reactance [Ω]
x''_q	q-axis subtransient reactance [Ω]
E'_d	d-axis transient electromotive force [V]

E'_q	q-axis transient electromotive force [V]
T'_{do}	d-axis open circuit transient time constant [s]
T'_{qo}	q-axis open circuit transient time constant [s]
T''_{do}	d-axis short-circuit subtransient time constant [s]
T''_{qo}	q-axis short-circuit subtransient time constant [s]
v_{do}	d-axis initial voltage [V]
v_{qo}	q-axis initial voltage [V]
i_{do}	d-axis initial current [A]
i_{qo}	q-axis initial current [A]
E_{qo}	q-axis initial electric potential [V]
E'_{qo}	q-axis initial transient electric potential [V]
E'_{do}	d-axis initial transient electric potential [V]
E_{fo}	d-axis initial excitation current [A]
V_t	Terminal voltage [V]
I_t	Terminal current [A]
I_{go}	Initial generator current [A]
V_{g0}	Initial generator voltage [V]
T_{em0}	Initial electromechanical torque [N.m]
P_g	Active power of synchronous machine [W]
Q_g	Reactive power of synchronous machine [VAr]
S	Apparent power of synchronous machine [VA]
P_L	Active power of load [W]
Q_L	Reactive power of load [VAr]
$\cos \varphi$	Power factor [-]
V_s	Stabilize signal voltage [V]
V_F	Feedback signal voltage [V]
V_R	Regulator voltage [V]
V_{Rmax}	Maximum regulator voltage [V]
V_{Rmin}	Minimum regulator voltage [V]

Chapter 1

Introduction

In the recent years, modern electrical power systems have grown to a large complexity due to increasing interconnections, installation of large generating units and - high voltage tie lines, etc. Especially, the integration of renewable energy resources as solar power units and wind power units into the electric networks has become one of the most important and challenging subjects of the power industry. In a proper integration of distributed energy sources, power system stability, control, protection, and operational restrictions should be taken into account. Therefore, excitation control, power system stabilizer (PSS), static VAR compensators, and other power system controllers play important roles in increasing dynamic performance and maintaining the power system stability and reliability. On other hand, the power system is a highly nonlinear system, which changes its operations continuously. Therefore, it is very challenging and uneconomical to make the system be stable for all disturbances.

In the last decade, several major blackouts were reported separately in many research papers. The first massive power failure properly reported was the Northeast power failure on 9th November 1965 in the United States [1]. The main cause was the weak transmission line between northeast and southwest. At heavy loading conditions, the backup protection tripped one line out of five. This is mainly due to relay was set to low load level. This major failure affected 30 million people, New York City was in darkness for 13 hours and it was the major failure in 85 years of electrical industries in the United States.

The second power failure was on 13th July 1977, which was a collapse of the Con Edison system. This left 8 million people in darkness, including New York City for periods from 5 to 25 hours. This collapse resulted from a combination of natural events, equipment malfunction, questionable system design features and operating errors as lack of preparation for major emergencies [2]. Severe thunderstorm and lightning strikes hit two lines; protective equipment of each line was imperfectly operated and resulted in three of the four lines tripping. Transmission ties increasingly overloaded for about 35 minutes and all ties were opened. After another 6 minutes, the entire system was out of operation.

A power failure in Tokyo, Japan occurred on 23rd July 1987 affecting 2.8 million customers with the outage of 3.4 GW power out of the maximum power demand of 38.5

GW. The reserve was kept at 1.52 GW and it was sufficient to manage the usual demand increase. The cause of this failure was reported [3] as unusual high peak demand due to extreme hot weather. Increase in demand (400MW/minute) exceeded the expected level. This increasing demand gradually reduced the voltage of the 500 kV trunk network within 5 minutes to 460 kV. The power transmission route was changed through sub transmission network to minimize tie line power. This minimizes the reactive power consumption and reduces the stress on the low voltage network.

A cascaded power interruption was reported [4] on 2nd July 1996, leading to a failure of the Western North American power system. This was initiated with a flashover to a tree, which created a short circuit on a 345 kV transmission line, causing a 2 GW power interruption. The total power consumption was the peak summer load of 118 GW. To prevent further down process, the system control managed to balance its operations by forming five islanded sub systems with controlled and uncontrolled load shedding, uncontrolled generator tripping and blackout in southern Idaho.

The US Canadian blackout on 14th August 2003 affected about 50 million people, 63 GW load was interrupted, which was 11% of the total power, served by the network. In this event 400 transmission lines and 531 generating units at 261 power plants tripped [5][6]. The major reason was found to be insufficient reactive power, which leads to voltage instability.

In Europe, the Swedish/Danish system had a blackout on 23rd September 2003 [7]. The system was moderately loaded with few outages for maintenance within the acceptable limits. The contingency started with the loss of a 1200 MW nuclear unit in the southern part of Sweden. After five minutes a fault occurred at a substation due to equipment failure and tripped another 1800 MW plant. These two events are unrelated. This tripping consequence very high power flow from north to south and system experienced voltage collapse. As a result separation of regions occurred. Finally, the islanded system also collapsed in both voltage and frequency, which lead to a blackout. This made a total of 6550 MW load lost in Sweden and Denmark affecting 4 million people.

The other major blackout occurred in Italy on 28th September 2003 [8]. Tree flashover hit the Italy Switzerland tie line. Connection was not re-established by auto re-closer due to a large phase difference across the line, as it was heavily loaded before tripping. Since the power was not redistributed effectively on time, a cascading trend continued. Within few seconds, the power deficit in Italy started to produce loss of synchronism with the rest of Europe. The interface line between Italy and France tripped due to a distance

relay and the same thing happened to the line between Italy and Austria. Finally, the transmission corridor between Italy and Slovenia got overloaded and tripped. These outages caused Italy with a shortage of 6,400 MW and the frequency of the Italian system dropped rapidly. After several minutes, the entire Italian system collapsed as the nationwide blackout. The frequency decay was not controlled sufficiently to stop generation from tripping.

A major interruption was caused on 16th January 2007 in Victoria, Australia [9]. This was mainly caused by a bushfire in extreme weather conditions thus tripping two key 330 kV power lines. Then the rapid cascaded line failures split the system into three islands within a few seconds. The value of unserved energy was revealed as AUS$ 60,000/MWh and the value of Loss Load was AUS$ 10,000IMWh.

Two severe power blackouts affected most of northern and eastern India on 30 and 31 July 2012 due to relay problems [16]. The 30 July 2012 blackout affected over 300 million people and was briefly, the largest power outage in history by number of people affected, beating the January 2001 blackout in Northern India (230 million affected). The blackout on 31 July is the largest power outage in history. The outage affected more than 620 million people, about 9% of the world population, or half of India's population, spread across 22 states in Northern, Eastern, and Northeast India. An estimated 32 GW of generating capacity was taken offline

Due to the geographical characteristics of Vietnam and different operational modes, the 500kV line linking North-Central-South power system often transmit the high capacity. Power transfer over this long line leads to heavy reactive losses and subsequent degradation of voltages at 500kV substations. These create high power swings in the regions and outweigh transmission capacity of power system. According to the calculated results with the 2014 power infrastructure, voltage collapse occurred in the peak load hours on the Central linking line when it transmitted over 2400/1980MW with 2/1 feeders. The transient stability limit of the 500kV line is violated when the system becomes unstable after large disturbance such as the tripping of a 500kV circuit breaker. When one 500kV line in system was cut off, the expected transmission limit on North-Central-South, line was approximately 1600MW and 2300MW in 2014 (adequately three 500kV feeder lines).

These above mentioned failures and blackouts in different parts of the power network have forced power systems researchers to look beyond the traditional approach of analyzing power system functionalities in steady state, pay serious attention to their dynamic characteristics, and that too in a global or wide-area sense. In the post-event

investigations of the blackout at several above countries, it was found out that large phase-angle differences in voltage and currents between two operating regions caused a series of generators to trip out, leaving insufficient power to run the grid. That, in turn, tripped out the few remaining generators still on line. However, a major road to wide-area analysis of large scale power systems is the absence of concrete mathematical models that capture the electromechanical dynamics coupling one area of the system with another. For example, we often hear power system operators mentioning how northern network oscillates against southern network in response to various disturbance events.

Recent articles have proposed various dynamical models of power sources. However, it is always assumed that these sources are connected to an infinite bus, and thus, dynamic multi-generator power system has not been utilized for stability analysis. In addition, in conventional power system dynamics analyses, the multi-machine ac power system is modeled by a set of nonlinear differential-algebraic equations. In these analyses, the differential equations represent the synchronous generators' dynamics whereas the algebraic equations model the power balance in the network buses. However, such a model has not been sufficiently developed for multi-generator power system in the presence of the new energy sources. These sources developments are related to frequency dynamics and power system operation. Since frequency dynamics are faster in power systems with low rotational inertia, this can lead to large transient frequency and power oscillations in multi-area power systems [10]. Moreover, the system stability can be lost due to these unexpected oscillations.

In addition, with the expansion of modern interconnected power system, inter-area low-frequency oscillations are becoming a phenomenon of concern in power system operations. Poorly damped inter-area oscillation is an especially serious threat to the safe and stable operation of the system. Currently, researchers have come up with many effective methods to analyze the low-frequency oscillation problem such state matrix, linear participation factors, the eigenvalue sensitivity and modal analysis. However, the relationship between the relative oscillation energy and the actual oscillating active power is still unclear. When a low-frequency oscillation occurs, the state variables, such as bus voltage and branch active power, will oscillate along with the generator rotor angle. There is an oscillation and a transformation between kinetic energy and potential energy. The potential energy exists in the form of branch potential energy, which will change during the low-frequency oscillation. The oscillation energy distribution in generators and branches will reflect the properties of power system oscillation and it can be used to identify the

oscillation mode and to determine the strongly correlated generators associated with the inter-area oscillation mode.

Above mentioned disadvantages lead to the wide discussion about power system stability. Ensuring stability, reliability and security in power systems is importance to system operators and the end users [11]. In recent studies, some main areas of interest were given broadly as modelling of power system leading to better understanding and control of the power system [12][13], and the electromechanical behavior of the power system. Those studies are based on the particular studies which are analyzing the influence of generator rotational inertia and long transfer distances among power plants on the power system fluctuations e.g. frequency, voltage, etc. [14].

Synchronous machines, specifically synchronous generators, are extremely important components in power generation systems worldwide. Many large synchronous generators connected to the power grid are usually found in recent power system, which is common in several countries around the world. Synchronous machines are used in many industrial applications due to their high power ratings and constant speed operation. The electrical and electromechanical behavior of most synchronous machines can be predicted from the equations that describe the three-phase salient pole synchronous machine [15].

Based on such two-generator model behavior, this work shows how the electromechanical dynamic of one generator in system may swing against each other when a disturbance sets in. The modes of study in this work represent prototypes of two transfer systems linked by long transmission line. First of all, the model must to be identified, and then derive analytical results showing how the voltage, phase angle, and frequency oscillations at two ending buses on the transfer path, follow a small-signal oscillations or transient disturbances. The focus in this dissertation is to present the simulation dynamic model of two synchronous generators connected via the long AC transmission line, and shows behavior characteristics of system through stability of voltage and frequency responses.

Chapter 2

Literary Research

The stability of power systems has been and continues to be of major concern in system operation. The grow of modern electrical power systems are a large complexity such as increasing interconnections, installation of large generating units and extra-high voltage tie-lines, etc. Since the first appearance, the fields of electrical machine and drive systems have been continuously enriched by introduction of many important topics. Progress in power electronics, microcontrollers, new materials and advances in numerical modeling have led to development of new types of electrical machines and different electrical drives. Their verification is usually done by simulation during system design, thus the effort is concentrated to development of simulation models.

Synchronous machines are used in many industrial applications due to their high power ratings and constant speed operation. The electrical and electromechanical behavior of most synchronous machines can be predicted from the equations that describe the three-phase salient pole synchronous machine. These equations can be used directly to predict the performance of hydro/steam turbine synchronous generators and synchronous motors. The rotor of synchronous machine is equipped with field winding and one or more damper windings, which is magnetically unsymmetrical. Simulation of the synchronous machine is well documented in the literature researches.

Despite the study of synchronous machines were mentioned in much research and numerous publications, some problems remain unsolved. One of the main problems is the providing stable operation during changing process conditions of system.

It is important to develop mathematical models for studying of synchronous machines, which adequately describe their behavior. Incorrect mathematical modeling leads to instability zone in corresponding models, which is lacking in real electrical machines. For example, increasing the supply voltage proportionally to increasing the torque load gives stable mathematical model, however, in practice the rotor sometimes starts rotating with acceleration or deceleration, synchronous machine is unstable. Therefore, the error mathematical models of synchronous machines cause the incorrect conclusions about stability of machines. The mathematical models of synchronous machines are often described by high-order differential equations with trigonometric nonlinearities. Due to the

complexity of these models, they practically cannot be studied by analytical methods, therefore, numerical methods are also used for investigation of these equations. However, some complicated effects such as semi-stable cycle solutions and hidden oscillations, which may occur in electromechanical systems, cannot be found and studied only by numerical methods. Hence, it is necessary to develop analytical methods for stability analysis of mathematical models.

The electrical machines and their controls are developing rapidly in the recent years. To get their operating characteristics under normal/fault condition needs implementation of modeling process. Simulation model of Permanent Magnet Synchronous Machine (PMSM) was presented mathematically in [22]. A current and speed controller is designed to implement fault tolerance and its stability analysis in this paper. Further use of permanent magnets helps in reduction of size and gives higher current, torque and speed compared to machine with electromagnets. The principles and methodology of virtual models development in GUI MATLAB for few chosen electrical machines and controlled drives were described in [26]. Strong advantage of these models does not need to know the complexity of dynamical system whose simulation scheme is working in the background. However, the only drawback of them are higher cost of magnets. In addition to higher accuracy, Iso Geometric Analysis (IGA) is used to simulate a permanent magnet synchronous machine [29]. IGA uses Non-Uniform Rational B-splines (NURBS) to parameterize the domain and to approximate the solution space, thus allowing for the exact description of the geometries even on the coarsest level of mesh refinement.

The Permanent Magnet Synchronous motor is a rotating electric machine where stator is a classic three-phase Induction Motor and rotor has permanent magnets. Mathematical modelling of Permanent Magnet Synchronous Motor is carried out and simulated using MATLAB [19]. The most important features of motor is its high efficiency given with the ratio of input power after deduction of loss to the input power. There is no field current or rotor current in the motor. Two mathematical models of four-pole rotor synchronous motors with damper windings at series and parallel connections were constructed based on laws of classical mechanics, electrodynamics and some simplifying assumptions [30]. The steady-state stability analysis and the dynamical stability of the idle synchronous machines is performed.

Another improved Simulink method, a nonlinear model of the Permanent Magnet Linear Synchronous Motor and an analogy between the rotary motor and the linear motor was described in [31]. A novel control of this motor is designed by which the system

nonlinearity is cancelled. In addition, a linear state feedback control law based on pole placement technique to achieve zero steady state error with respect to reference current specification is employed to improve the dynamic response. Based on a model and computer program simulation, the dynamic model and simulation of a three-phase salient pole synchronous motor are presented in [27]. Using rotor reference frame is to avoid the complexity involved in the course of solving time varying differential equations obtained from the dynamic model. An embedded MATLAB toolbox is utilized in this paper due to its uniqueness in offering the user the opportunity of programming the differential equations rather than obtaining the complete block diagram representation of those equations. In addition, it enables the user the opportunity to easily crosscheck the model for ease of identification of errors. Including PID controller, the modeling and simulation of the permanent magnet synchronous motor was realized by Simulink in [23][33]. A hybrid control strategy based on the nonlinear time-varying neural network and traditional PID parallel control is adopted. The results showed that the composite control strategy using nonlinear neural network PID and traditional PID parallel control had obvious superiority in time-varying response, robustness and anti-jamming capability. Therefore, it is superior to the traditional PID control strategy.

Besides synchronous motor, synchronous generator is also the main part of the power system. It has a complex dynamic behavior. This behavior influences on the entire power system. Hence, in order to analyze different problems of the power system, one must build the mathematical model of the synchronous generator.

Many works include the theory and performance of the synchronous generator. The different mathematical models of synchronous generators, described by ordinary differential equations or partial differential equations are used. Their models and analysis has always been not easy. Modeling synchronous generators when they operate in stationary or dynamic regime is currently widely used due to obvious advantage which modeling the excitation - generator - load system offers in different operating conditions of the generator. The model of the synchronous generator with damper windings is described by the system of six differential equations [23]. The solution of these equations is not an easy task. However, the art of modeling is the ability to convert the original complex system into a simple one without losing the main properties of the phenomenon. Therefore, the models of the synchronous generator to calculate the steady state and transient regimes. The ability to use different mathematical approximations of the generator models depending on the spatial distance of the disturbance point in system.

Study on the model of the whole system behavior allows predetermination of actual functioning of both steady and transient regime for different electric charges of the generator. The system model for determining the internal angle was designed and implemented by stroboscopic method [21]. Due to the development of modern computer technology, the numerical methods and several software solutions for simulations, control and scientific visualization have been reported such as Authorware, Hypertext, Labtech, Visual C, Visual Basic, LabVIEW and Matlab/Simulink. A new information about the behavior of trajectories can be obtained. Simulations of the same synchronous generator in Matlab/Simulink and LabVIEW verify the accuracy of the model in LabVIEW [25]. Modeling the synchronous generator with an excitation system in Matlab/Simulink and Sim-Power Systems allows full analysis in both static and dynamic states [28].

The main objectives of electricity networks operation is to ensure the functioning of a system in good condition and keep it in a stable state when it faces to a sudden disturbance, as in the cases of line faults or electric generator separations. In transient stability studies, generator model with AVR and PSS will constitute the worst-case scenario with respect to system stability following a disturbance [27]. The transient stability of electrical system was studied in [34], it based on the stability of the rotor angle while a three-phase fault, to determine the number of lines to be built under a voltage of 1200 kV and to transport a power of 9000 MW.

The widespread application of Renewable Energy Sources (RES) requires the use of advanced internet techniques both for monitoring system operation and control of its operation. The modeled plant consists of Hydropower turbine connected to synchronous generator with excitation system, and the generator is connected to public grid [20]. In this paper, the development of a data acquisition system based on switched Ethernet network for remote monitoring and control of hydroelectric power plants is presented. During disturbances, the generation and the corresponding loads can separate from the system to isolate the micro-grid's loads from the disturbance without harming the transmission grid's integrity. The improvement of voltage stability in the distributed generation system was focused on [32] by connecting a micro-grid with a synchronous generator to the utility grid.

Transient stability analysis has recently become a major issue in the operation of power systems due to the increasing stress on power system networks. This problem requires evaluation of a power system's ability to withstand disturbances while maintaining the quality of service. Many different techniques have been proposed for transient stability analysis in power systems, especially for a multi-machine system. Simulation of multi-

machine power system was described [38]. This model is very useful to study of stability analysis but is limited to the study of transients for only the “first swing” or for periods on the order of one second. The system is made stable by removing faulted line of given multi-machine.

Rotor angle stability denotes the ability of synchronous machines in the grid to remain in synchronism following large or small disturbance, and sustaining or re-establishing the equilibrium between electromagnetic torque and mechanical torque at each synchronous machine in the system. Large disturbance rotor angle stability, frequently called transient stability, parallels the ability of generators to sustain synchronism when subjected to harsh disturbances, including transmission system faults, sudden load changes, and loss of generating units or line switching. The novel didactic procedure is specially developed for transient stability simulation of a multi-machine power system given full details in [40].

Historically, simulation of transient phenomena related to power systems has been carried on using the electromagnetic transients program (EMTP) or one of its variants, such as the alternative transient program (ATP) or electromagnetic transients for d.c. (EMTDC), which are all based on the trapezoidal integration rule and the nodal approach. It contains models for basic circuit elements (R, L, C, independent and controlled sources, transformer, and transmission line), switches and most common semiconductor devices. However, there are no specific models for power systems and drives, such as electrical machines, circuit breakers, surge arresters, thyristors, etc. In order to simulate a power system, the user has to build the needed models using basic elements, so the simulation setup can be highly time consuming. Simulink is particularly useful for studying the effects of nonlinearity on the behavior of the system, and as such, is also an ideal research tool. Excitation systems, turbine and governor blocks can be readily used with Simulink blocks and when required. In [41], it have demonstrated a simplified and an efficient approach to study the transient stability performance of a practical power system, with Simulink as a tool.

Mathematical modeling of dynamic equivalents of an electric power system has seen some 40 years of long and rich research history. Simulink models for examining dynamic interactions involving electromechanical oscillations in systems were paid more attention. The dynamic modelling of synchronous machine based on low and medium voltage distribution systems for interaction studies involving electro-mechanical oscillations are presented clearly [35]. The respective interactions were observed in case of the low inertia low voltage units. Modelling and simulation studies are an integral part of power system

analysis. They are used in the electricity related industry from the early days of digital computers and the operation, stability of the system, controllers design and testing, operator training. A dynamic simulation program for a single machine infinite bus test system was developed by using MATLAB/Simulink software [39]. The program is useful to demonstrate various operational and stability challenges in power system operations.

In order to carry out analytical purpose and study the transient stability performance of a test system, a complete model for transient stability study of a multi-machine power system was developed using MATLAB/Simulink [42]. This model possesses interactive capacity for a detailed transient stability study, which facilitated fast and precise solution of nonlinear differential equation i.e. the swing equation. Due to these advantages, this study can be utilized for initiating rapid fault clearing and immediate restorative actions to maintain normal power flow.

With the expansion of modern interconnected power system as penetration of renewable energy sources, which is represented as a multi-machine interconnected system, inter-area low frequency oscillations are becoming a phenomenon of concern in power system operations. Currently, researchers have come up with many effective methods to analyze the low-frequency oscillation problems and loss of synchronism between generators. Between two synchronous machines, the relative rotor angle determines instability. When a synchronous machine losses synchronism or "fall out of step" with the rest of the system, its rotor runs at a higher or lower than that required to generate voltages at system frequency. System stability depends on the existence of both components of torque for each of the synchronous machines. From any small or large disturbance in the power system, electromechanical oscillations could result and could be damped and consequently the system can return to a stable operating state.

The main reasons of loss of synchronism, which led to accidents, were the increasing of load torque and voltage collapse such as the accident happened due to the multiple additional variable loads on a hydraulic aggregate connected with transition through non-recommended operation domain of a turbine. The loss of synchronism can occur between one machine and the rest of the system or between groups of machines. Because of these reasons, the qualitative analysis of transient processes in synchronous machines under sudden change of load is required. It is well known that a 0.25 Hz inter-area swing mode exists between the north-south interconnections of the Western Electricity Coordinating Council (WECC) extending from Alberta, Canada, to northern Baja Mexico [44], with additional 0.4–0.7Hz modes along the pacific intertie and the east-west interconnection.

Stability is a condition of equilibrium between opposing forces. Under steady-state conditions, there is equilibrium between the input mechanical torque and the output electrical torque of each machine, and the speed remains constant. If one generator temporarily runs faster than another does, the angular position of its rotor relative to that of the slower machine will advance. The resulting angular difference transfers part of the load from the slow machine to fast machine, depending on power-angle relationship. This tends to reduce the speed difference and hence the angular separation. Beyond a certain limit, an increase the angular separation is accompanied by a decrease in power transfer; this increase the angular separation further and leads to instability. For any given situation, the stability of the system depends on whether or not the deviations in angular positions of the rotors result in sufficient restoring torques.

It is known that, an initial generator rotor angle swing, which does not exceed 160°, is considered stable (practical limit). A rotor angle swing exceeding 160° only has a small margin before pole slipping (180°), and an initial rotor swing angle higher than 160° may result in a pole slip or repeated pole slipping, which is considered unstable [45]. The characteristics of inter-area oscillation are studied by analyzing the distribution of the oscillation energy [24]. A modal kinetic energy participation factor is proposed for evaluating the participation of each generator in the oscillation. The distribution characteristics of voltage angle oscillation and branch potential energy in inter-area oscillation is developed.

The dynamic stability of synchronous machines can be increased by implementing a controller. The controller may influence either on stator and rotor currents or directly on the torque of the rotor. A variable frequency drive is frequently used as a controller, which allows one to change amplitude and frequency of current. Stability of a multi-generator representation of the power system is achieved by employing novel controllers. When a fault or a disturbance occurs in the power system, the generator angles and speeds deviate from their normal operating range. Unless there is a controller to mitigate the oscillations, which bounce back and forth among multiple generators, the power system will not return to its normal operating state after the fault is removed. Since the disturbance is a function of the power network voltages and angles as well as generator states, it is generally hard to design a centralized damping controller for the complex interconnected power network. A damping controllers are developed with the application of conventional multi-machine stabilizing techniques such as Power System Stabilizer (PSS) and Automatic Voltage Regulator (AVR) [43]. The result is a feedback controller that makes possible for power

systems with penetration of renewable energy sources. This thesis is based on the major publications [12] [14] [20] [22] [24] [26] [28] [30] [34] [36] [37]**.**

Taking motivation from above discussion, this dissertation is modeling two synchronous generators connected via long transmission line to see how the system behaves when subject to disturbances. The major objectives of this work are dynamic model of the synchronous generators and behavior characteristics of system through voltage and frequency stability index.

Chapter 3

Aim of dissertation

According to the discussion and analysis in chapter 2, the main aims of my dissertation are:

(i) To implement the complete system model for electromechanical oscillation of connected generators including mechanical components under steady state and disturbances condition.

(ii) To analysis the influence of the length of line for oscillation of power system using the complete system model.

Based on analyzing oscillation problems in chapter 2, almost authors in the articles tended to cut mechanical part and electrical part separately. In fact, two these parts have a tight connection through electromechanical oscillation. This oscillation limits to power transfer capacity. New modes of oscillation, involving the interaction between the dynamics of the different machines, which are not modeled in the single machine models. It is necessary to have comprehensive modelling and analysis techniques of all the components that may interact to produce oscillations. Each component of the power system i.e. prime mover, generator rotor, generator stator, transformers, transmission lines, load, controlling devices and protection systems should be mathematically represented to assess the rotor angle, voltage and frequency stability through appropriate analysis tools. For the correct representation of a generating unit, both the electrical and the associated mechanical phenomena must be modeled

Power transfer capability in power system has been limited by stability considerations under the long transmission distance between load centers and power sources. This dissertation work will give dynamic model of system and respect length of long lines as influent index to oscillations. It is due to the big blackouts in history was mostly in large countries with long lines. My country Vietnam with long transmission distance from Northern to Southern is facing to some dangerous blackouts for long lines. Therefore, the length of line needs to be considered as one of the most influent factors to system oscillation.

Chapter 4

System Modeling

The investigated systems are described in this chapter. Consider that the system (a generator) is connected to another similar system by a tie line (power line). This tie line should be strong enough to survive the loss of any one generator. Tie line oscillations are very likely to occur, especially at heavy line loading. These tie line oscillations are the restriction on the allowable power transfer, as relatively large oscillations are taken as the precursor to instability.

In this chapter, in order to analysis the electromechanical oscillations of generators and the influence of length of power line to system stability, a dynamic model of synchronous generator is presented, along with the interconnecting long transmission line model and aggregated load model.

The modelling of the systems are based on per unit (pu) quantities, with the exception of time expressed in seconds (s), and base values, expressed in their corresponding physical values. The base values are defined from the apparent power ratings and the rated peak phase to neutral voltages.

System equations are derived and linearized for the small disturbance stability analysis **[PVI] [PVII]** and some large disturbances **[PIII].** Results of transient simulations are provided to compare the time-domain response of the test systems in some disturbance cases. These results can also serve to define stability margin of a power system under the different connection conditions of network. The electromechanical oscillation frequency between synchronous generators in a power system typical lies between 0.5 to 3 Hz **[PV] [PVI]**. The sub-transient time constant of most machines is between 0.03 to 0.04 seconds [49], which is short compared to the typical period of the electromechanical oscillations of machines [Appendix (B)].

4.1 Synchronous Generator Modeling

Synchronous machines have been widely used in power system, they are not only the main generation units in large scale conventional power stations, but also in small and remote standalone systems. A detailed and accurate model is essential to investigate the performance of a synchronous machine and its control strategies.

The modelling, analysis and control of synchronous machines are implemented in rotating reference frames. The transformations from the stationary reference frame into rotating reference frames are based on the amplitude-invariant Park transformation, with the quadrature (q) axis leading the direct (d) axis by 90^0 [22] [23].

In order to be simple, balanced three-phase conditions have been assumed, so no zero sequence components are included. The sub-indexes d and q denote the d-axis and q-axis components of a transformed variable, respectively. The magnitude of the current and voltage vectors is in per unit (pu) at rated conditions.

This project presents important aspects regarding dynamic characteristic of a direct phase synchronous machine model which has been implemented in MATLAB/SIMULINK under various conditions of system.

The electrical and electromechanical behavior of most synchronous machines can be predicted from the equations that describe the three phase salient pole synchronous machine [15][17]. The rotor of synchronous machine is equipped with field winding and damper windings. Salient pole synchronous machine is used to provide independent control of mechanical torque and deliver electric power. Slip power recovery systems can provide both the mechanical and electrical power transmission, but these are coupled and not independently controllable [18]. To obtain the phase currents from the flux linkages, the inverse of the time varying inductance matrix will have to be computed at every time step [38] [39]. Stator winding quantities need transformation from three phases to two-phase d-q rotor rotating reference frame.

Simulation of the synchronous machine is well documented in the literature and digital computer solutions can be performed using various methods such as numeric programming [25][26][39]. Fig 4.1 shows an internal block diagram representation of a synchronous machine model. It consists of three blocks, namely torque-angle loop, rotor electrical block, and excitation system block **[PVI]** [46].

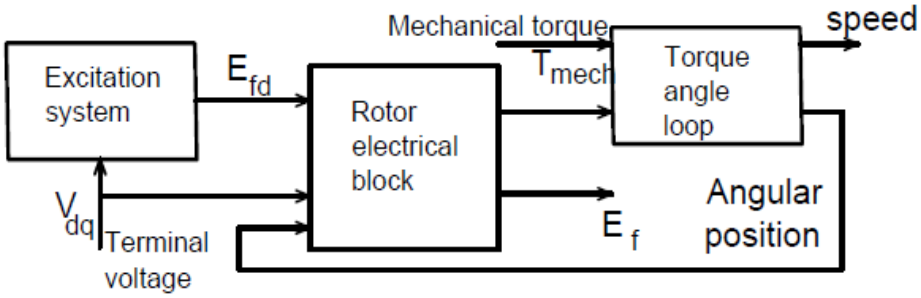

Fig. 4.1. Block diagram representation of synchronous machine model

The torque angle loop represents turbine and generator mechanical system. Input to this block are mechanical and electrical torques, and outputs are rotating speed and rotor position.

The rotor electrical block represents flux dynamics in the machine windings. The excitation system block compares terminal voltage magnitude with a reference voltage, and outputs field voltage. There are two inputs for the synchronous machine model. One of them is the mechanical torque, which is assumed to be constant or changed during the course of simulation. The second one is terminal voltage V_t obtained from the network. The output of the model is current I_t which is fed to the network block.

The mathematical description and model developed in this section is based on the concept of an ideal synchronous machine with two basic poles. For the salient-pole rotor machine, two additional windings are used, one on the d-axis and the other on the q-axis. Damper windings in the equivalent machine model are used to represent physical amortisseur windings, or the damping effects of eddy currents in the solid iron portion of the rotor poles. Fig. 4.2 shows a circuit representation of an idealized machine model of the synchronous machine commonly used in stability analysis **[PII].**

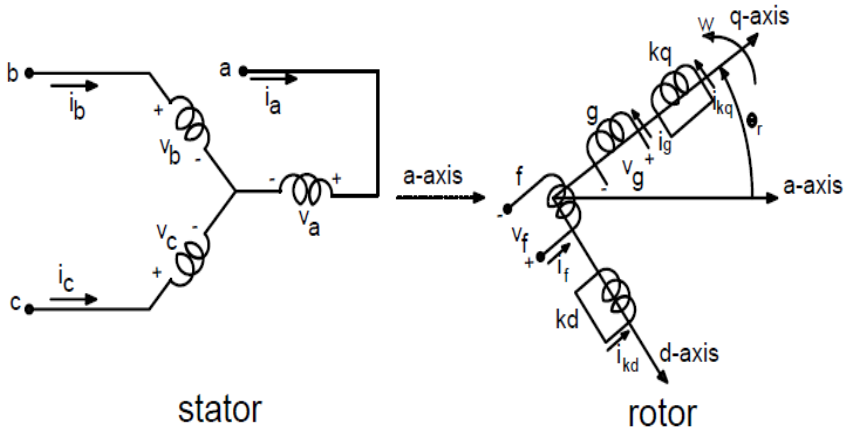

Fig. 4.2. Diagram of idealized synchronous machine

4.1.1 Mathematical model

The circuit of an idealized synchronous machine, three phase windings a-b-c, field winding f and two equivalent damper coils k_d-k_q are shown in Fig. 4.2.

The performance of a synchronous generator is described by the voltage equations in direct phase quantities for the three armature phases, the field and two equivalent damper coils. The position of the rotor at any instant is specified with reference to the axis of phase a by the angle θ_r. In terms of flux linkage, the voltage equations of the stator and rotor windings in the circuit are expressed in phase frame as [20]:

$$\begin{bmatrix} v_s \\ v_r \end{bmatrix} = \begin{bmatrix} r_s & 0 \\ 0 & r_r \end{bmatrix} \begin{bmatrix} i_s \\ i_r \end{bmatrix} + \frac{d}{dt} \begin{bmatrix} \Psi_s \\ \Psi_r \end{bmatrix} \quad (4.1)$$

Where:

$$[v_s] = [v_a \ \ v_b \ \ v_c]^T \quad (4.2)$$

$$[v_r] = \left[v_f \ \ v_{kd} \ \ v_g \ v_{kq}\right]^T \quad (4.3)$$

$$[\Psi_s] = [\Psi_a \ \ \Psi_b \ \ \Psi_c]^T \quad (4.4)$$

$$[\Psi_r] = [\Psi_f \ \ \Psi_{kd} \ \ \Psi_g \ \ \Psi_{kq}]^T \quad (4.5)$$

$$[i_s] = [i_a \ \ i_b \ \ i_c \ ]^T \quad (4.6)$$

$$[i_r] = \left[i_f \ \ i_{kd} \ \ i_g \ \ i_{kq}\right]^T \quad (4.7)$$

$$[r_s] = diag[r_a \ \ r_b \ \ r_c \ ] \quad (4.8)$$

$$[r_r] = diag\left[r_f \ \ r_{kd} \ \ r_g \ \ r_{kq} \ \right] \quad (4.9)$$

Transform the stator quantities to a rotating qd0 reference frame that is attached to the machine rotor.

In vector forms, the transformation of coordinate's abc-dq0, known also as the park transform, valid for voltages, currents and fluxes:

$$\left[v_{qd0}\right] = \left[P_{qd0}(\theta_r)\right][v_s] = \left[v_q \ \ v_d \ \ v_0\right]^T \quad (4.10)$$

$$\left[\Psi_{qd0}\right] = \left[P_{qd0}(\theta_r)\right][\Psi_s] = \left[\Psi_q \ \ \Psi_d \ \ \Psi_0\right]^T \quad (4.11)$$

$$\left[i_{qd0}\right] = \left[P_{qd0}(\theta_r)\right][i_s] = \left[\ i_q \ \ i_d \ \ i_0\right]^T \quad (4.12)$$

Where:

$$\left[P_{qd0}(\theta_r)\right] = \frac{2}{3}\begin{bmatrix} cos\theta_r & \cos\left(\theta_r - \frac{2\pi}{3}\right) & \cos\left(\theta_r + \frac{2\pi}{3}\right) \\ sin\theta_r & \sin\left(\theta_r - \frac{2\pi}{3}\right) & \sin\left(\theta_r + \frac{2\pi}{3}\right) \\ \frac{1}{2} & \frac{1}{2} & \frac{1}{2} \end{bmatrix} \quad (4.13)$$

$$\omega_r = \frac{d\theta_r}{dt} \quad (4.14)$$

4.1.2 Voltage and currents equations

The main inputs to the machine simulation are the stator a-b-c phase voltages, the excitation voltage applied to the field windings, and the applied mechanical torque to the rotor.

Performing the transformation to qd0 reference frame of voltages yields:

$$v_q = \frac{2}{3}\left\{v_a \cos\left(\theta_r(t)\right) + v_b \cos\left(\theta_r(t) - \frac{2\pi}{3}\right) + v_c \cos\left(\theta_r(t) + \frac{2\pi}{3}\right)\right\} \quad (4.15)$$

$$v_d = \frac{2}{3}\left\{v_a \sin\left(\theta_r(t)\right) + v_b \sin\left(\theta_r(t) - \frac{2\pi}{3}\right) + v_c \sin\left(\theta_r(t) + \frac{2\pi}{3}\right)\right\} \tag{4.16}$$

$$v_0 = \frac{1}{3}(v_a + v_b + v_c) \tag{4.17}$$

Where:

$$\theta_r(t) = \int_0^t \omega_r(t)\, dt + \theta_r(0) \tag{4.18}$$

In simulation, the values of $\cos\left(\theta_r(t)\right)$ and $\sin\left(\theta_r(t)\right)$ obtained from a variable-frequency oscillator circuit which has a provision for setting the proper initial value of θ_r.

The qd0 voltage equations are used in the integral equations of flux linkages of the windings.

$$\Psi_q = \omega_b \int \left\{v_q - \frac{\omega_r}{\omega_b}\Psi_d + \frac{r_s}{x_{ls}}(\Psi_{mq} - \Psi_q)\right\} dt \tag{4.19}$$

$$\Psi_d = \omega_b \int \left\{v_d + \frac{\omega_r}{\omega_b}\Psi_q + \frac{r_s}{x_{ls}}(\Psi_{mq} - \Psi_d)\right\} dt \tag{4.20}$$

$$\Psi_0 = \omega_b \int \left\{v_0 - \frac{r_s}{x_{ls}}\Psi_0\right\} dt \tag{4.21}$$

$$\Psi'_{kq} = \frac{\omega_b r'_{kq}}{x'_{lkq}} \int (\Psi_{mq} - \Psi'_{kq}) dt \tag{4.22}$$

$$\Psi'_{kd} = \frac{\omega_b r'_{kd}}{x'_{lkd}} \int (\Psi_{md} - \Psi'_{kd}) dt \tag{4.23}$$

$$\Psi'_f = \frac{\omega_b r'_f}{x_{md}} \int \left\{E_f + \frac{x_{md}}{x'_{lf}}(\Psi_{mq} - \Psi'_f)\right\} dt \tag{4.24}$$

Where:

$$\Psi_{mq} = x_{mq}\left(i_q + i'_{kq}\right) = x_{mq}\left(\frac{\Psi_q}{x_{ls}} + \frac{\Psi'_{kq}}{x'_{lkq}}\right) \tag{4.25}$$

$$\Psi_{md} = x_{md}\left(i_d + i'_{kd} + i'_f\right) = x_{md}\left(\frac{\Psi_d}{x_{ls}} + \frac{\Psi'_f}{x'_{lf}} + \frac{\Psi'_{kq}}{x'_{lkq}}\right) \tag{4.26}$$

$$E_f = x_{md}\frac{v'_f}{r'_f} \tag{4.27}$$

$$\Psi_q = x_{ls} i_q + \Psi_{mq} \tag{4.28}$$

$$\Psi_d = x_{ls} i_d + \Psi_{md} \tag{4.29}$$

$$\Psi_0 = x_{ls} i_0 \tag{4.30}$$

$$\Psi'_f = x'_{lf} i'_f + \Psi_{md} \tag{4.31}$$

$$\Psi'_{kd} = x'_{lkd} i'_{kd} + \Psi_{md} \tag{4.32}$$

$$\Psi'_{kq} = x'_{lkq} i'_{kq} + \Psi_{mq} \tag{4.33}$$

The above equations are in motoring convention, that is the currents, i_q and i_d, are in the positive polarity of the stator windings terminal voltages.

The mutual flux linkages are expressed in terms of the total flux linkages of the windings:

$$\Psi_{mq} = x_{MQ}\left(\frac{\Psi_q}{x_{ls}} + \frac{\Psi'_{kq}}{x'_{lkq}}\right) \tag{4.34}$$

$$\Psi_{md} = x_{MD}\left(\frac{\Psi_q}{x_{ls}} + \frac{\Psi'_{kq}}{x'_{lkq}} + \frac{\Psi'_{f}}{x'_{lf}}\right) \tag{4.35}$$

Where:

$$\frac{1}{x_{MQ}} = \frac{1}{x_{mq}} + \frac{1}{x'_{lkq}} + \frac{1}{x_{ls}} \tag{4.36}$$

$$\frac{1}{x_{MD}} = \frac{1}{x_{md}} + \frac{1}{x'_{lkd}} + \frac{1}{x'_{lf}} + \frac{1}{x_{ls}} \tag{4.37}$$

The winding currents are determined by the values of the flux linkages of windings and the mutual flux linkages among the d- and q-axes.

$$i_q = \left(\frac{\Psi_q - \Psi_{mq}}{x_{ls}}\right) \tag{4.38}$$

$$i_d = \left(\frac{\Psi_d - \Psi_{md}}{x_{ls}}\right) \tag{4.39}$$

$$i'_{kd} = \left(\frac{\Psi'_{kd} - \Psi_{md}}{x'_{lkd}}\right) \tag{4.40}$$

$$i'_{kq} = \left(\frac{\Psi'_{kq} - \Psi_{mq}}{x'_{lkq}}\right) \tag{4.41}$$

$$i'_{f} = \left(\frac{\Psi'_{f} - \Psi_{md}}{x'_{lf}}\right) \tag{4.42}$$

The stator winding qd currents are transformed back to abc winding currents using the following rotor to stationary qd, and stationary qd0 to abc transformations:

$$i_q^s = i_q \cos\big(\theta_r(t)\big) + i_d \sin\big(\theta_r(t)\big) \tag{4.43}$$

$$i_d^s = -i_q \sin\big(\theta_r(t)\big) + i_d \cos\big(\theta_r(t)\big) \tag{4.44}$$

$$i_a = i_q^s + i_0 \tag{4.45}$$

$$i_b = -\frac{1}{2}\, i_q^s - \frac{1}{\sqrt{3}} i_d^s + i_0 \tag{4.46}$$

$$i_c = -\frac{1}{2} i_q^s + \frac{1}{\sqrt{3}} i_d^s + i_0 \tag{4.47}$$

4.1.3 Power and torque equations

The expression for the electromagnetic torque developed by the machine obtained from the component of the input power that transferred across the air-gap.

$$P_{in} = \frac{3}{2}\left(r_s\left(i_q^2 + i_d^2\right) + i_q\frac{d\Psi_q}{dt} + i_q\frac{d\Psi_d}{dt} + \omega_r(\Psi_d i_q + \Psi_q i_d)\right) + 3i_0^2 r_0 + 3i_0\frac{d\Psi_0}{dt} + 3\,i_f^2 r_f + 3i_f\frac{d\Psi_f}{dt} \tag{4.48}$$

Eliminating the ohmic losses and the rate of change in magnetic energy, the electromechanical power developed as:

$$P_{em} = \frac{3p}{4}\omega_{rm}(\Psi_d i_q - \Psi_q i_d) \tag{4.49}$$

The electromechanical torque developed by a p-pole machine:

$$T_{em} = \frac{P_{em}}{\omega_{rm}} = \frac{3p}{4}(\Psi_d i_q - \Psi_q i_d) \tag{4.50}$$

Equation motion of rotor is given by:

$$T_{em} - T_{mech} - T_{damp} = \frac{2J}{p}\frac{d(\omega_r(t) - \omega_e)}{dt} \tag{4.51}$$

In per unit system, the base power, S_b, is the rated VA of the machine.

For transient studies, the peak value of the rated phase voltage is to be chosen as the base voltage:

$$V_b = \frac{\sqrt{2}}{\sqrt{3}}V \tag{4.52}$$

Similarly, choosing the peak value of the rated current as the base current:

$$I_b = \frac{2}{3}\frac{S_b}{V_b} \tag{4.53}$$

The base values for the stator impedance, torque, mechanical angular frequency, flux and flux linkage:

$$Z_b = \frac{V_b}{I_b} \tag{4.54}$$

$$T_b = \frac{S_b}{\omega_{bm}} \tag{4.55}$$

$$\omega_{bm} = \frac{2\omega_b}{p} \tag{4.56}$$

$$\psi_b = \frac{V_b}{\omega_b} \tag{4.57}$$

$$H_b = \frac{J\omega_{bm}^2}{2S_b} \tag{4.58}$$

The torque in per unit reduces to:

$$T_{em}(pu) = \Psi_d(pu) i_q(pu) - \Psi_q(pu) i_d(pu) \tag{4.59}$$

Equation of the motion of the rotor assembly, expressed in per unit:

$$T_{mech}(pu) - T_{em}(pu) - T_{damp}(pu) = 2H \frac{d(\Delta\omega(pu))}{dt} \tag{4.60}$$

$$\frac{d\delta_e}{dt} = \omega_r - \omega_e \tag{4.61}$$

$$\omega(pu) = \Delta\omega(pu) + 1 \tag{4.62}$$

Where:

$$T_{damp}(pu) = D\left(\frac{\omega_r - \omega_e}{\omega_b}\right) \tag{4.63}$$

$$V_t(pu) = \sqrt{v_q^{s2} + v_d^{s2}} \tag{4.64}$$

$$I_t(pu) = \sqrt{i_q^{s2} + i_d^{s2}} \tag{4.65}$$

$$P_g(pu) = Re\{(v_q - jv_d)(i_q - ji_d)^*\} = v_q i_q + v_d i_d \tag{4.66}$$

$$Q_g(pu) = Im\{(v_q - jv_d)(i_q - ji_d)^*\} = v_q i_d - v_d i_q \tag{4.67}$$

4.1.4 Transient model

Considering that x'_d, x'_q are d- and q-axis transient generator reactance, E'_d, E'_q are d- and q-axis transient electromotive forces and T'_{do}, T'_{qo} are the transient open circuit time constants.

The stator winding equations:

$$v_q = -r_s i_q - x'_d i_d + E'_q \tag{4.68}$$

$$v_d = -r_s i_d + x'_q i_q + E'_d \tag{4.69}$$

Rotor winding equations:

$$T'_{do} \frac{dE'_q}{dt} = -E'_q - (x_d - x'_d) i_d + E_f \tag{4.70}$$

$$T'_{qo} \frac{dE'_d}{dt} = -E'_d + (x_q - x'_q) i_q \tag{4.71}$$

The torque and motion equation:

$$T_{em} = E'_d i_d + E'_q i_q + (x'_q - x'_d) i_d i_q \tag{4.72}$$

$$2H \frac{d\left(\frac{\omega_r - \omega_e}{\omega_b}\right)}{dt} = T_{mech} - T_{em} - T_{damp} \tag{4.73}$$

4.1.5 Initial values of the synchronous generator

The primary step in initializing the model is to obtain a power flow solution of the system. A more detailed explanation is available in [48]. The subscript 0 in the following equations indicates initial value or steady state value of the state variables.

Initial values of current, load angle, rotor angle, electromotor force in the machine, terminal voltage, real power, exciter voltage, and reference terminal voltage are calculated using the equations below:

$$I_{g0}\angle\varphi_0 = (P_g - jQ_g)/(V_{g0}\angle(-\theta_{g0})) \tag{4.74}$$

$$E_{q0}\angle\delta_0 = V_{g0}\angle\theta_{g0} + (r_s + jx_q)I_{g0}\angle\varphi_0 \tag{4.75}$$

$$i_{d0} = -I_{g0}sin(\delta_0 - \varphi_0) \tag{4.76}$$

$$i_{q0} = I_{g0}cos(\delta_0 - \varphi_0) \tag{4.77}$$

$$v_{d0} = -V_{g0}sin(\delta_0 - \varphi_0) \tag{4.78}$$

$$v_{q0} = V_{g0}cos(\delta_0 - \varphi_0) \tag{4.79}$$

$$E'_{q0} = v_{q0} + x'_d i_{d0} + r_s i_{q0} E_{f0} \tag{4.80}$$

$$E'_{d0} = v_{d0} - x'_d i_{q0} + r_s i_{d0} \tag{4.81}$$

$$E_{f0} = E'_{q0} + (x_d - x'_d) i_{d0} \tag{4.82}$$

$$T_{em0} = E'_{d0} i_{d0} + E'_{q0} i_{q0} + (x_d - x'_d) i_{d0} i_{q0} = T_{mech0} \tag{4.83}$$

4.2 Excitation system modelling

Synchronous generator excitation control is one of the most important measures to enhance power system stability and to guarantee the quality of electrical power it provides. The main control function of the excitation system is to adjust the field voltage with respect to the variation of the terminal voltage. It must be able to respond quickly to a disturbance enhancing the transient stability and the small signal stability.

The generator excitation system consists of an exciter and an Automatic Voltage Regulator (AVR) [28]. Fig 4.3 shows block diagram of simplified excitation system with Automatic Voltage Regulator and Power System Stabilizer (PSS).

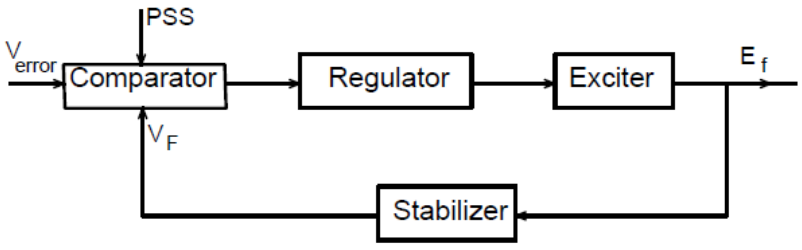

Fig 4.3 Block diagram of the Excitation System with AVR and PSS.

The AVR regulates the generator terminal voltage by controlling the amount of current supplied to the generator field winding by the exciter. AVR consists of an error amplifier in limiter with whose function is to protect the AVR, exciter and generator from excessive voltages and currents [20] [28]. A power system stabilizer (PSS) is added to the AVR subsystem to help damp power swings in the system.

In this work, the simplified IEEE type 1 excitation system is used followed Fig. 4.4. **[PVI] [PVII]** [50].

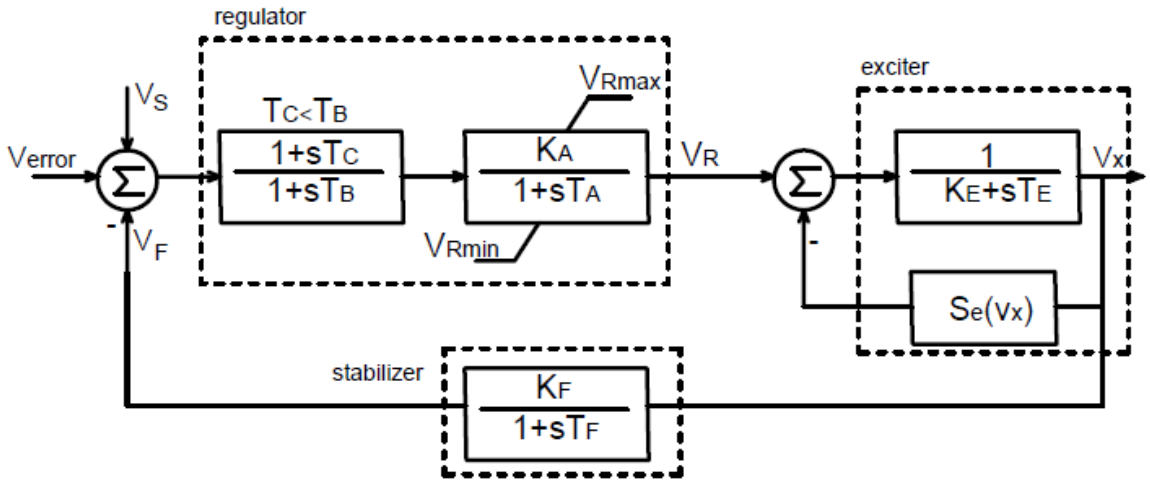

Fig 4.4. IEEE type 1 excitation system

4.3 Network modelling

Transmission network mainly consists of transmission lines, transformers and loads. The modelling of these components are discussed in the following sections:

4.3.1 Transmission lines

Models for transmission lines for using in network analysis are usually categorized by line lengths (short, medium, long). In this thesis content, the long line will be used for connecting two synchronous generators via step up transformers. The parameters and calculated values are analyzed clearly followed the long transmission line model.

The long line model involves partial differential equations, which in some sense represent an infinite number of ordinary differential equations. For the line over 250km, the fact that the parameters of a line are not lumped but distributed uniformly throughout its length [36] [37], must be considered in Fig.4.5 **[PI-PIII].**

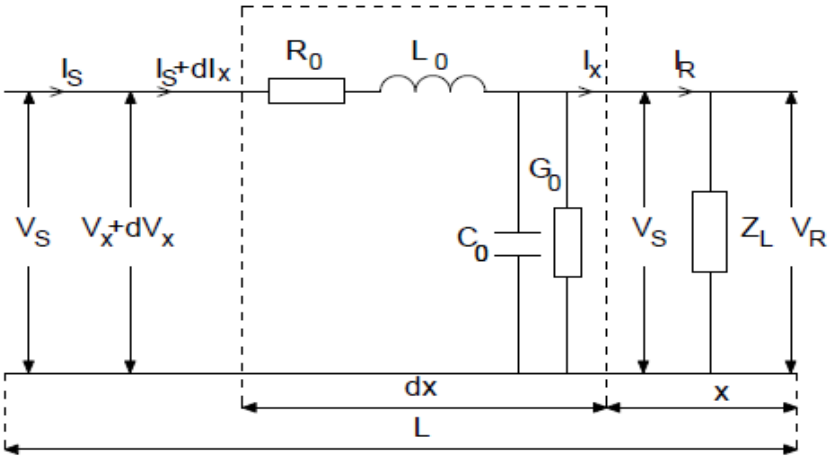

Fig. 4.5 Schematic diagram of a long transmission line

dx be an element section of the line at a distance x from the receiving end having a series impedance Z_0dx and shunt admittance Y_0dx. The rise in voltage to neutral over the element section in the direction of increasing x is dVx.

Where

$Z_0=R_0+j\omega L_0$ (Ω/km)

$Y_0= G_0+j\omega C_0$ (S/km)

R_0 (Ω/km), L_0 (H/km), G_0 (S/km) and C_0 (F/km) are resistance, inductance, conductance and capacitance per line length unit.

The differential relationships across the element section

$$dV_x = I_x Z_0 dx \quad or \quad \frac{dV_x}{dx} = I_x Z_0 \tag{4.84}$$

$$dI_x = V_x Y_0 dx \quad or \quad \frac{dI_x}{dx} = V_x Y_0 \tag{4.85}$$

Derivation two side of (4.84) and substitute (4.85) yields:

$$\frac{d^2V}{dx^2} = Z_x \frac{dI_x}{dx} = Z_0 Y_0 V_x \tag{4.86}$$

Equation (4.86) is a linear differential equation whose general solution can be written as follows:

$$V_x = C_1 e^{\gamma x} + C_2 e^{-\gamma x} \tag{4.87}$$

Where

$\gamma = \sqrt{Z_0 Y_0}$ is the propagation constant

And C_1, C_2 are arbitrary constants to be evaluated

Differentiating (4.87) with respect to x

$$\frac{dV_x}{dx} = C_1 \gamma e^{\gamma x} - C_2 \gamma e^{-\gamma x} = Z_0 I_x \tag{4.88}$$

$$I_x = \frac{C_1 e^{\gamma x}}{Z_c} - \frac{C_2 e^{-\gamma x}}{Z_c} \tag{4.89}$$

Where

$Z_c = \sqrt{\frac{Z_0}{Y_0}}$ is the characteristic impedance

Let x=0, V_x=V_R and I_x=I_R

$$\begin{cases} V_x = \frac{(V_R + Z_c I_R)}{2} e^{\gamma x} + \frac{(V_R - Z_c I_R)}{2} e^{-\gamma x} & (4.90) \\ I_x = \frac{(V_R/Z_c + I_R)}{2} e^{\gamma x} + \frac{(V_R/Z_c - I_R)}{2} e^{-\gamma x} & (4.91) \end{cases}$$

A more convenient form of expression for voltage and current is obtained by introducing hyperbolic functions.

$$\begin{cases} V_x = V_R cosh\gamma x + Z_c I_R sinh\gamma x & (4.92) \\ I_x = \frac{V_R}{Z_c} sinh\gamma x + I_R cosh\gamma x & (4.93) \end{cases}$$

When x=l, V_x=V_S, I_x=I_S

$$\begin{bmatrix} V_S \\ I_S \end{bmatrix} = \begin{bmatrix} cosh\gamma x & Z_c sinh\gamma x \\ \frac{1}{Z_c} sinh\gamma x & cosh\gamma x \end{bmatrix} \begin{bmatrix} V_R \\ I_R \end{bmatrix} = \begin{bmatrix} A & B \\ C & D \end{bmatrix} \begin{bmatrix} V_R \\ I_R \end{bmatrix} \tag{4.94}$$

Where

A=D= $cosh\gamma x$ (per unit)

B=$Z_c sinh\gamma x$ (Ω)

C=$\frac{1}{Z_c} sinh\gamma x$ (S)

And γ is a complex number which can be expressed as:

$$\gamma = \alpha + j\beta \tag{4.95}$$

Where

α is the attenuation constant

β is the imaginary part (phase constant)

The equivalent circuit of a transmission line can be established in the form of a π-network. The parameters of the equivalent network are easily obtained by comparing the performance equations of a π-network and a transmission line in terms of end quantities in Fig.4.6 **[PIII].**

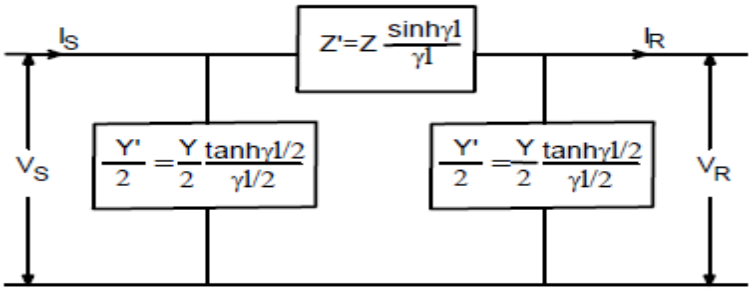

Fig. 4.6 Equivalent π-network of a long transmission line

$$\begin{bmatrix} V_S \\ I_S \end{bmatrix} = \begin{bmatrix} (1+\frac{1}{2}Y'Z') & Z' \\ Y'(1+\frac{1}{4}Y'Z') & (1+\frac{1}{2}Y'Z') \end{bmatrix} \begin{bmatrix} V_R \\ I_R \end{bmatrix} \tag{4.96}$$

According to exact solution of a long line

$$\begin{bmatrix} V_S \\ I_S \end{bmatrix} = \begin{bmatrix} cosh\gamma l & Z_c sinh\gamma l \\ \frac{1}{Z_c} sinh\gamma l & cosh\gamma l \end{bmatrix} \begin{bmatrix} V_R \\ I_R \end{bmatrix} \tag{4.97}$$

Where

$$Z' = Z_c sinh\gamma l;\ Z' = \sqrt{\frac{Z_0}{Y_0}} sinh\gamma l = \frac{Z_0 l}{l\sqrt{Z_0 Y_0}} sinh\gamma l = \frac{Z}{\gamma l} sinh\gamma l$$

$$1+\frac{1}{2}Y'(Z_c sinh\gamma l) = cosh\gamma l; \frac{Y'}{2} = \frac{Y}{2}\frac{tanh\frac{\gamma l}{2}}{\frac{\gamma l}{2}}$$

In the case of a lossless line, the terminology surge impedance is used for Z_c instead of characteristic impedance. A lossless line operating at its nominal voltage, terminated in its surge impedance Z_c, is called to be surge impedance loaded (SIL). The transmitted per phase power in this case is designed P_{SIL}.

$$P_{SIL} = \frac{|V|^2}{Z_c} \tag{4.98}$$

4.3.2 Transformers

Transformers are generally used as inter-connecting and generator transformers. These transformers are usually with off-nominal-turns-ratio and are modelled as equivalent π circuit [46] as shown in Fig 4.7.

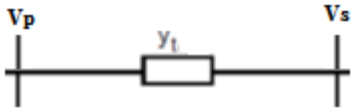

Fig. 4.7 Transformer model

Where:

$y_t=1/z_t$

z_t: represents the series impedance

V_p: primary voltage

V_s: secondary voltage

4.3.3 Loads

The load admittance Y_L can be absorbed and is given by [Appendix (A.2)]:

$$Y_L = \frac{P_L - jQ_L}{V^2} \tag{4. 99}$$

The load at bus is represent by an equivalent circuit as shown in Fig 4.8 **[PVI]**. The load admittance Y_L has been absorbed into bus admittance Y_{bus}. Therefore, the net equivalent load current to be injected at load bus is given by:

$$I_L = -\left(\frac{S_L}{V}\right)^* - (-Y_L V) \tag{4.100}$$

$$= -\left(\frac{S_L}{V}\right)^* + Y_L V = g(V, f)$$

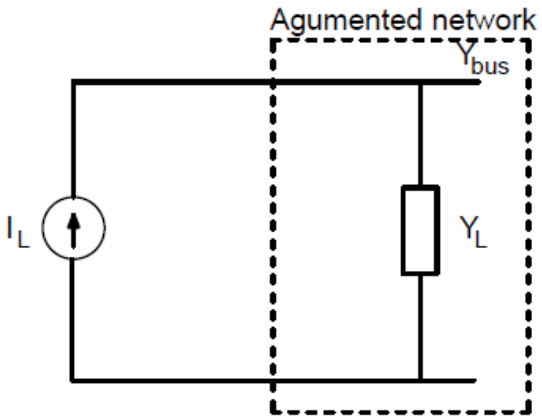

Fig. 4.8 Equivalent circuit of load

4.4 Mathematical model of the proposed power system

A power system comprises several buses which are interconnected by means of transmission lines. Power is injected into a bus from generators, while the loads are tapped from it. There may be buses with only generators and no-loads, and there may be others with only loads and no generators. In order to the analysis of connected networks becomes simpler, each network has been reduces to a multiphase equivalent circuit in which only terminals at the connection points are retained and all other terminals are eliminated. Such a situation exists when generators are connected to a transmission system. Only terminals

connected to generators are retained, making all the rest of terminals concealed. It means that the network can be reduce to the retained terminals only.

In real power system, there are many generators which are connected together via the power lines to become complicated model for stability analysis problems. With the typical long shape of countries, the power transfer capacity and the synchronization between two sources through long lines took more attentions. Studies are routinely conducted to ensure that generators will operate properly in the event of probable faults or changes in system conditions. When dealing with a large power system, it is not practical to present every component in full detail. The electromechanical oscillation frequency between synchronous generators in a power system typical lies between 0.5 and 3 Hz. Electromechanical oscillations are those associated with the tendency for the generators to remain in synchronism when interconnected.

In the proposed work, a four-bus system is considered as shown in Fig.4.9. The system consists of two generator buses and two loads buses. The synchronous generators used for the study are modeled with standard IEEE type 1 excitation system.

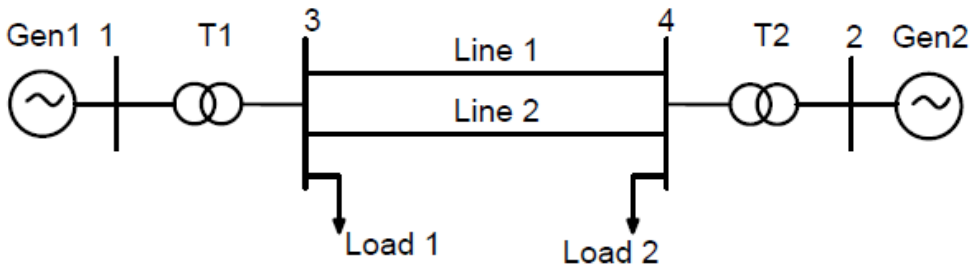

Fig. 4.9. Simulation system

In the content of this work, the test system model includes two synchronous generators connected via two step-up transformers, long transmission line. Fig.4.10 shows the equivalent circuit of two-bus system with generators, transformer and loads at each bus. Node 0 is the reference node (neutral). Node 1, 2 are the internal machine buses, or the buses to which the voltages behind transient reactance are applied. Passive impedances connect the various nodes and connect the nodes to the reference nodes. The initial values $E'_1\angle\delta_1$, $E'_2\angle\delta_2$ are determined from the pre-transient conditions [Appendix (A.1)].

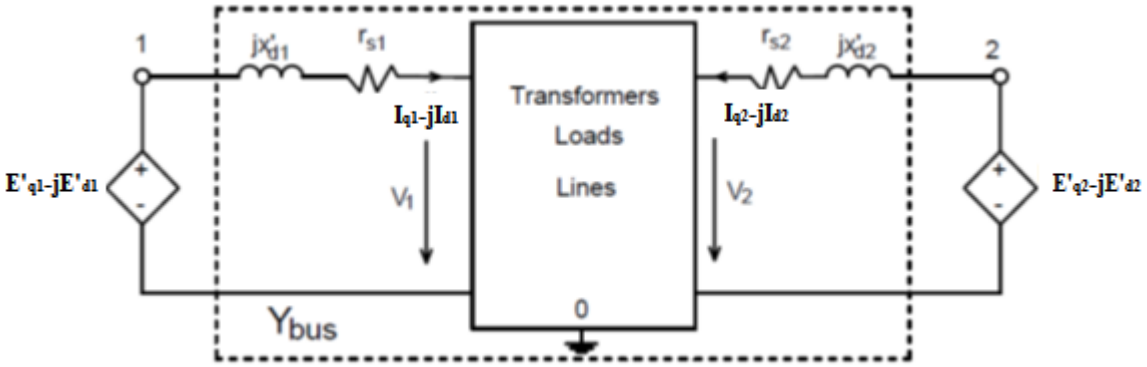

Fig.4.10 Equivalent circuit of system model

To arrive at the network model of power system, it is sufficiently accurate to represent a long line by a nominal-π model (equivalent-π model). For systematic analysis, it is convenient to regard loads as load impedance and lump together transformer and line impedances at the buses.

The simplification can be made in the two-axis model x_d' and x_q' with neglecting transient saliency in the synchronous machines x_d'= x_q'.

The stator equations of the generator model, which are a set of dynamic equations, are to be interfaced with the static equations of the network. However, when the time derivative terms of the stator qd flux linkages are dropped from the stator voltage equations, the resulting stator voltage equations will become algebraic. Algebraic loops will be formed if these algebraic stator equations and those of the static network representation are to be solved separately. To avoid algebraic loops, it is desirable to combine them. With one machine and a simple radial line, it can easily incorporate the network equations into the stator qd equations. However, for a system with more than one machine or where the dimension of the network equations are large, the stator voltage equations are best incorporated into those of the network. To incorporate these stator voltage equations into those of the network equations, which are in terms of qd variables in the machine's own rotor reference frame, expressed in the synchronously rotating reference frame.

The stator equation is given by:

$$v_{qi} - jv_{di} = -(r_{si} + jx'_{di})(i_{qi} - ji_{di}) + e^{j\delta_i}(e'_{qi} - je'_{di}) \qquad (4.101)$$

These simplified stator voltage equation in phasor form can be modeled by a Thevenin's equivalent, whose fixed impedance of $(r_{si} + jx'_{di})$ can now be easily added to the Z_{bus} or Y_{bus} of network. To use the Thevenin's equivalent, the value of the internal voltage E'_i is to be obtained from the simulation of the rotor's field winding equation. When the transient impedances of the machines are incorporated in the network admittance matrix,

the injected current I_i, can be determined by multiplying the resultant admittance matrix with the vector of internal voltages. The value of $I_i = I_{qi} - jI_{di}$ is then transformed to obtain $i_{qi} - ji_{di}$ that is needed for the rest of the machine simulation, including that of the terminal bus voltage of the machine.

The Simulink model for the two-machine power system (four buses) is developed as shown in Fig 4.11. The stator qd currents in the synchronously rotating reference frame injected by the machine into the network are used as input. Among its outputs are the internal transient voltage E'_q and E'_d of the machine in the synchronously rotating reference frame. The Fig.4.13 shows the excitation system block schematic for IEEE type 1 excitation system used. The parameters of the generators are also expressed in the common system base. In the simulation, the parameters of the generators in the 'generator' block as shown in the generator schematic (Fig.4.12) remain in their own respective bases. As such, their currents must be scaled by the ratio of the system to generator base VA, which is equivalent to the ratio of system base current to generator base current when the base voltages of the system and generator per unit system are the same at the generator buses. In addition to the scaling of the generator current, to account for the difference in per unit system between the generator and network, the stator transient impedance must also be appropriately scaled when it is incorporated into the network admittance matrix. The stator and rotor equations are in implemented in Fig.4.14 and Fig.4.15.

The seven state variables assumed are q and d axes voltage, rotor angle, three variables from excitation system which are exciter voltage and rotor slip, stabilizer voltage and regulator voltage each generator.

x=[$E'_q(1)$; $E'_d(1)$; $\delta o(1)$; $E'_q(2)$; $E'_d(2)$; $\delta o(2)$; $E_f(1)$; slip(1); $V_S(1)$; $V_R(1)$; $E_f(2)$; slip(2); $V_S(2)$; $V_R(2)$]

The input variables considered for developing linear system are field voltage, mechanical torque for generator buses, dq axes current for load buses.

u = [$E_{fo}(1)$; $T_{mech}(1)$; $E_{fo}(2)$; $T_{mech}(2)$; i_{qe3}; i_{de3}; i_{qe4}; i_{de4}]

The output variables are terminal voltage, real power and reactive power generation for each generator buses.

y =[$V_{to}(1)$; $P_{emo}(1)$; $Q_{emo}(1)$; $V_{to}(2)$; $P_{emo}(2)$; $Q_{emo}(2)$]

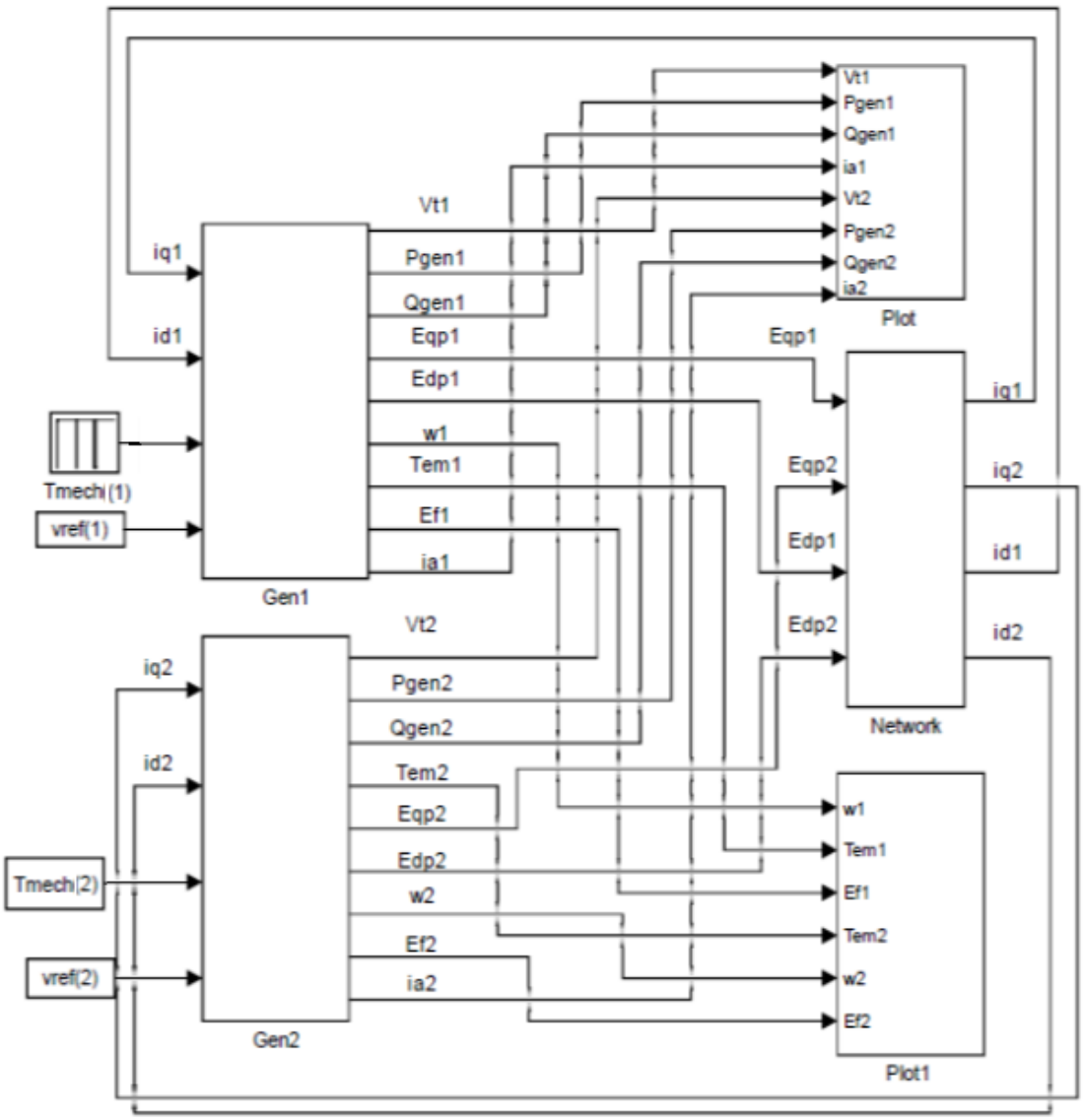

Fig. 4.11. Two-machine power system-simulation schematic

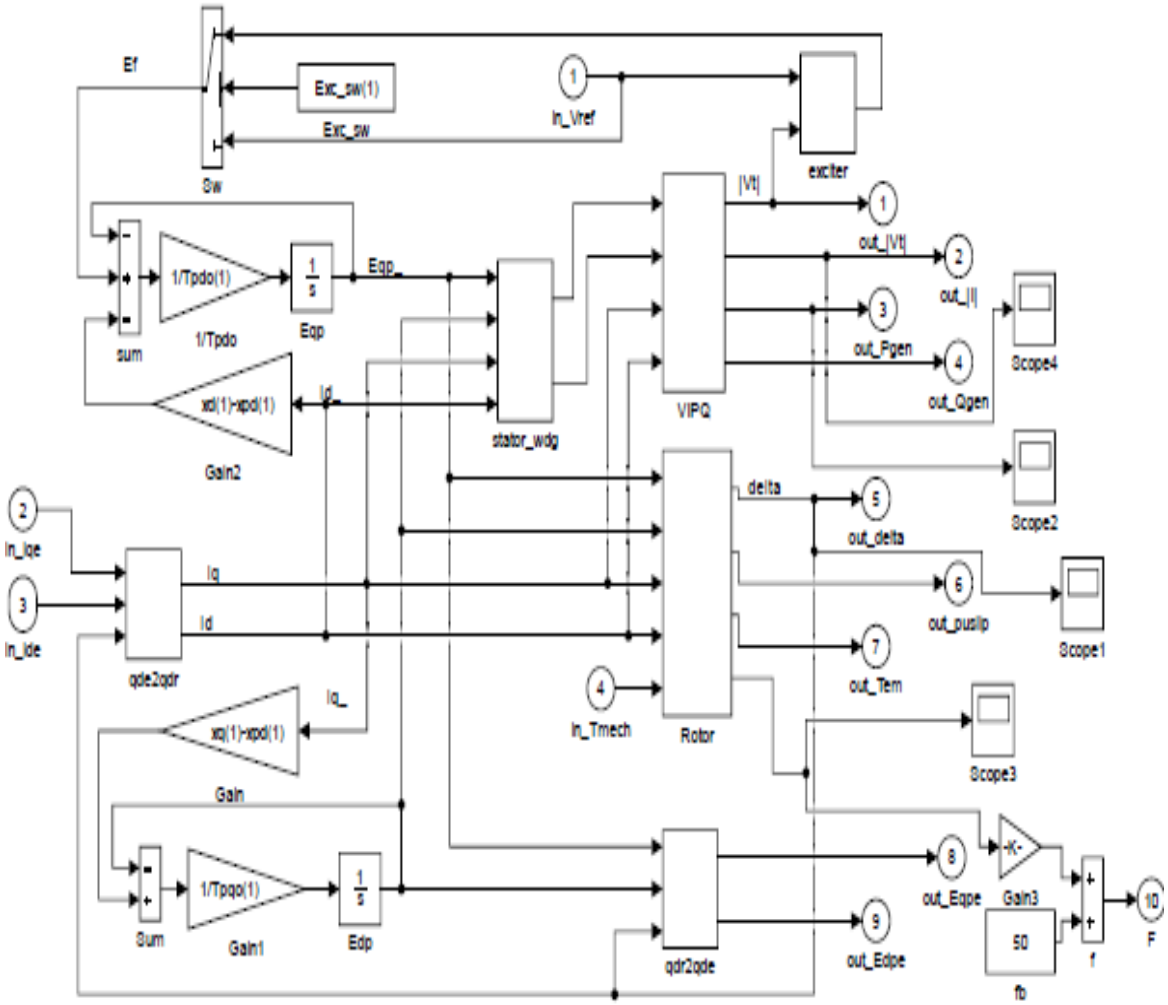

Fig. 4.12. Synchronous generator schematic

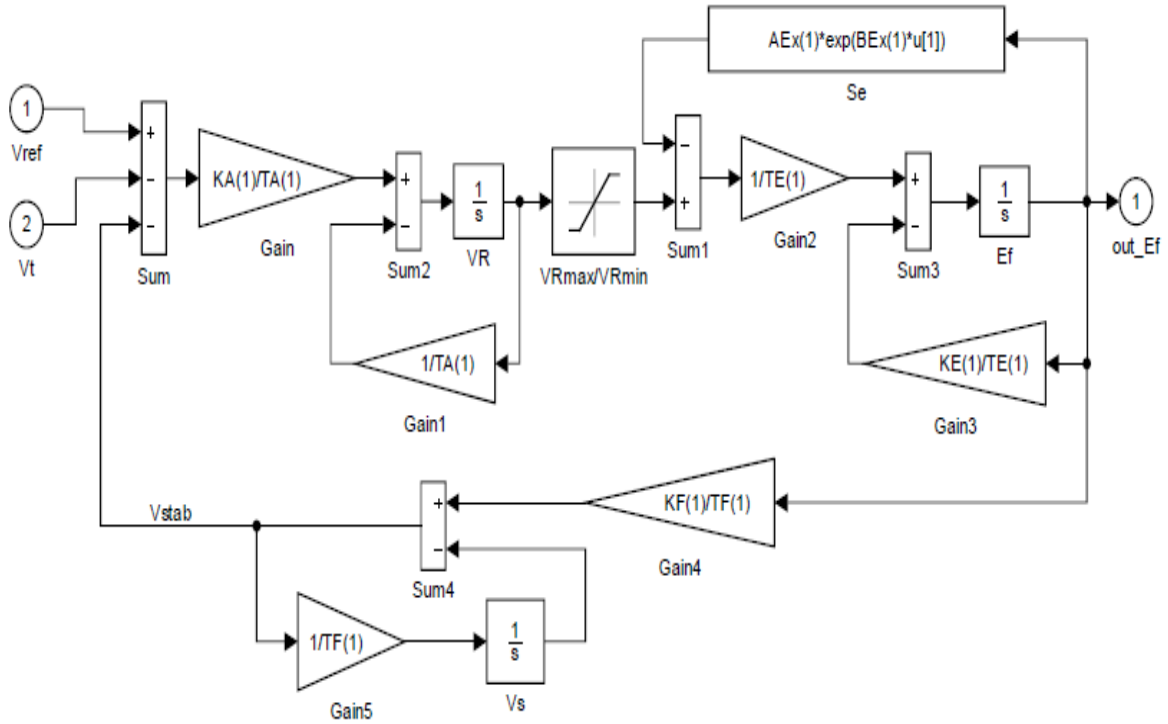

Fig. 4.13. Schematic of IEEE Type I exciter system

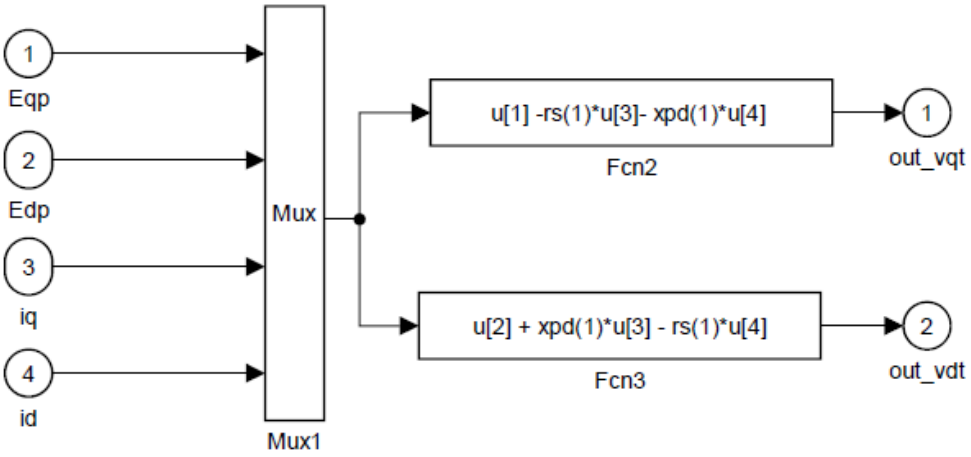

Fig. 4.14. Schematic of stator winding block

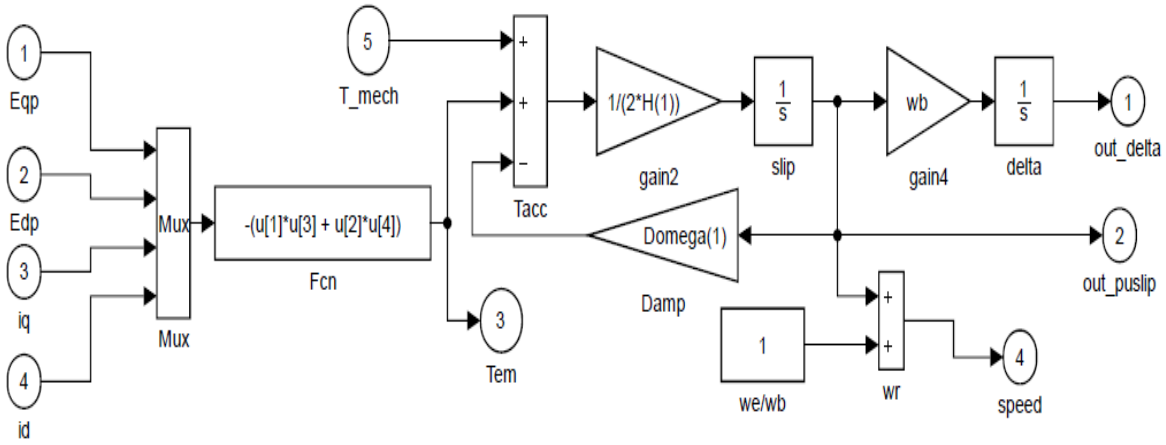

Fig. 4.15. Schematic of rotor winding block

As shown in Fig.4.11, the synchronous generator model gets the values for the mechanical torque T_{mech}, as physical input signals. From these input values, the model can calculated the electrical output torque T_{em}, the terminal voltage, the armature winding current, generated real and reactive powers P_{gen}, Q_{gen}, rotor angle.

The mathematical equations used to develop the Simulink model of two-machine system are described below.

The machine-network transformation gives:

$$\begin{bmatrix} E'_1 \\ E'_2 \end{bmatrix} = \begin{bmatrix} E'_{q1} - jE'_{d1} \\ E'_{q2} - jE'_{d2} \end{bmatrix} = \begin{bmatrix} e'_{q1} - je'_{d1} \\ e'_{q2} - je'_{d2} \end{bmatrix} \begin{bmatrix} e^{j\delta_1} \\ e^{j\delta_2} \end{bmatrix} \tag{4.102}$$

$$\begin{bmatrix} I_1 \\ I_2 \end{bmatrix} = \begin{bmatrix} I_{q1} - jI_{d1} \\ I_{q2} - jI_{d2} \end{bmatrix} = \begin{bmatrix} i_{q1} - ji_{d1} \\ i_{q2} - ji_{d2} \end{bmatrix} \begin{bmatrix} e^{j\delta_1} \\ e^{j\delta_2} \end{bmatrix} \tag{4.103}$$

To prepare the system data for a stability study, the following preliminary calculations are made:

1. The system data are converted to a common system base. The procedure to perform this transformation has been described above.
2. The load data from the prefault, power flow are converted to equivalent impedances or admittances. The necessary information for this step is obtained from the result of the power flow. If a certain load bus has a voltage solution V_{Li} and complex power demand $S_{Li}=P_{Li}+jQ_{Li}$, then using $S_{Li}=V_{Li}I^{*}_{Li}$.

$$Y_{Li} = \frac{I_{Li}}{V_{Li}} = \frac{S^{*}_{Li}}{|V_{Li}|^2} = \frac{P_{Li} - jQ_{Li}}{|V_{Li}|^2} \tag{4.104}$$

   where $Y_{Li}=g_{Li}+jb_{Li}$ is the equivalent shunt load admittance.
3. The internal voltages of the generators are calculated from the power flow data using the pre-disturbance terminal voltages $V_i\angle\theta_i$. The stator algebraic equation is simplified as:

$$\begin{bmatrix} E'_{q1} - jE'_{d1} \\ E'_{q2} - jE'_{d2} \end{bmatrix} = \begin{bmatrix} V_1\angle\theta_1 \\ V_2\angle\theta_2 \end{bmatrix} + \begin{bmatrix} r_{s1} + jx'_{d1} \\ r_{s2} + jx'_{d2} \end{bmatrix} \begin{bmatrix} I_{q1} - jI_{d1} \\ I_{q2} - jI_{d2} \end{bmatrix} \tag{4.105}$$

4. The Y_{bus} matrices for the prefault, faulted, and postfault network conditions are calculated.
5. In the final step eliminating all the nodes except the internal generator nodes using Kron reduction [Appendix (A.3)]. The system Y_{bus} for each network condition provides the following relation between the voltage and currents:

$$I = Y_{bus}V \tag{4.106}$$

   Where the current vector I is given by the injected currents at each bus. In the classical model considered, injected currents exist only at the internal generator buses. All other currents are zero. As a result, the injected current vector has the form:

$$I = \begin{bmatrix} I_1 \\ I_2 \\ \cdots \\ 0 \end{bmatrix} \tag{4.107}$$

Partition the matrices Y_{bus} and V appropriately to obtain:

$$\begin{bmatrix} I_1 \\ I_2 \\ \cdots \\ 0 \end{bmatrix} = \begin{bmatrix} Y_{11} & Y_{12} \\ Y_{21} & Y_{22} \\ \cdots & \cdots \\ Y_{r1} & Y_{r2} \end{bmatrix} \begin{bmatrix} E'_1 \\ E'_2 \\ \cdots \\ V_r \end{bmatrix} \tag{4.108}$$

The subscript r is used for all remaining nodes and n is used to denote the internal generator nodes. The voltage at the internal generator nodes are given by the internal emf's E'_i. Expanding (4.108):

$$I_n = Y_{nn}E'_n + Y_{nr}V_r \tag{4.109}$$

$$0 = Y_{rn}E'_n + Y_{rr}V_r \quad (4.110)$$

Eliminating V_r to determine I_n:

$$I_n = (Y_{nn} - Y_{nr}Y_{rr}^{-1}Y_{rn})E'_n = Y_{red}E'_n \quad (4.111)$$

The matrix Y_{red} is the desired reduced admittance matrix. It has dimensions (n x n), where n is the number of the generators. In this work, n=2. The reduced admittance matrix provides a complete description of all the injected currents in terms of the internal generator bus voltages.

In the other cases, some load buses can be keep in the admittance matrix to inject fault current to system.

Chapter 5

Simulation and Results

5.1 Three Phase Synchronous Generator Steady-State Model

In this section, the dynamic model of a single generator is investigated as the simple reference for stability analysis before coming to the more complicated power system.

The parameter of single three phase synchronous generator model in steady-state condition are shown in Tab. 5.1. These are one of the machines which is used for modelling the Vietnamese 500kV transmission system in [**PI**] (Generator A) and one machine used in Radlická metro in Prague (Generator B). It is easy to compare to the results of the real measurement machine and verify the mathematical model of the proposed machine used in the test system.

The suitable initial values of flux linkages, speed and oscillator were adjusted to avoid transient and starting conditions in simulation. Voltages v_a, v_b and v_c are applied to stator wingdings are three balanced phases which are:

$$v_a = V_m \sin(\omega_r t) \tag{5.1}$$

$$v_b = V_m \sin\left(\omega_r t - \frac{2\pi}{3}\right) \tag{5.2}$$

$$v_c = V_m \sin\left(\omega_r t + \frac{2\pi}{3}\right) \tag{5.3}$$

In this case, the operation conditions are similar to conditions in which the generator is connected directly to infinite network given in Fig.5.1.

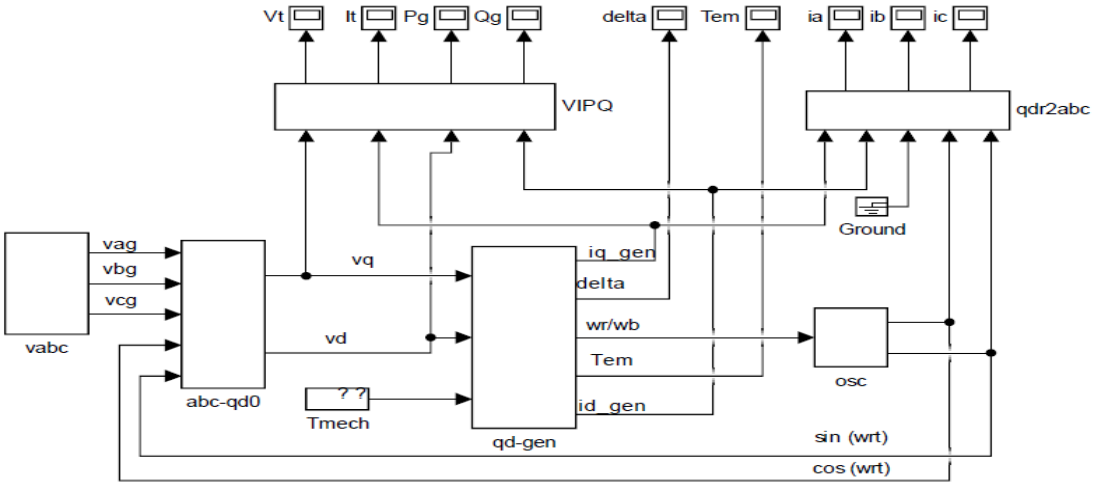

Fig.5.1 Three phase synchronous generator model

The simulation programme has been implemented in MATLAB/SIMULINK 2016a version by change of small disturbance into machines. The dynamics of the stator current may be neglected in the small signal stability analysis by setting the differentials of the stator currents equal to zero in [53].

The initial condition calculations have been performed by the writing script (one_machine.m files) in Appendix (C.1).

Tab.5.1. The parameters of the proposed generator and real measurement generator

			Generator used in modelling the Vietnamese 500kV transmission system in [PI] (Generator A)			**BEZ Gen.type FB 443 /34_6 Metro Prague (Generator B)**		
			Variant A			**Variant B for comparation with real measurement**		
Parameter	**Dem. technic.**	**SI**	**Technic.**	**SI units**	**Per units**	**Technic.**	**SI units**	**Per units**
Nominal S	kVA	VA	353000	$3.53x10^8$	1	1900	$1.90 x10^6$	1
cosφ	-	-	0.85	0.85		0.8	0.8	
$U_{between\ phase}$	kV	V	15.75	$1.58 x10^4$	1	6.3	$6.30 x10^3$	1
$U_{phase\ .midle}$	kV	V	9.09	$9.09 x10^3$	1	3.64	$3.64 x10^3$	1
I_{phase}	A	A	12939.977	$1.29 x10^4$	1	174	$1.74 x10^2$	1
f	Hz	Hz	50	50	1	50	50	1
Rotor speed	rpm	rpm	3000	3000		1000	1000	
Poles			2	2		6	6	
$Z_{nominal}$	Ω	Ω	0.7027	0.703	1	20.90	20.9	1
r_s	Ω	Ω	0.0032	$3.16 x10^{-3}$	0.0045	0.18	0.175	0.0084
x_{ls}	Ω	Ω	0.1047	0.105	0.149	3.97	3.97	0.19
X_d	Ω	Ω	1.4125	1.41	2.01	30.52	30.5	1.46
X_q	Ω	Ω	1.3773	1.38	1.96	18.81	18.8	0.9
X'_d	Ω	Ω	0.1785	0.178	0.254	5.23	5.22	0.25
X'_q	Ω	Ω	0.3092	0.309	0.44	4.39	4.39	0.21
X''_d	Ω	Ω	0.1462	0.146	0.208	3.55	3.55	0.17
X''_q	Ω	Ω	0.1462	0.146	0.208	2.51	2.51	0.12
T'_{d0}	s	s	8.43	8.43		2.5	2.5	
T'_{q0}	s	s	0.94	0.94		0.44	0.44	
T''_{d0}	s	s	0.043	0.043		0.045	0.045	
T''_{q0}	s	s	0.075	0.075		0.029	0.029	
J	kgm^2	kgm^2	14300	14300		693.74	693.74	

Tab. 5.2. Excitation system parameters of the proposed generator

Parameter	Value in SI unit
T_A	0.067 s
K_A	50
T_E	0.058 s
K_E	-0.0465
K_F	0.0832
T_F	1.1234 s
V_{Rmax}	15.75×10^3 V
V_{Rmin}	-15.75×10^3 V
A_{ex}	0.0012
B_{ex}	1.264

The simulation 1 is implemented when the field voltage of generator at the initial voltage in the beginning of simulation, then increasing more 0.3 pu at time 1.5 seconds and continues increase more 0.3 pu at 3 seconds, it keeps at this value until simulation end. The mechanical torque of generators implemented during simulation is constant at the initial values. The results of simulation 1 are given in Fig.5.2 and Fig.5.3 below.

Generator A- 353 MVA used in modelling the Vietnamese 500kV transmission system in [PI]	Generator B- 1.9 MVA BEZ Generator, type FB 443 /34_6 Metro Prague
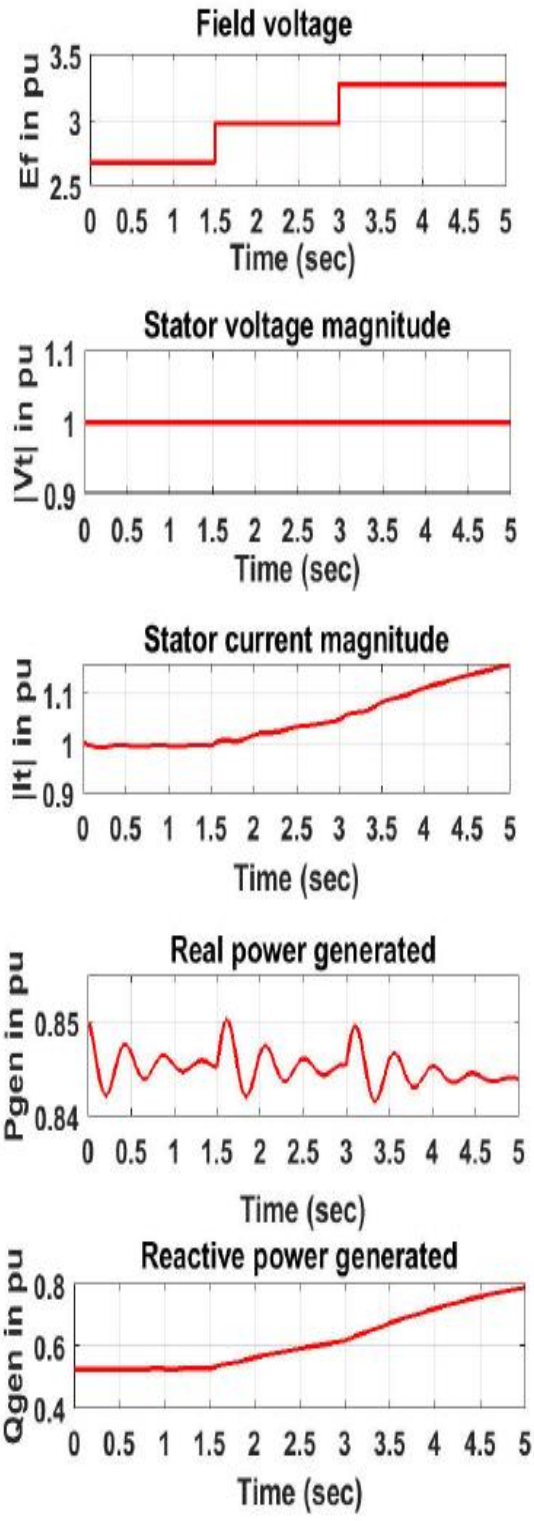	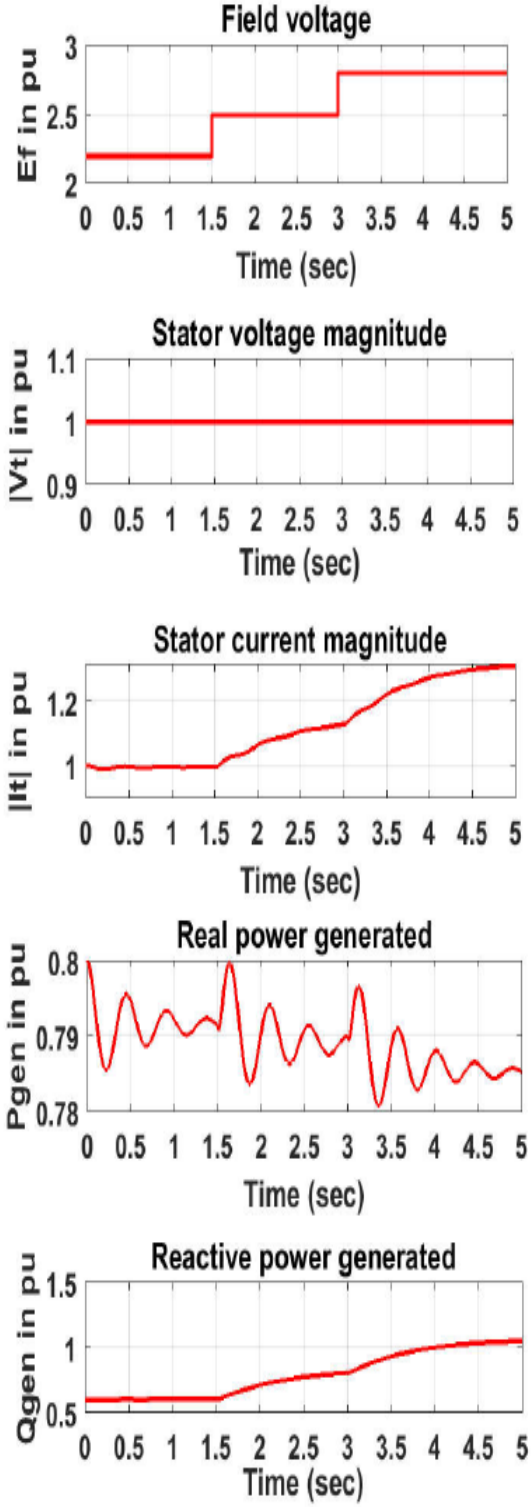

Fig.5.2 Performance of generator with variation of the excitation voltage (excitation voltage, terminal voltage, terminal current, real power, reactive power)

Generator A- 353 MVA used in modelling the Vietnamese 500kV transmission system in [PI]	Generator B- 1.9 MVA BEZ Generator, type FB 443 /34_6 Metro Prague

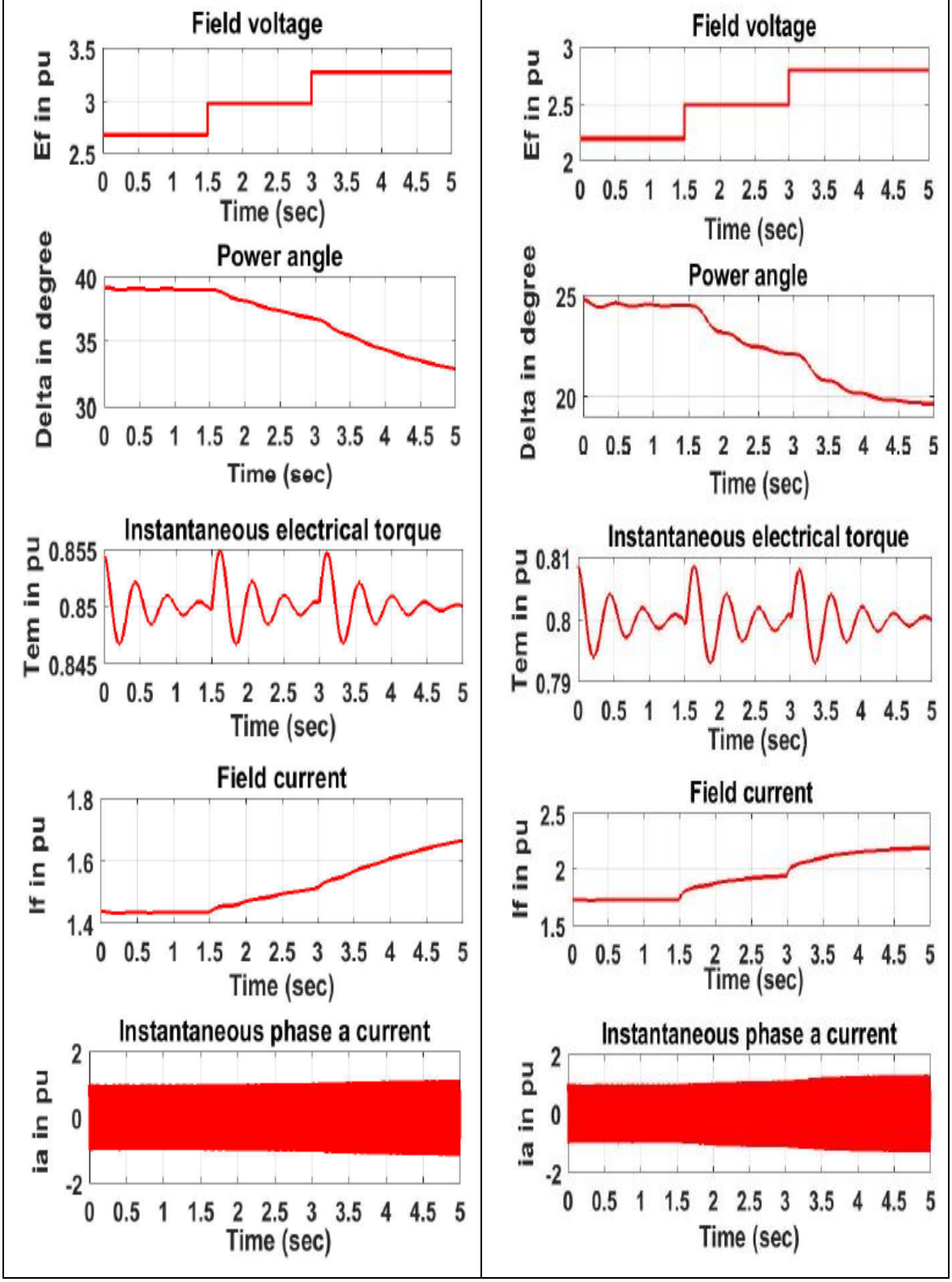

Fig.5.3 Performance of generator with variation of the excitation voltage (excitation voltage, power angle, electrical torque, field current, phase a current)

The results in simulation 1 illustrated that when changing the field voltage, the active generating power of Generator A oscillated significantly at 2.5 Hz and about 2 seconds it came back the original stable state at each increase of field voltage, this results were proved and analyzed in **[PV] [PVI].** However, the active generating power of Generator B oscillates at larger amplitudes and in the same frequency 2.5 Hz given in the Fig.5.2**.** That also happened similarly to electrical torques in the Fig.5.3. In meanwhile, the rotor angles of generators tended to reduce to maximal 4 degree with Generator A and 3 degree with Generator B after each changes of the field voltages. In the other hand, the field current rises to 0.3 pu with Generator A and 0.25 pu with Generator B. And, the currents of phase a of generator in simulation 1 oscillated gradually in the Fig.5.3.

The simulation 2 is implemented when the mechanical torque of generator at the initial torque in the beginning of simulation, then increasing more 0.1 pu at time 0.5 seconds continues increase more 0.1 pu at 2 seconds, it keeps at this value until simulation end. The field voltage of generator implemented during simulation is constant at the initial values. The results of simulation 2 are given in Fig.5.4 and Fig.5.5 below.

Generator A- 353 MVA used in modelling the Vietnamese 500kV transmission system in [PI]	Generator B- 1.9 MVA BEZ Generator, type FB 443 /34_6 Metro Prague
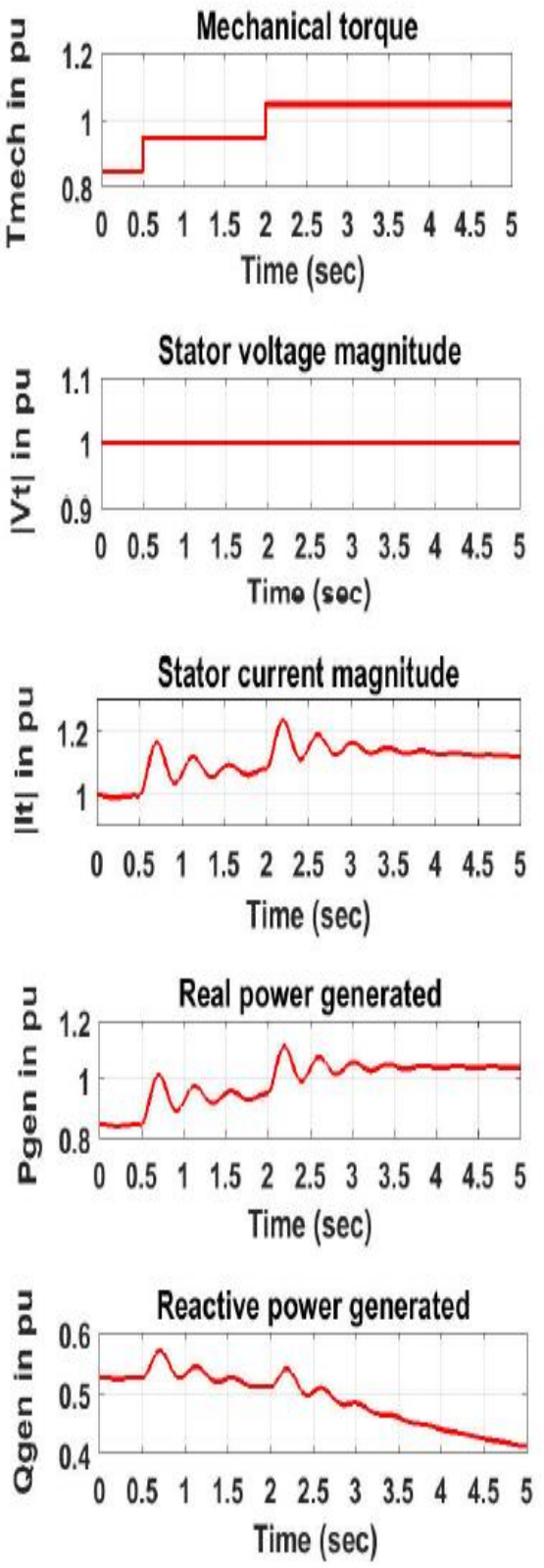	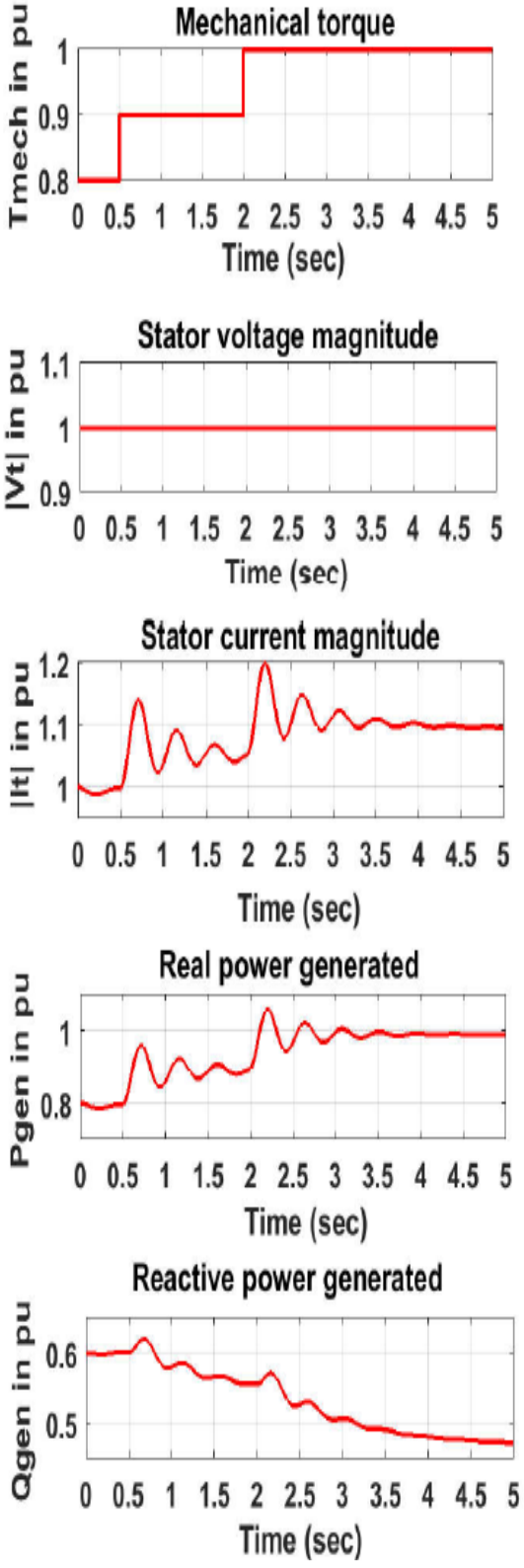

Fig.5.4 Performance of generator with variation of the mechanical torque (mechanical torque, terminal voltage, terminal current, real power, reactive power)

Generator A- 353 MVA used in modelling the Vietnamese 500kV transmission system in [PI]	Generator B- 1.9 MVA BEZ Generator, type FB 443 /34_6 Metro Prague
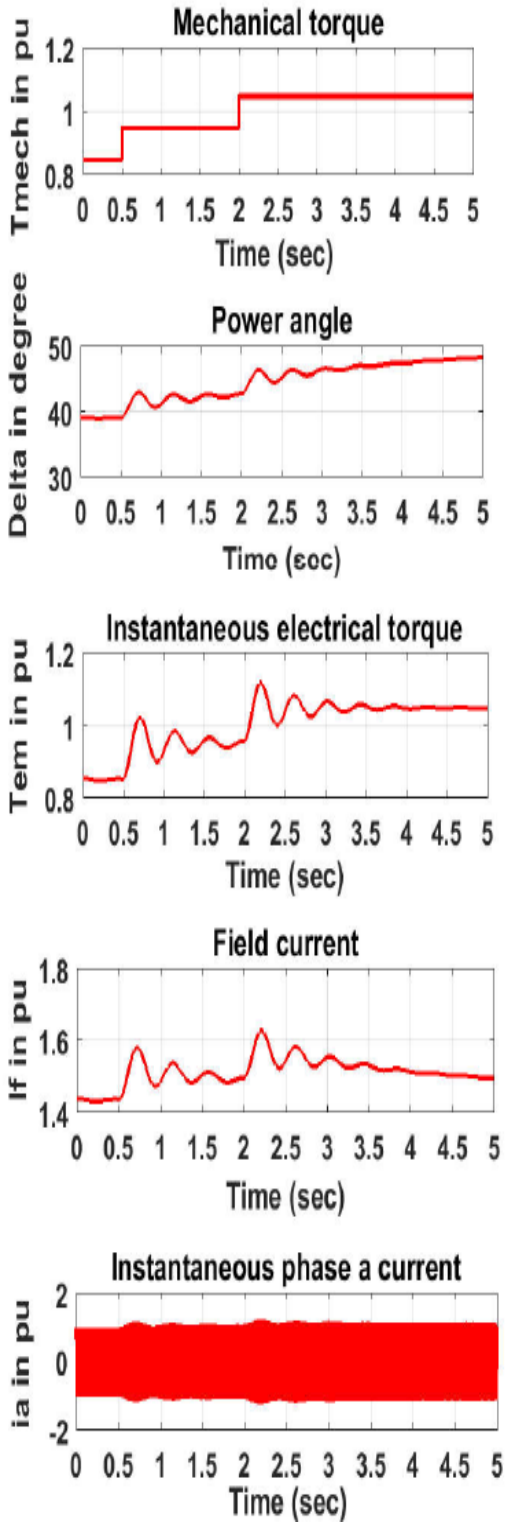	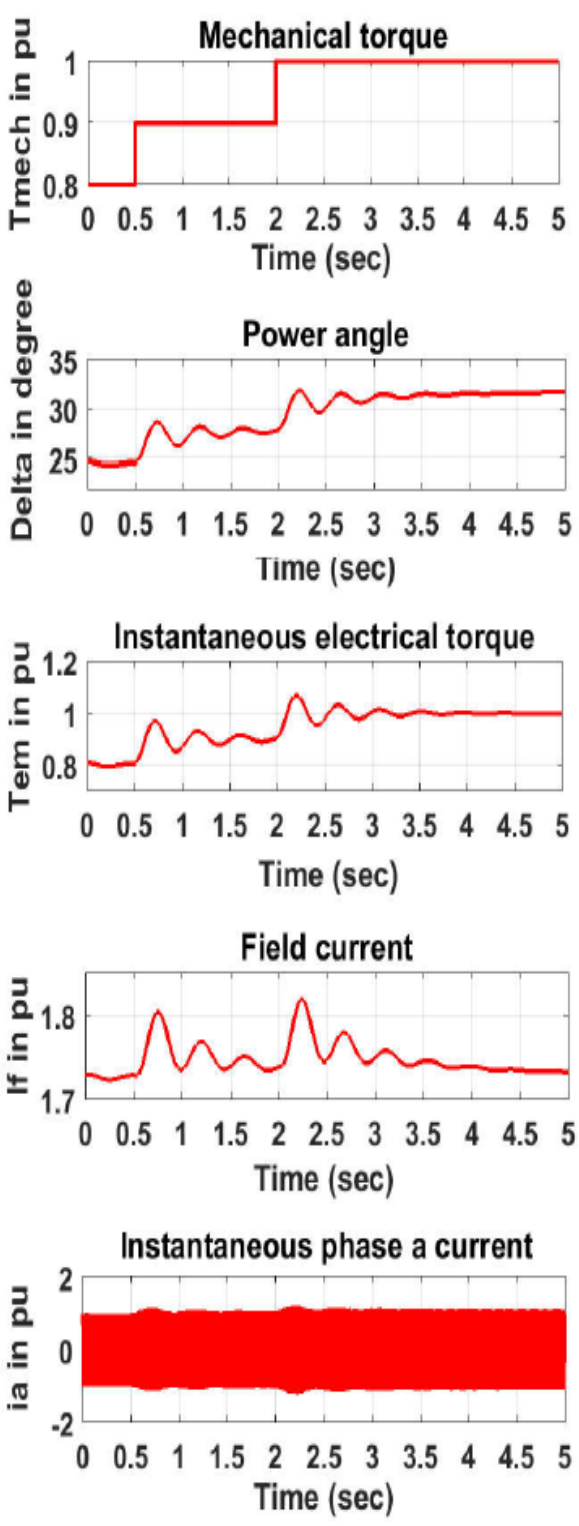

Fig.5.5 Performance of generator with variation of the mechanical torque (mechanical torque, power angle, electrical torque, field current, phase a current)

The results in simulation 2 showed out the performance of generators when changing the mechanical torque, the active generating power of Generator A oscillates significantly in 2.5 Hz and about 1.5 seconds it came back the original stable state after each increase of the mechanical torque, but the active generating power of Generator B oscillates at the smaller amplitudes given in the Fig.5.4. That also happens similarly to electrical torque in the Fig.5.5. Obviously, the rotor angles of the generators tends to increase to maximal 3 degree after each change of the mechanical torques. In the same time, the field current rise to 0.16 pu with Generator A and 0.8 pu with Generator B. Finally, the currents of phase a of generators in simulation 2 oscillated significantly given in the Fig.5.5.

Implement to compare modeling results of two machines between one generator used in modelling the Vietnamese 500kV transmission system in **[PI]** (Generator A) and one generator used in Radlicka metro in Prague with real measurement (Generator B), it can be seen that the modeling results of two machines are similar. Therefore, parameters and modeling method of the generator used in modelling the Vietnamese 500kV transmission system in **[PI]** are reliable and verified. This machine can apply in the proposed system in next sections.

The previous discussion of transient behaviour of synchronous machines is based on a single machine connected to a good approximation of an infinite bus. An example is the typical industrial situation where a synchronous motor of at most a few thousand horsepower is connected to a utility company system with a capacity of thousands of megawatts. Under these conditions, we can safely neglect the effect of the machine on the power system.

A system consisting of only two machines of comparable size connected through a transmission link, however, becomes more complicated because the two machines can affect each other's performance. The medium through which this occurs is the air-gap flux. This is a function of machine terminal voltage, which is affected by the characteristics of the transmission system, the amount of power being transmitted, the power factor, etc.

In the steady state, the rotor angles of the two machines are determined by the simultaneous solution of their respective torque equations. Under a transient disturbance, as in the single-machine system, the rotor angles move toward values corresponding to the changed system conditions. Even if these new values are within the steady-state stability limits of the system, an overshoot can result in loss of synchronism. If the system can recover from the disturbance, both rotors will undergo a damped oscillation and ultimately settle to their new steady-state values.

An important concept here is synchronizing power. The higher the real power transfer capability over the transmission link between the two machines, the more likely they are to remain in synchronism in the face of a transient disturbance. Synchronous machines separated by sufficiently low impedance behave as one composite machine, since they tend to remain in step with one another regardless of external disturbances.

The modelling of two generators connected via long line is going to implement in the next section. In order to demonstrate the importance of accurate modeling, small and large signal stability analyses of time domain simulation are used. Before implement modeling two-generator system connected through long line, the proposed system will be taken to calculate the load-ability of line followed the length (L) increase.

5.2 Load capacity limit of lines

Assumed that all the generators, transformers, lines and loads at two generator sides are the same respectively. Further, the mutual admittance between lines is assumed to be zero. The long lines are replaced as a matrix [A B; C D].

The equivalent of two-machine Simulink model is illustrated in Fig.5.6.

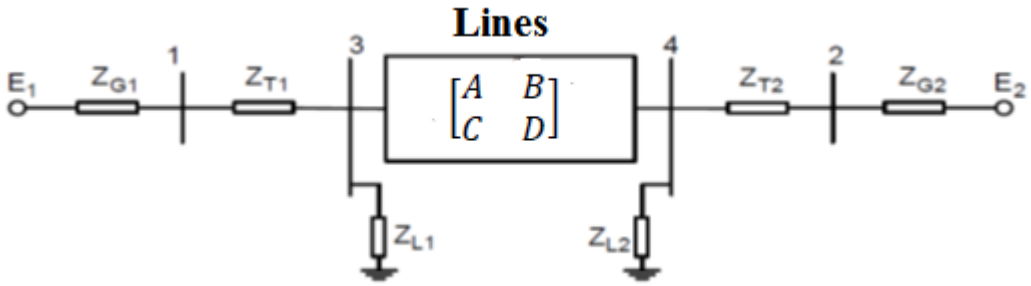

Fig. 5.6. Equivalent simulation network

Parameters of generators, transformer and transmission lines are given from Tab.5.3-Tab.5.4.

Under the steady state condition, the generators deliver 0.85 pu power to the buses of voltage magnitude at 1 pu and the length of lines at 250 km. The rotor rotates at the synchronous speed.

The initial condition calculations have been performed by the MATLAB writing script (Two_machine.m file) in Appendix (C.2).

The parameters of the two-machine test system are given in Tab.5.1-5.4.

Tab. 5.3. Transformers and loads parameters

Parameter		Value in SI unit	Primary side (15.75×10^3 V)	Secondary side (230×10^3 V)	Per units (pu) to secondary side
Base power	Power	VA	353×10^6	1000×10^6	1
Transformer (T_1, T_2)	Power	VA	350×10^6		0.35
	Voltage	V	15.75×10^3	230×10^3	1
	Impedance	Ω	(0.001+j0.068)	(0.29+j14.5)	0.0055+j0.2741
Load1	Power	VA	-	$(199+j149.2) \times 10^6$	0.199+j0.1492
Load2	Power	VA	-	$(399+j299.2) \times 10^6$	0.399+j0.2992

Tab. 5.4. Lines parameters

Parameter	Symbols	SI	SI units
Resistance	R_0	Ω/m	0.045×10^{-3}
Inductance	L_0	H/m	1.401×10^{-6}
Conductance	G_0	S/m	22.22×10^3
Capacitance	C_0	F/m	0.012×10^{-9}
Velocity	v	m/s	$\approx 2.44 \times 10^8$
Characteristic impedance	Z_c	Ω	≈350
Wavelength	λ	m	488×10^4
A quarter of wavelength	λ/4	m	122×10^4

Power lines from bus 3 to bus 4 in system are limited in their ability to deliver power. The two most important limits can be thermal effect and stability. With limitations on maximum current and voltage, there is a corresponding limitation on the active power that can safely be transmitted [46]. For the long transmission lines, the stability limit should be considered. Assumed that the voltage magnitudes are equal at each end of line ($|V_3| = |V_4| = 1\ pu$). And the length of lines are 250 km.

The parameters of line:

$$V_3 = |V_3|\angle\theta_3;\ V_4 = |V_4|\angle\theta_4;\ \theta = \theta_3 - \theta_4; \tag{5.4}$$

$$A = D = cosh\gamma L\ = |A|\angle a;\ B = Z_c sinh\gamma L|B|\angle b; \tag{5.5}$$

$$P_{SIL} = \frac{|V_3|^2}{Z_c} \tag{5.6}$$

The active power is able to transmit from bus 3 to bus 4 [45]:

$$P_{34} = \frac{|D|}{|B|}|V_3|^2 \cos(b-a) - \frac{|V_3||V_4|}{|B|}\cos(b+\theta) \quad (5.7)$$

From (5.4)- (5.6) substituted into (5.7), the load-ability of line 34 yields:

$$P_{34} = P_{SIL}\left[\frac{\cos(b-a)}{tanh\gamma L} - \frac{\cos(b+\theta)}{sinh\gamma L}\right] \quad (5.8)$$

From (5.7), it can be seen that for fixed $\theta = 5.5\ degree$, as the length is increased, γL increases and P_{34} decreases.

Under the values of system are calculated in the initial condition, the stability limit of line 34 is shown in Fig. 5.7.

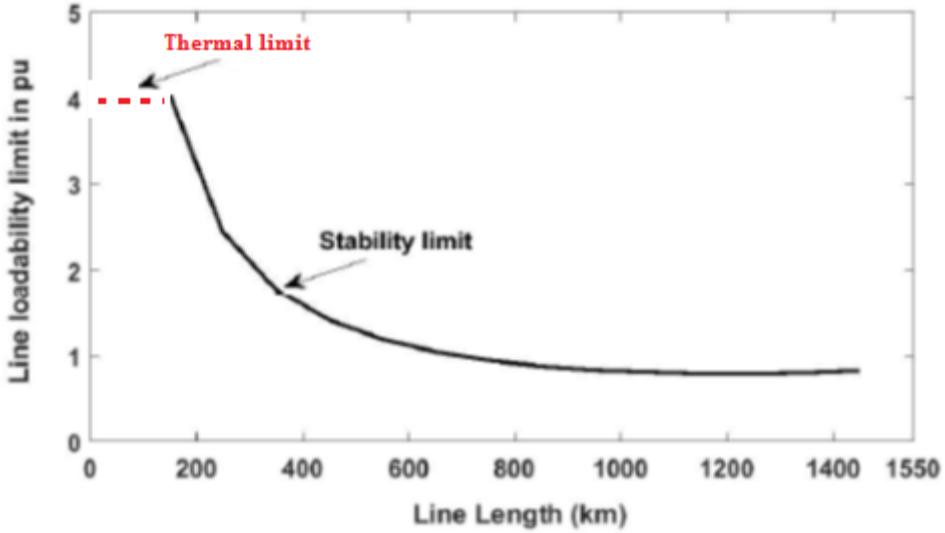

Fig. 5.7. The stability limit of line 34 in the proposed system.

5.3 Synchronization of two three Phase Synchronous Generators in a small disturbance.

This section implements modelling the synchronization of two synchronous generator connected via parallel long lines in a small disturbance condition.

The small disturbance is applied to the generator's mechanical torques that excite the different modes of oscillation, and examine the resulting responses of the generator frequencies. The parameters of the test system are given from Tab.5.1-5.4.

The initial condition calculations have been performed by the MATLAB writing script (Two_machine.m file) in Appendix (C.2). A MATLAB Two_machine.m file is created to initialize the MATLAB workspace with the system parameters and to determine the linear model of the system and its eigenvalues at some desired operating condition.

The network is represented by help of the admittance matrix. Simulation file receives parameters from Two_machine.m files and then simulates the system.

The simulation is implemented when increasing in mechanical torque at generator 1 on the generator base. The field voltages are changed by the excitation systems.

The simulated results of the oscillations in the terminal voltage, terminal current, active and reactive power, rotor angle and speed of each generator obtained in Fig.5.8-Fig.5.10 by changing transmission distances [250; 700; 1200] km in case [1; 2; 3] respectively.

-Case 1: L=250 km

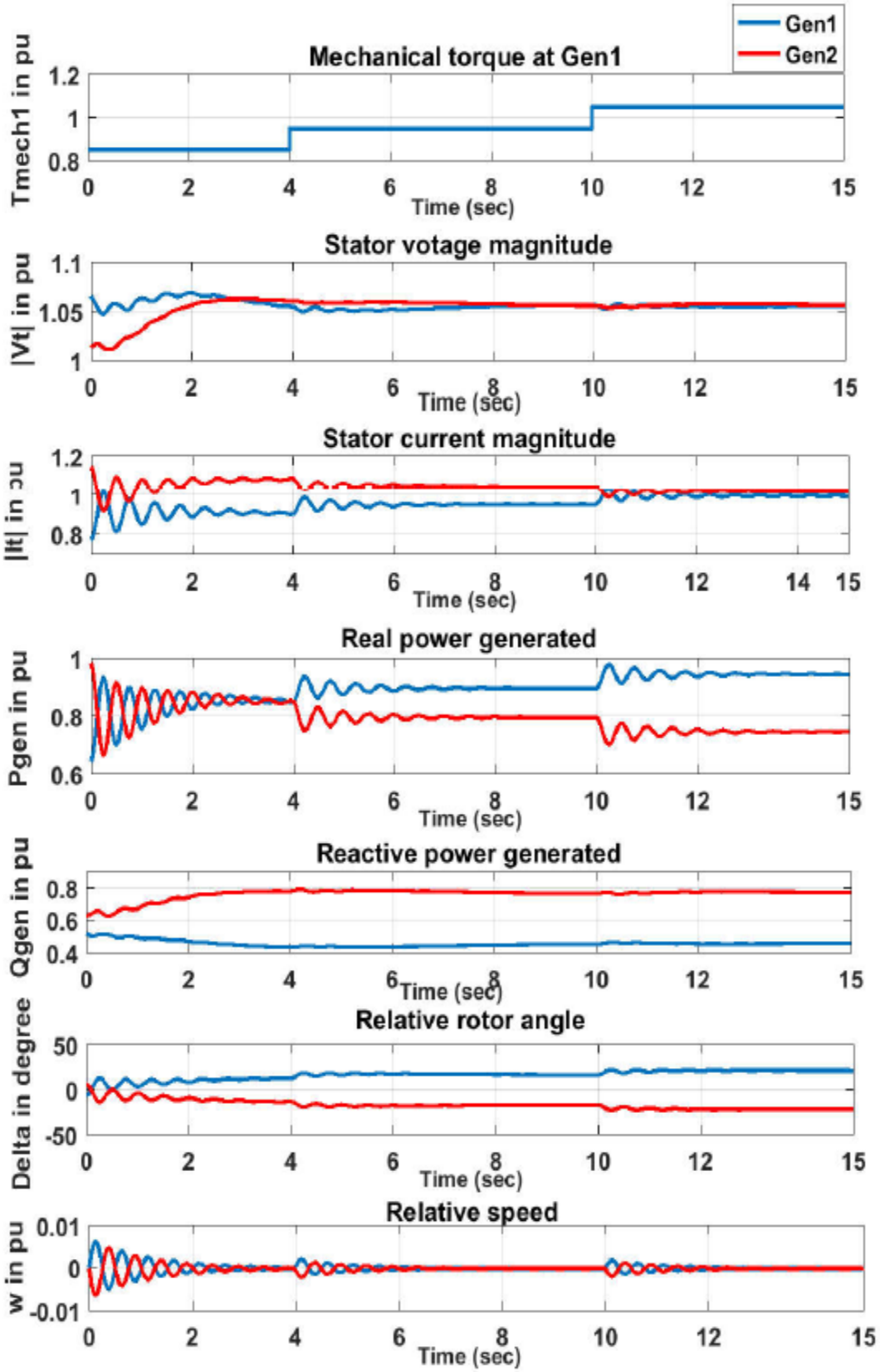

Fig.5.8 Performance of system with variation of the mechanical torque at generator 1 at length 250 km (mechanical torque, terminal voltage, terminal current, real power, reactive power, rotor angle and speed)

The machine is driven by an externally applied mechanical torque T_{mech}. By varying the mechanical torque at generator 1 T_{mech1}, the practical load variation is attained in the Simulink model. A sharp variation in T_{mech1} of generator bus 1 is created. At t= 4 sec, T_{mech1} is increased from 0.85 pu to 0.95 pu, and at t = 10 sec, T_{mech1} is increased from 0.95 pu to 1.05 pu and keeps until simulation end. Fig.5.8 depicts the variation of terminal voltage for changes in mechanical torque at two generator buses. This is made clearly that when torque at Gen 1 is increased, the terminal voltages of Gen1 and Gen2 oscillate slightly, they settle to a steady-state value of 1.05 pu.

The terminal current I_t, active power P_{gen}, reactive power Q_{gen}, relative rotor angle and relative speed of two generators are recorded during the variation of externally applied T_{mech1}, are shown in Fig.5.8. From the 'rotor winding' block in Fig.4.15, it is well known that the angles of two generators varies proportionally with T_{mech} and oscillated against-phase in frequency 2 Hz. In addition, the relative speeds of generators also oscillated slightly in against-phase. It is also clearly observed that the synchronous generators are stable for the applied sharp variations in the mechanical input.

When the length of line increases in 700 km, the mechanical oscillations of generating powers, terminal voltages and currents, angles and speeds are larger given by Fig.5.9. However, these oscillations still keep two generators in synchronism.

When increasing line distance up to 1200 km, there is a totally loss synchronism between generator 1 and generator 2 shown in Fig.5.10.

-Case 2: L=700 km

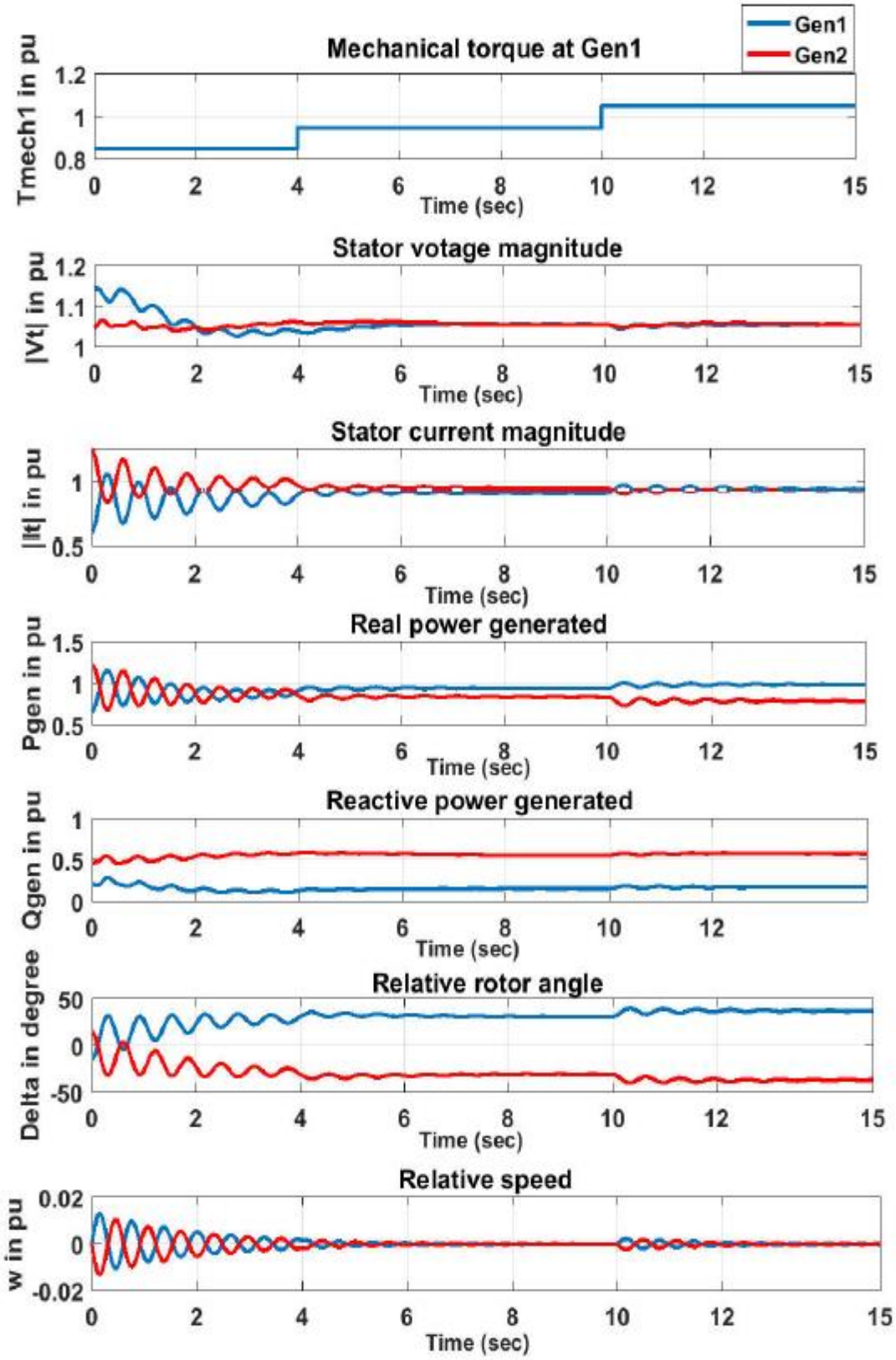

Fig.5.9 Performance of system with variation of the mechanical torque at generator 1 at length 700 km (mechanical torque, terminal voltage, terminal current, real power, reactive power, rotor angle and speed)

-Case 3: L=1200 km

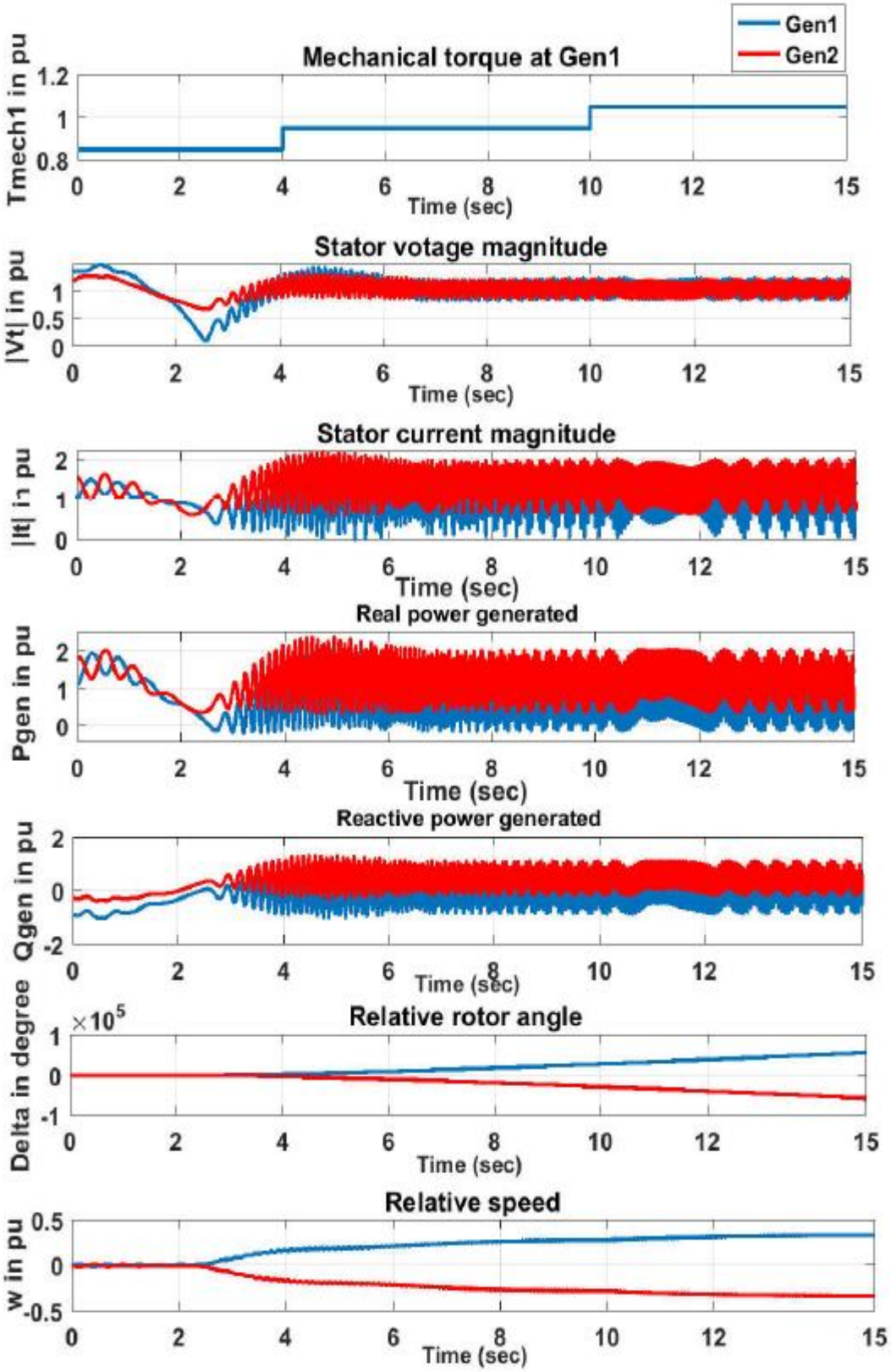

Fig.5.10 Performance of system with variation of the mechanical torque at generator 1 at length 1200 km (mechanical torque, terminal voltage, terminal current, real power, reactive power, rotor angle and speed)

The generators's controls change the field voltages and the rotor mechanical torques during simulation. The responses of the generators's angle to a step change in the mechanical torque at generator 1 are shown in Fig.5.8-5.10. It can be seen that there are oscillations in angle and the amplitudes of these oscillations change gradually over the time of the transient. When the length of double lines is 250 km, the generators are in rating power operation. At the start of the transient, the angles oscillate about 2.5 Hz. The angle changes of generator 1 and generator 2 are in antiphase, generator 1 is oscillating against generator 2. The power oscillations of generators increase when the length of lines increase at 700 km and 1200 km in Fig.5.9 and Fig.5.10 respectively. In order to adjust the balance between the generating power and the loads, the speeds of generators toward to change significantly. When the length of lines is 700 km, at the start of the transient, the generators move in phase opposite at a lower frequency (1.43 Hz) and established the new steady state positions. However, when the length of lines reach to 1200 km, the oscillations of generators tend to be unstable through the oscillations of the generating power and angle. The frequencies of the oscillations depend on the length of the network.

Obviously, the longer transmission lines are, the more oscillate the speed and power transmission capacity of generators do **[PII][PIV]**. When the length of lines reach to 1200 km, there will exist a loss of synchronism between two generators through power and rotor angle index**.** These results may be compared to the power oscillations before blackout in [Appendix Fig.B.1 and Appendix Fig.B.3].

The 1200 km length of line is the maximal capacity of double lines which allow to synchronize between the generator 1 and generator 2. This length should be considered as a maximal index to design the connected network in the practical design section.

5.4 Synchronization of two three Phase Synchronous Generators in a large disturbance

It is essential to analyze the performance of a power system with fault condition for stability analysis and hence a sudden fault is created at bus 4 in the test system.

Before the fault occurs, the power system is operating at some stable steady-state conditions. Assumed that a three phase short circuit occurs at bus 4 shown in Fig. 5.11. If a fault occurs and is then cleared by operating the circuit breaker at the generator end of the line, the prefault and postfault impedance between the generators are the same. The modelling parameters is equal to them in 5.3 section.

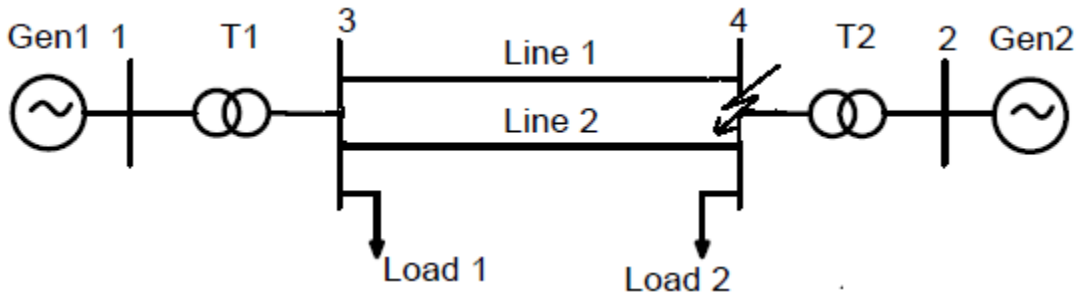

Figure 5.11 Three phase short circuit at bus 4 in system

The initial condition calculations have been performed by the MATLAB writing script (Two_machine.m files) in Appendix (C.2).

The system simulation is implemented when in three phase short circuit at bus 4 closed to generator 2 (Gen 2). During fault time, the system operates only with one source and all transferred powers in the system make stress to generator 1 (Gen1). After 200 ms (milliseconds) the fault will be cleared.

In the network, the load bus 4 is purposely retained so that the injected current to introduce a fault at that bus. With this change in network, the reduced bus admittance matrix equation of the network including the transient impedances of the generators is formed. The Simulink model for the network is created considering the pre-fault nature of that network. At about t=3 s, fault is applied and cleared after 0.2 s.

Similarly, simulation in section 5.3, the synchronism analyses of two generators and transmission capacity of power line under a large disturbance are investigated through changing of power line distance L from 250 km to 1210 km.

It is evident from the Fig.5.12-5.14 that the system comes back to steady-state condition after the clearance of fault. In the cases L=250 km and L=700 km, the blackout does not lead to loss of synchronism. However, power, angle, speed and voltage undergo

“swings” which are caused by relative motions of the generator rotors. These swings are acceptable and will usually die down due to effect of damper and field windings in a generator. Due to the slight lower voltages at buses 1 and 2 after tripping fault, the total power drawn by the resistive loads decreases. Since the mechanical power is not changed, the angles of both generators keep increasing. In case 1 and case 2, the relative speeds settle down to a value zero due to the governors of two generators adjust the mechanical input to the generators.

-Case 1: L=250 km

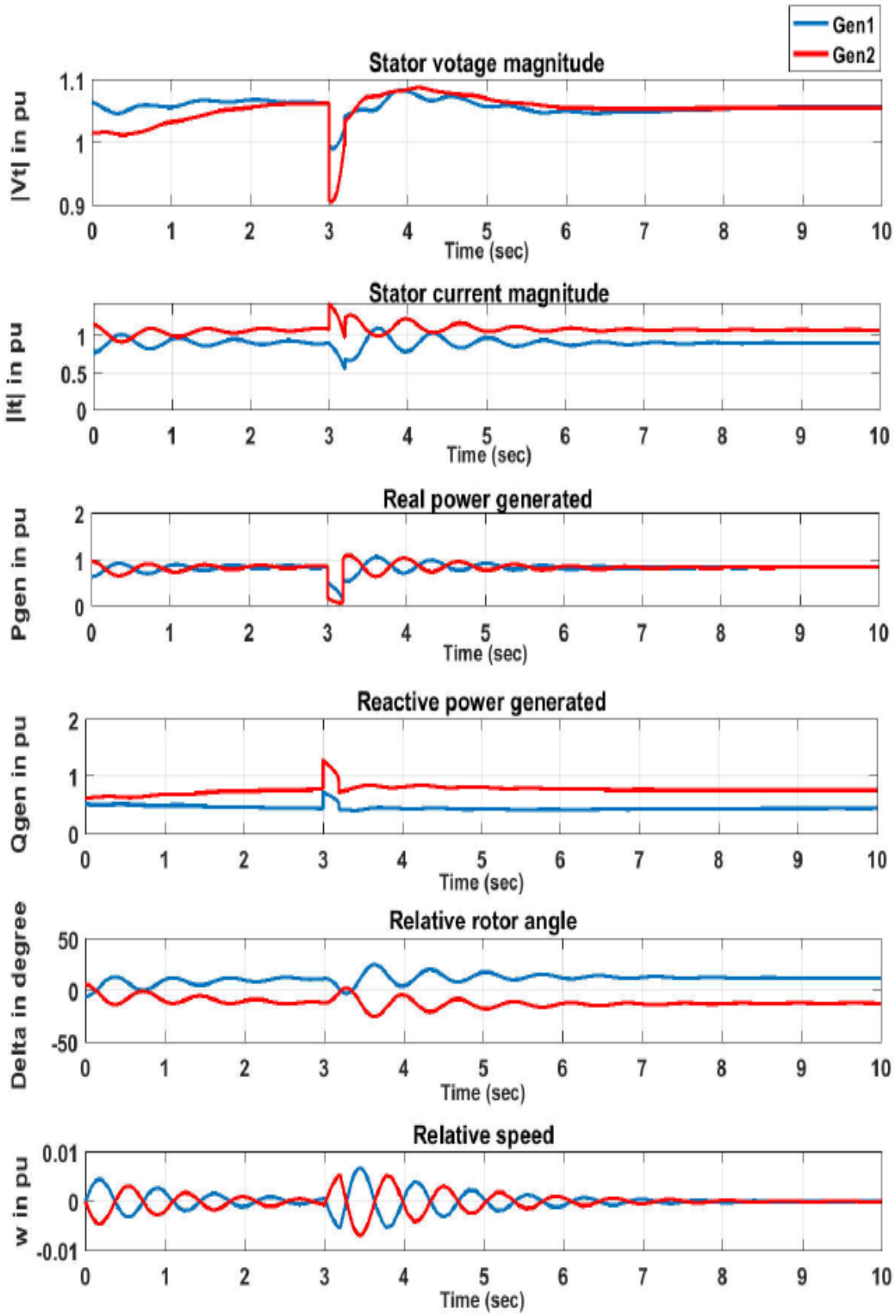

Fig.5.12 Response of system when fault occurs at bus 4 at length 250 km (terminal voltage, terminal current, real power, reactive power, rotor angle and speed)

-Case 2: L=700 km

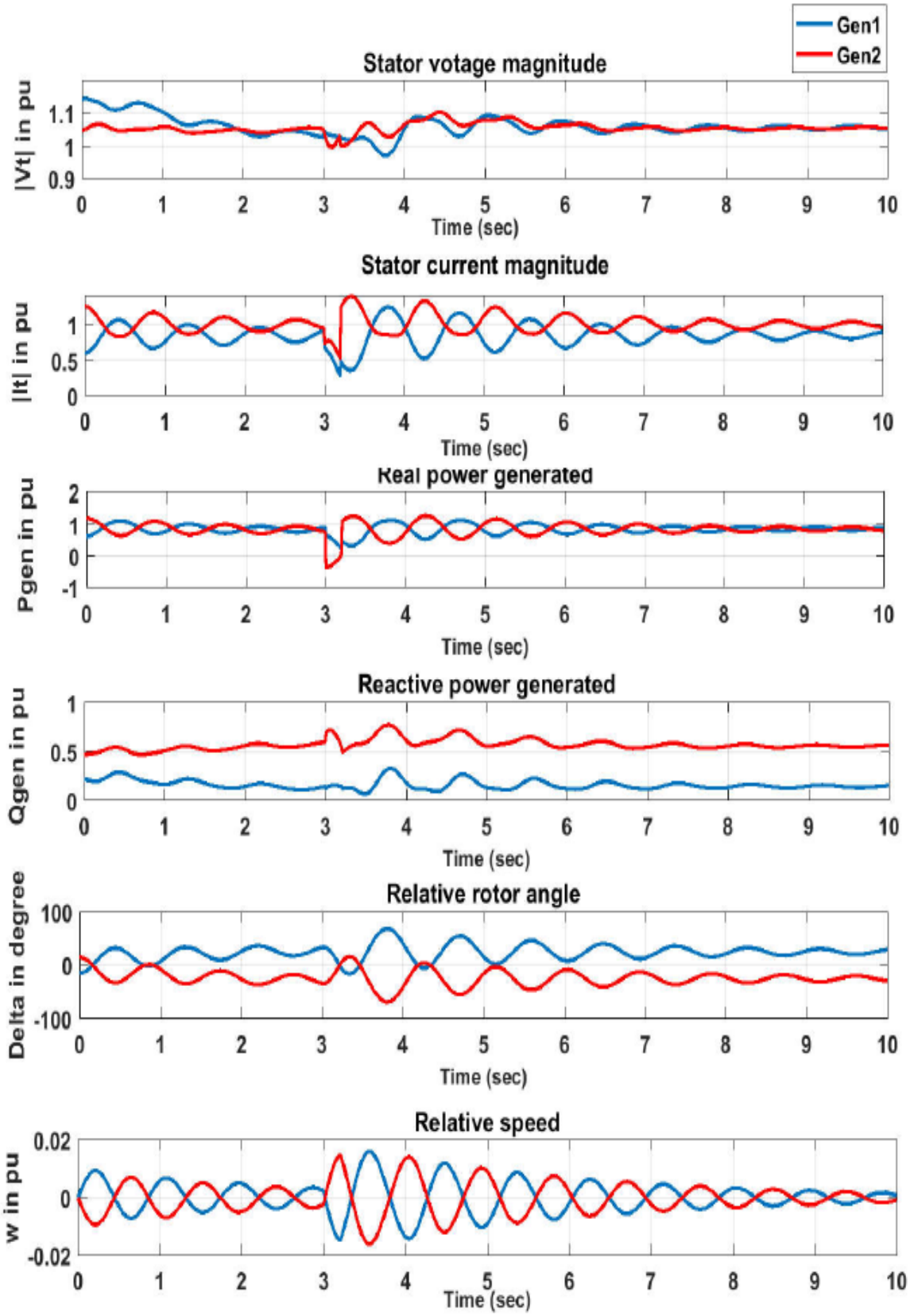

Fig.5.13 Response of system when fault occurs at bus 4 at length 700 km (terminal voltage, terminal current, real power, reactive power, rotor angle and speed)

-Case 3: L=1210 km

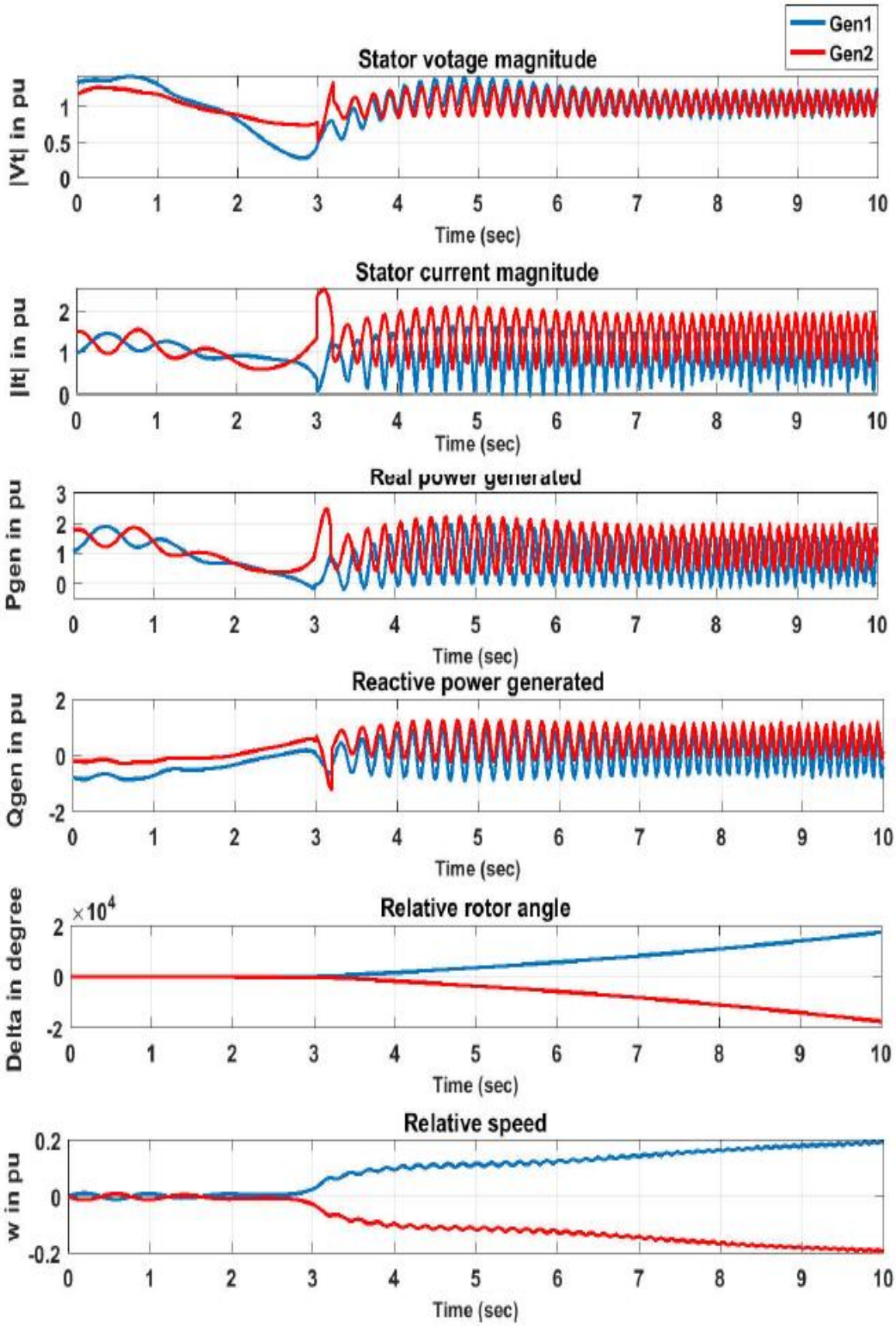

Fig.5.14 Response of system when fault occurs at bus 4 at length 1210 km

(terminal voltage, terminal current, real power, reactive power, rotor angle and speed)

The presented results in above show that when three phase fault at the bus 4 closed to generator 2. As the results, the length of line reached to 1210 km in case 3, there is a instability of generators. The disturbance causes the two generators to lose synchronism. The angles of the two generators “separate out” and electrical power and voltage undergo violent pulsations. Normally this case will not be allowed to continue.

This instability also occurs similar to the case that exists three short circuit in one of the parallel lines closed to bus 4. There is a loss synchronization between two generators. Therefore, it is necessary to find out somehow to improve the un-synchronization in this system. These results may be compared to the power oscillations versus time in **[PI] [PIII]** and [Appendix (B)].

Chapter 6

Practical Design

Obviously, the system of two generators connected via double lines shown in Fig.4.9 has a longitudinal structural consists of two weakly connected subsystems. Any disturbance leading to the loss of synchronism and a natural sprit of the network into two subsystems operating asynchronously.

A transmission network is usually meshed and parallel transmission corridors. These double transmission corridors are loaded in inverse proportion to the reactances of the corridors, assuming no quadrature boosters are present. Hence, it may occur that short transmission lines are overloaded while long ones are under loaded. If that happens, a desired loading of lines can be enforced using quadrature boosters. Improvement a transfer capacity between areas can be implemented by reducing the flow on overloaded lines and increasing the flow on under loaded lines. Large interconnected networks may suffer from circulation of power between subsystems when power enters a subsystem through one transmission corridor and returns through another. This means that there may be large power transfers between regions while net power exchanges, when circulating power is taken away, are small. Quadrature boosters may eliminate or significantly reduce circulation of power. This usually results in reduced load on some transmission corridors at the cost of a small increase in transmission losses.

For very long lines voltage level cannot be raised beyond the limits placed present day high voltage technology. To increase power transmitted in such cases, the only choice is to reduce the line reactance. This is accomplished by adding series capacitors in the line. A method of tuning power lines which is being presently experimented with, uses series capacitors to cancel the effect of the line inductance and shunt inductors to neutralize line capacitance. A long line is divided into several sections which are individually tuned.

The performance of long AC transmission systems can be improved by reactive compensation of series or shunt (parallel) type. Series capacitors and shunt reactors are used to reduce artificially the series reactance and shunt susceptance of lines and thus they act as the line compensators. Compensation of the lines results in improving of system stability and voltage control, in increasing the efficiency of power transmission, facilitating line energization, reducing temporary and transient overvoltage. So far the practical method of

improving line regulation and power transfer capacity is to add series capacitors to reduce line inductance; shunt capacitors under heavy load conditions; and shunt inductors under light or no-load conditions.

However, the above methods are impractical and uneconomical for power frequency lines, in the content of this work a proposed improved method for increasing transfer capacity of lines is change of connected network model. The maximal of length of the transmission line (1200 km) to keep the system stability obtained in the results of section 5.3 is a criteria to design a mesh connected system.

The one-line diagram of a twelve-bus system shown in Fig.6.1 is a meshed network connected by the same relatively tie-lines (power line). This situation is typical of an interconnected system. The weakness of connections may lead to asynchronous rotations in tie-lies following a disturbance. Therefore, the interconnected system plays important role in improving reliability and stability of power system compared to previous tested system in **[PI][PII] [PIII]**. The modelling parameters is equal to them in section 5.3. Assumed that all the lines in this design network are considered as long lines (>250 km). The equivalent of these lines are presented in π model with impedances and susceptance.

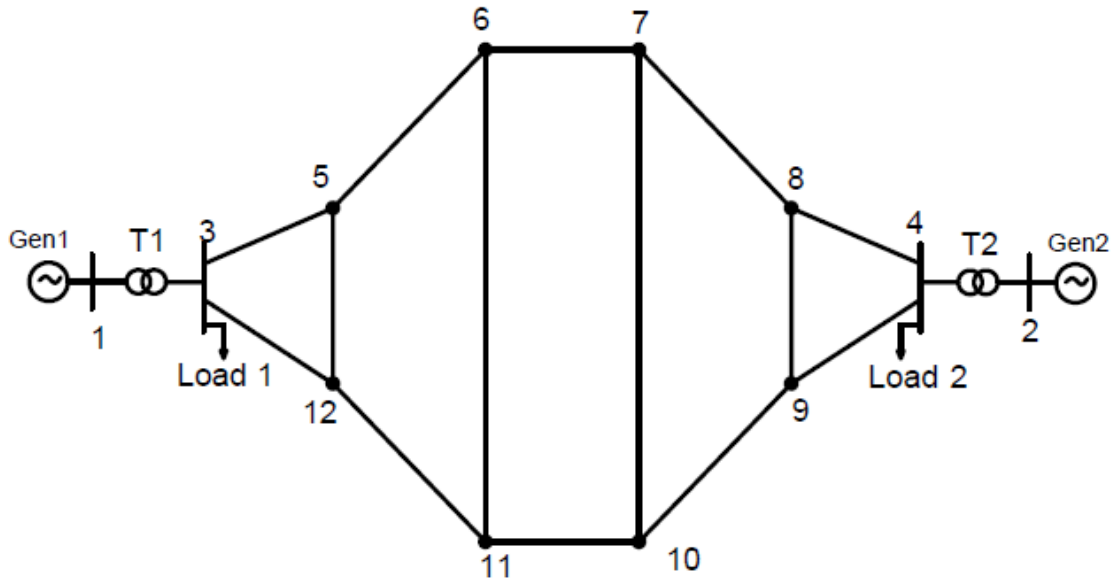

Figure 6.1 Two generators connected via the mesh network

6.1 Steady state operation

The Fig.6.2 shows the network model of the sample power system prepared on the above lines after lumping the shunt admittances Y/2 at the buses. The equivalent power source at each bus is represented by a shaded circle. The equivalent power source at the i^{th} bus injects current I_i into the bus. It may be observed that the structure of power network is

such that all the sources are always connected to a common ground node. Besides the ground node, there are two other nodes (buses) at which the current from the sources is injected into the network. The line admittance between nodes i and k is depicted by $y_{ik}=y_{ki}=1/z_{ik}=1/Z$. Further, the mutual admittance between lines is assumed to be zero.

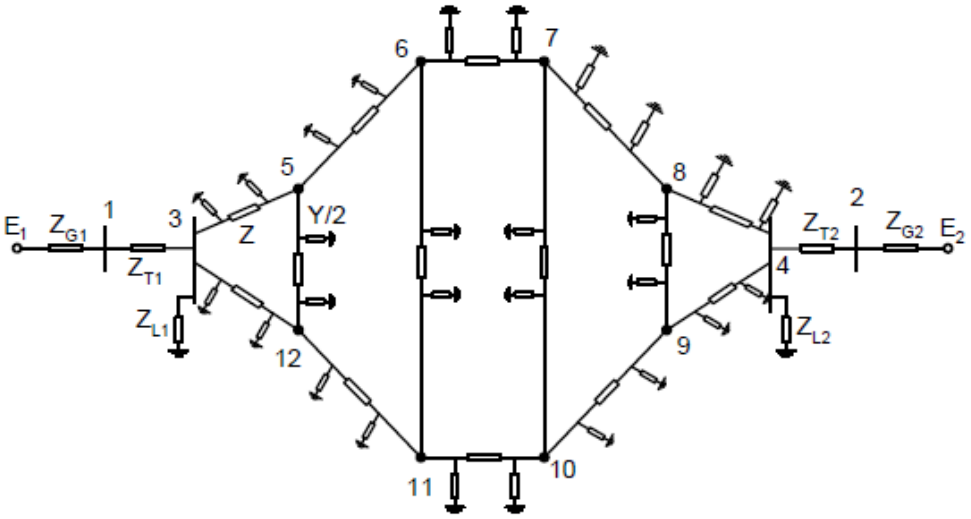

Fig. 6.2 Equivalent diagram of two generators connected via the mesh network

Applying Kirhhoff's current law (KCL) at 12 nodes, we get the following equation set:

$$\begin{bmatrix} I_1 \\ I_2 \\ 0 \\ 0 \\ 0 \\ 0 \\ 0 \\ 0 \\ 0 \\ 0 \\ 0 \\ 0 \end{bmatrix} = \begin{bmatrix} \left(\frac{1}{Z_{G1}+Z_{T1}}\right) & 0 & \left(\frac{-1}{Z_{G1}+Z_{T1}}\right) & 0 & 0 & 0 & 0 & 0 & 0 & 0 & 0 & 0 \\ 0 & \left(\frac{1}{Z_{G2}+Z_{T2}}\right) & 0 & \left(\frac{-1}{Z_{G2}+Z_{T2}}\right) & 0 & 0 & 0 & 0 & 0 & 0 & 0 & 0 \\ \left(\frac{-1}{Z_{G1}+Z_{T1}}\right) & 0 & \left(\frac{1}{Z_{G1}+Z_{T1}}+\frac{1}{Z_{Load1}}+Y+\frac{2}{Z}\right) & 0 & \frac{-1}{Z} & 0 & 0 & 0 & 0 & 0 & 0 & \frac{-1}{Z} \\ 0 & \left(\frac{-1}{Z_{G2}+Z_{T2}}\right) & 0 & \left(\frac{1}{Z_{G3}+Z_{T3}}+\frac{1}{Z_{Load2}}+Y+\frac{2}{Z}\right) & 0 & 0 & 0 & \frac{-1}{Z} & \frac{-1}{Z} & 0 & 0 & 0 \\ 0 & 0 & \frac{-1}{Z} & 0 & \left(\frac{2}{Z}+Y+\frac{1}{Z_{5-12}}+\frac{Y_{5-12}}{2}\right) & \frac{-1}{Z} & 0 & 0 & 0 & 0 & 0 & \frac{-1}{Z_{5-12}} \\ 0 & 0 & 0 & 0 & \frac{-1}{Z} & \left(\frac{2}{Z}+Y+\frac{1}{Z_{6-11}}+\frac{Y_{6-11}}{2}\right) & \frac{-1}{Z} & 0 & 0 & \frac{-1}{Z_{6-11}} & 0 & 0 \\ 0 & 0 & 0 & 0 & 0 & \frac{-1}{Z} & \left(\frac{2}{Z}+Y+\frac{1}{Z_{6-11}}+\frac{Y_{6-11}}{2}\right) & \frac{-1}{Z} & 0 & \frac{-1}{Z_{6-11}} & 0 & 0 \\ 0 & 0 & 0 & \frac{-1}{Z} & 0 & 0 & \frac{-1}{Z} & \left(\frac{2}{Z}+Y+\frac{1}{Z_{5-12}}+\frac{Y_{5-12}}{2}\right) & \frac{-1}{Z_{5-12}} & 0 & 0 & 0 \\ 0 & 0 & 0 & \frac{-1}{Z} & 0 & 0 & 0 & \frac{-1}{Z_{5-12}} & \left(\frac{2}{Z}+Y+\frac{1}{Z_{5-12}}+\frac{Y_{5-12}}{2}\right) & \frac{-1}{Z} & 0 & 0 \\ 0 & 0 & 0 & 0 & 0 & \frac{-1}{Z_{6-11}} & 0 & 0 & \frac{-1}{Z} & \left(\frac{2}{Z}+Y+\frac{1}{Z_{6-11}}+\frac{Y_{6-11}}{2}\right) & \frac{-1}{Z} & 0 \\ 0 & 0 & 0 & 0 & 0 & \frac{-1}{Z_{6-11}} & 0 & 0 & 0 & \frac{-1}{Z} & \left(\frac{2}{Z}+Y+\frac{1}{Z_{6-11}}+\frac{Y_{6-11}}{2}\right) & \frac{-1}{Z} \\ 0 & 0 & \frac{-1}{Z} & 0 & \frac{-1}{Z_{5-12}} & 0 & 0 & 0 & 0 & 0 & \frac{-1}{Z} & \left(\frac{2}{Z}+Y+\frac{1}{Z_{5-12}}+\frac{Y_{5-12}}{2}\right) \end{bmatrix} \begin{bmatrix} E_1 \\ E_2 \\ V_3 \\ V_4 \\ V_5 \\ V_6 \\ V_7 \\ V_8 \\ V_9 \\ V_{10} \\ V_{11} \\ V_{12} \end{bmatrix} \quad (6.1)$$

Using Kron reduction [Appendix (A.3)] to remove buses having zero current injection. Rearranging and writing (6.1) in matrix form, we get:

$$\begin{bmatrix} I_1 \\ I_2 \end{bmatrix} = \begin{bmatrix} Y_{11} & Y_{12} \\ Y_{21} & Y_{22} \end{bmatrix} \begin{bmatrix} E_1 \\ E_2 \end{bmatrix} \quad (6.2)$$

From (6.2) the simulation of system is implemented similarly to the model with two lines in previous chapter in the length of each line in the twelve-bus network followed:

$L_{35}=L_{3\text{-}12}=L_{56}=L_{67}=L_{78}=L_{48}=L_{49}=L_{9\text{-}10}=L_{10\text{-}11}=L_{11\text{-}12}=250$ km.

$L_{5\text{-}12}=L_{8\text{-}9}=255$ km.

$L_{6\text{-}11}=L_{7\text{-}10}=260$ km.

The results of the terminal voltage, active and reactive generating power, phasor current, relative angle and relative speed are given in Fig.6.3. The initial condition calculations have been performed by the writing script (Two_machine_12bus.m files) in Appendix (C.3).

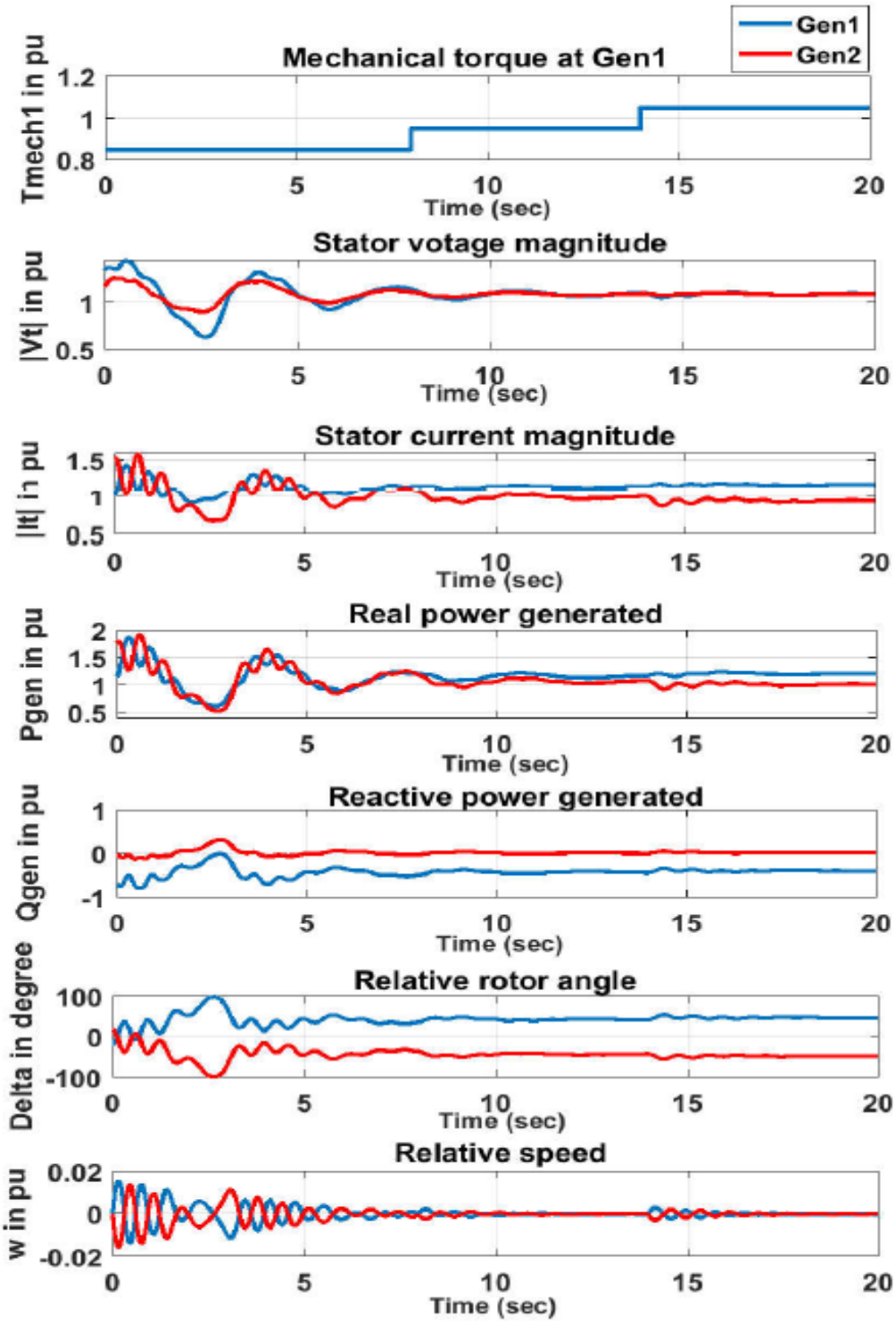

Fig.6.3. Performance of system with variation of the mechanical torque at generator 1 (mechanical torque, terminal voltage, terminal current, real power, reactive power, rotor angle and speed)

Compared with results of this network model to the network includes two power lines L_1 and L_2 in previous chapter, the proposed mesh network with 12 buses decreases the oscillation of output significantly and improves stability of system when changing the mechanical torque at Gen1.

6.2 Three phase short circuit at bus 4

Assumed that there is a three phase short circuit at bus 4 given in Fig.6.4. The calculation of parameters of network is implemented similarly to the section (6.1). The results of the terminal voltage, active and reactive generating power, phasor current, relative angle and relative speed are given in Fig.6.5. The initial condition calculations have been performed by the writing script (Two_machine_12bus.m files) in Appendix (C.3).

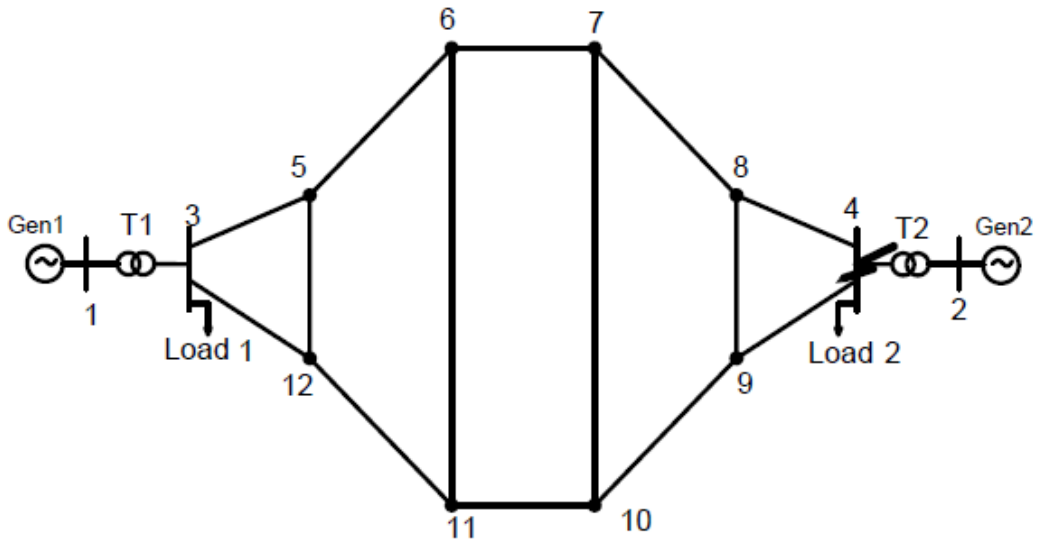

Fig. 6.4 Two generators connected via the mesh network when short circuit at bus 4

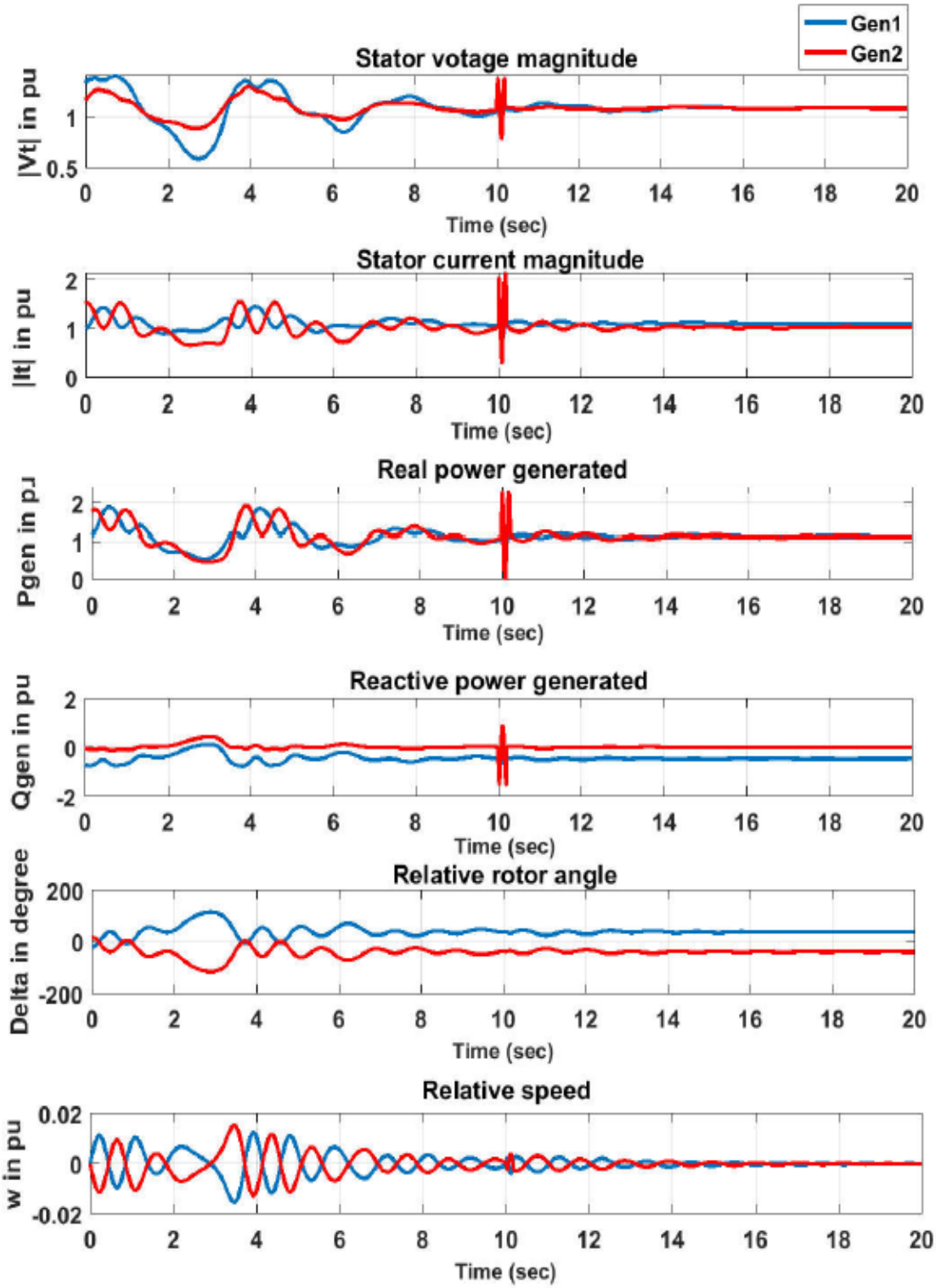

Fig.6.5. Response of system when fault occurs at bus 4 (terminal voltage, terminal current, real power, reactive power, rotor angle and speed)

Compared the above results to results of network model operating two power line L_1, L_2 and short circuit at bus 4 in previous chapter, the proposed mesh network with 12 buses improves stability and reliability of system with a short time response under disturbance condition.

Chapter 7

Conclusion and Future Work

7.1 Conclusion

The following conclusions are made:

- The synchronous machine models have been documented and explained in detail in this technical thesis, including the steady-state operation and transient operation.
- The two synchronous machine fundamental frequency models, connected via the long transmission lines, have been analyzed in synchronization in term of transient stability.
- Influence of length of line to the system oscillation is analyzed and determined as the important index of stability.

In this work, the modeled system consists of synchronous generator with excitation system and connected network model with transformer, transmission line and loads.

Two synchronous generator models, steady state model and transient model, were simulated using qd rotating reference frame. The modeled generator is connected to transmission line. Thevenin's equivalent circuit was considered to represent the generator connection. A transient stability study during three phase fault at one bus closed to generator terminal was performed, and the effect of using power system stabilizer on the system stability was discussed. The MATLAB library was used to simulate the network and to build up a data acquisition of system.

Three simulation parts were applied; the first part is steady state model of a single synchronous generator. In this part, the results of steady state operation of synchronous generator during small changes of mechanical torque and field voltage were shown. The considered generator in first part is connected directly to infinite grid.

In the second part, the steady state model of two synchronous generators with excitation system model connected via long double lines. The results of generator synchronism during small changes of mechanical torque were given. Also, the effect of using long line on the transmission system was discussed in this part.

In the third part, the transient model of two synchronous generators with excitation system model connected via long double lines were applied. In this part, the results of transient operation of system during small changes of mechanical torque and short circuit at bus in network were shown.

In these above parts, the possible consequences of a small disturbance as change mechanical torque and a large disturbance like a fault (followed by length of line) can be:

- The system settles to a new acceptable equilibrium after some initial transient die down
- The system settles to a new acceptable equilibrium but the equilibrium is violated of some steady-state equipment limit (leading to tripping out of that equipment)
- The system does not attain a new equilibrium due to angular and voltage instability.

Voltage instability leads to unacceptable low voltages (which can be corrected by under-lower load shedding), while angular instability (loss of synchronism) leads to violent excursions in current, voltage and power leading to equipment damage. Therefore, the generators which have lost synchronism have to be disconnected from each other. This may occur "naturally" due to distance relays or "intentionally" due to control system separation.

There are two methods can be used to improve stability of system. These methods are reactive compensation of series or shunt and change of connected network. In this work, the method of change of connected network was investigated to get more stable and reliable system operation **[PVI] [PVII].**

In the content of this thesis, the loading capacity of AC transmission at very long distance was presented through connecting two synchronous generators in system. The analyzed and simulated results show that: electric transmission at very long distance is quite different of what would be expected by simple model of medium and short distance transmission experience. The synchronism ability of generators and system behavior under steady state and transient operation depends on more the length of transmitted distances.

To optimize a very long distance transmission line, a more fundamental and open approach is given in this work. Instead of reactive compensation with high cost and technique requirements, the idea to restructure the network by a mesh network topology was shown. Each node in mesh network cooperates in the relaying of data or information in the network. The advantage of this mesh network followed as: A broken node won't distract the transmission of data in a mesh network. Each node is connected to several other nodes

which make it easier to relay data. A broken device will be ignored by the signals and will then find a new one that is connected with the node. Additional devices in a mesh topology will not affect its network connection. Hence it will improve the traffic in the network. Mesh topology makes a large data center that simulates useful information to its nodes. A mesh topology can also handle high amount of network traffic since every additional device into the network is considered a node. Interconnected devices can simultaneously transfer data smoothly and will not complicate the network connection. Based on all above discussion, the mesh network topology should be considered as the first criteria for decreasing the loss of synchronism and improving stability of network.

7.2 Future work

This thesis studied the system behavior when connecting two synchronous generators through long transmission line under steady state and transient operation. The chosen part of the power system to apply was synchronous generator, transformer, transmission line and load.

The electric transmission system plays a critical role in the stability of power system. It is an ever-changing system both in physical terms and how it is operated and regulated. These changes must be recognized and actions developed accordingly. The transmission components continue to get older and investment is not keeping up with needs when looking over a future horizon. Technology development and application undoubtedly will create a new look and advance methods to combat the congestion issues, increased electrical demand and new overhead or restructure of transmission lines will be only one of the solutions considered. In the other hand, DC (direct) transmission system is also optimal solution for improving transmission capacity and stability of power system.

In terms of measurement technique, extensive and powerful tools to facilitate the gathering of information on all aspects regarding system stability is possible through implementation of Phasor Measurement Unit (PMU) **[PII] [PIII] [PV].** Relay functions of PMU installed in two ends of transmission line. PMU measurements at both ends will provide voltages (magnitude and angle) and currents (magnitude and angle) in real time. They help for collecting data in global and overcoming disturbances occurred in system in limited time. Hence the behavior or characteristics of the power line is an excellent candidate for representation of system/network synchronism or stability.

In future work, the following paragraphs could be considered: that would be important for further refinement in the restructure to widen networks, in the improvement control system **[PVI]** and in application of DC transmission system. Having a reliable,

regional, uncongested transmission system will enable to ensure stability of system. Especially, as a teacher in the electrical power university in Hanoi, Vietnam, I would be continuing to research about the Vietnamese network. With the typical shape of country, the Vietnamese network is connected by the long transmission line from Northern to Southern **[PIII].** The transmission capacity and power quality is one of the difficult problems to the operators. The stability and reliability of network need to be improved. These are really related to the topic I have done in this dissertation.

The Vietnamese power system in Fig.7.1 has main high voltage levels of transmission lines: 500kV, 220kV and 110kV. Among them, the 500kV transmission lines are the most important interconnecting three regional power systems: North, Central and South. It plays an vital role in the economic development of the country. The Vietnamese 500 kV power system operated in 1994. Initially a 500kV transmission line with total length of 1483 km was constructed via five 500kV substation for liking all three separate systems into one interconnected network. In the period 1994-1999, the 500kV transmission lines transferred power from North to South via Central, but since 2000 it operated mainly in transferring power from South to North via Central with maximum active power ever reached being 1500MW in the 500kV Central Vietnam line. By 2007 the number of 500kV substation has grown to 11, the total 500kV line length reached 3466km and total 500kV transformer rating increased to 6600MVA. It reached the length of about 5690 km and total capacity of all the 500 kV substations of 22,800 MVA in 2015.

Following the report of Electricity Vietnam group in August 2018, the number of 500kV substation has increased to 28 with total rating power 30000MVA, the total 500kV line length reached 7500km and the transferring power from South to North via Central reached being 5920MW. The National Load Dispatch Center (NLDC) in Vietnam has the jurisdiction to control 500kV substations, transmission lines and the large power plants.

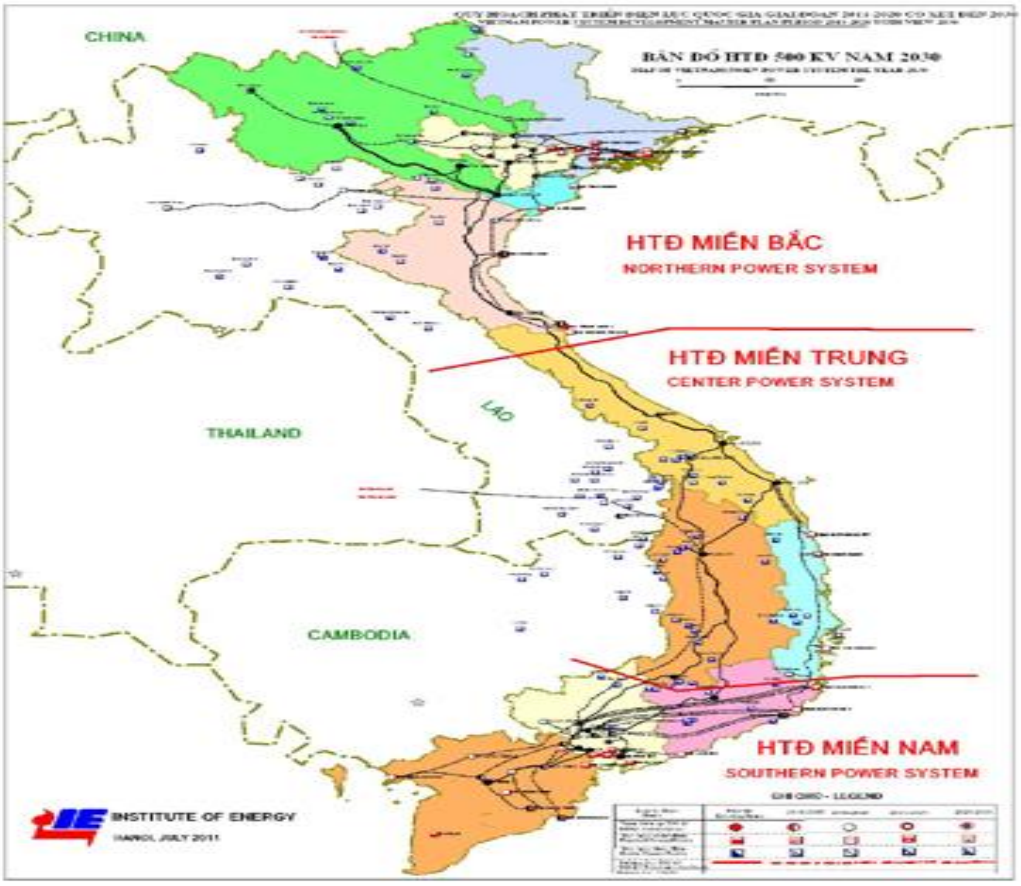

Fig.7.1 Vietnamese power system in geographical location

The master plan period of 2011-2030 for volume of the 500kV Vietnam transmission network to be constructed was reported in 2016 in Tab.7.1.

Tab.7.1: Quantity of transmission grids to be built up to 2030

Category	Unit	2011-2015	2016-2020	2021-2025	2026-2030
500kV substation	MVA	17100	26750	29400	33550
500kV transmission line	km	2533	2746	3592	3714

After more than 20 years of operation, the North-South 500kV transmission line has confirmed the importance, rapid development of power sector in science, technology as well as management, become a base for development, expansion of National power transmission grid, opening up a new era for power sector of Vietnam.

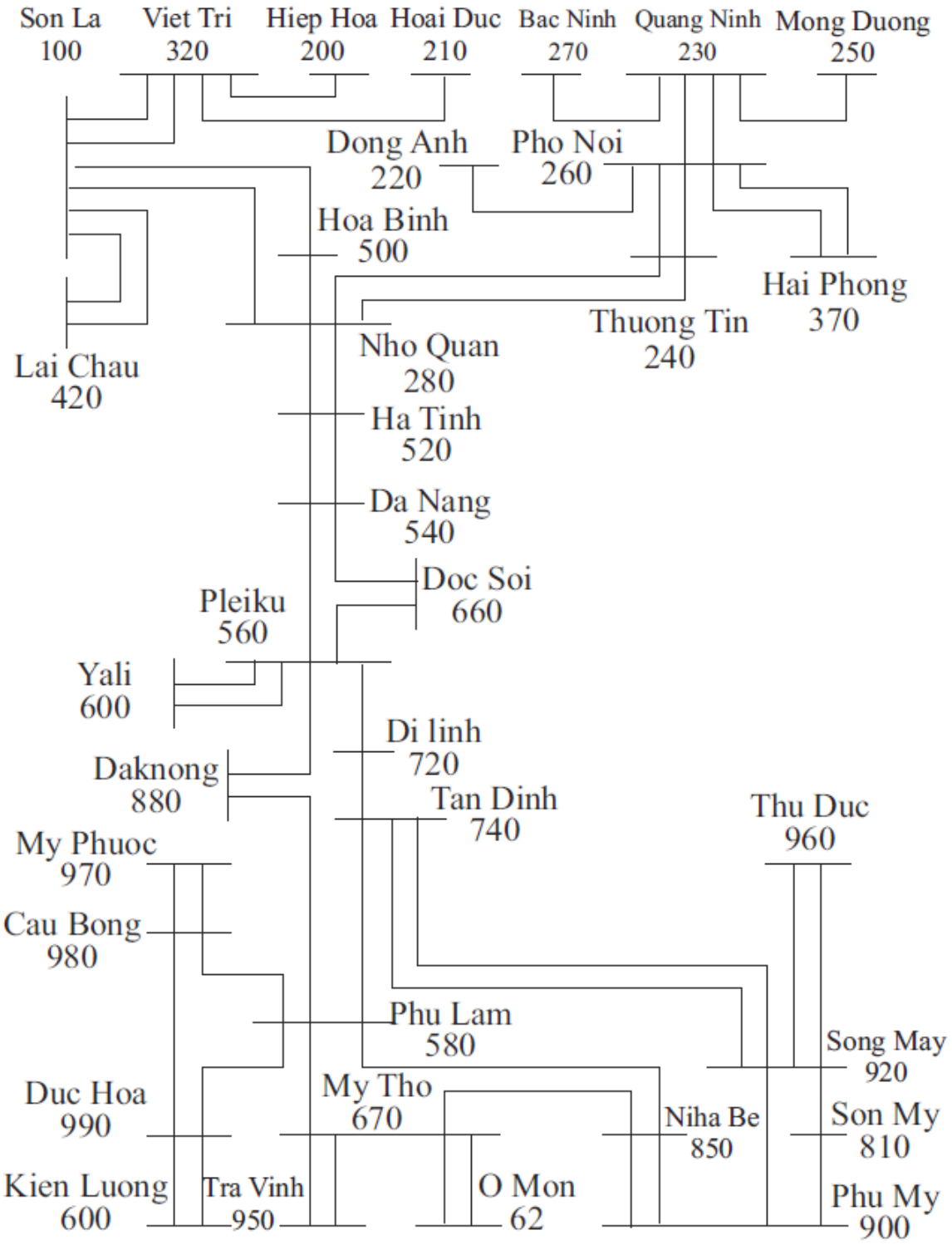

Fig.7.2 One line diagram of Vietnam Power System

In the future work, the stability analysis is focus on the Vietnam Power System which has a longitudinal network structure with the trunk 500KV transmission system as shown in Fig.7.2 (Tran-Quoc et al.., 2003; Hoang et al.., 2011).

APPENDIX (A) – Calculated formulas

A.1. The voltage behind the transient impedance of generator

$$E_i' = V_i + (r_s + jx_d')I_i \quad \text{(A.1)}$$

Where:

i is the i^{th} generator

V_i is the terminal voltage of i^{th} generator

I_i is the generator current

A.2. The load equivalent admittances

$$y_{io} = \frac{S_i^*}{|V_i|^2} = \frac{P_i - jQ_i}{|V_i|^2} \quad \text{(A.2)}$$

Where:

P_i and Q_i are the generator real and reactive power

A.3. The reduced bus admittance matrix

To simplify the analysis, all nodes other than the generator internal nodes are eliminated using Kron reduction formula. To eliminate the load buses, the bus admittance matrix is partitioned such that the n buses to be removed are present in the upper n rows.

$$Y_{bus}^{red} = Y_{mm} - Y_{nm}^T Y_{nn}^{-1} Y_{nm} \quad \text{(A.3)}$$

Where:

m is the number of generator

n is bus need to be removed

APPENDIX (B) – Verification plot

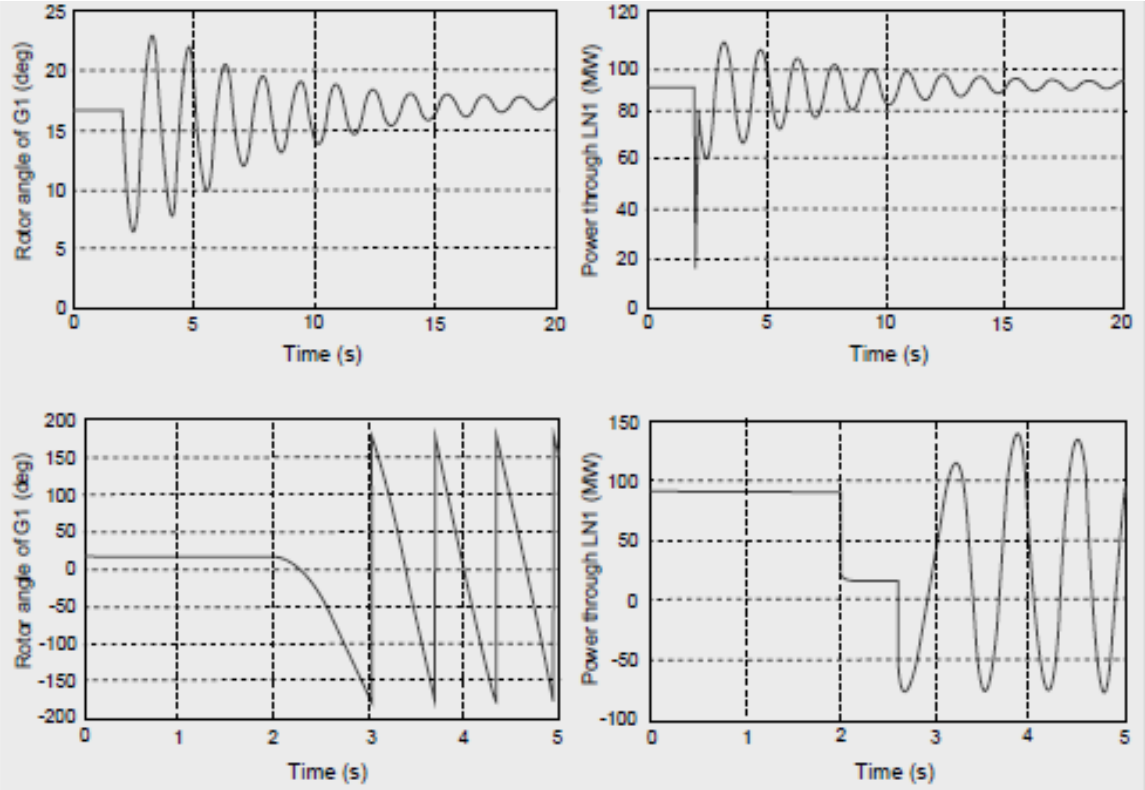

Fig. B.1. Angle of generator G1 and power through line LN1 before and after a fault at BUS 3. For 80ms clearance time (upper trace). For 400ms clearance time (lower trace) [52]

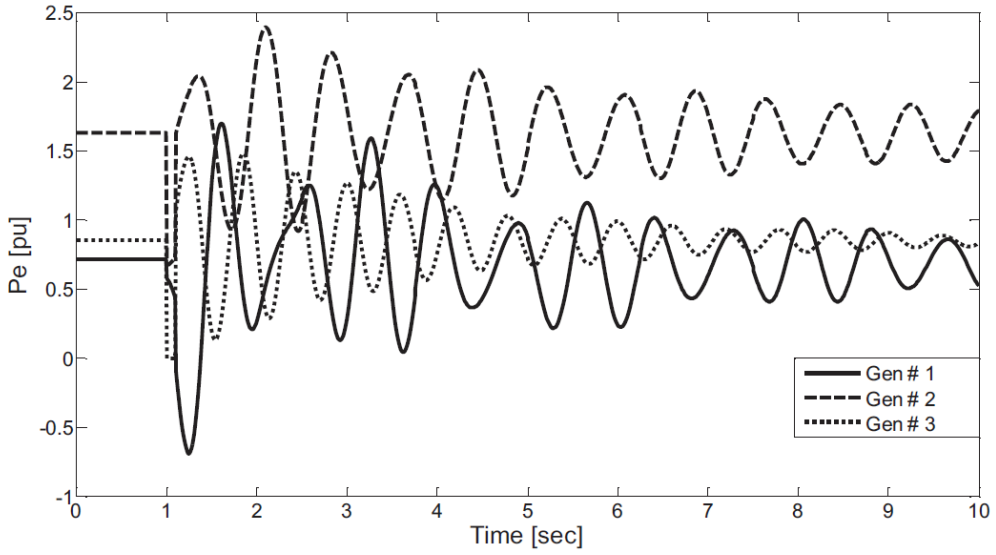

Fig. B.2. Plot of electrical power outputs versus time for a 100ms clearing time [40]

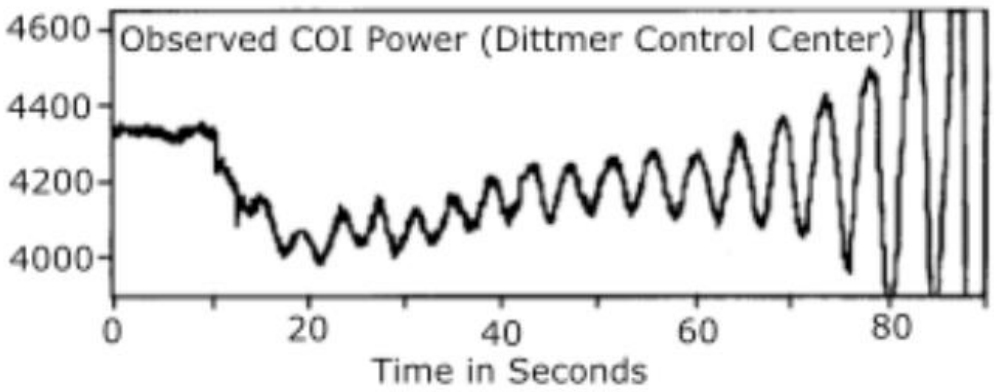

Fig.B.3. Phasor angle oscillation increment of voltage (the increment is proportional in relation to the active power) on 10.8.1996 in California, USA [51]

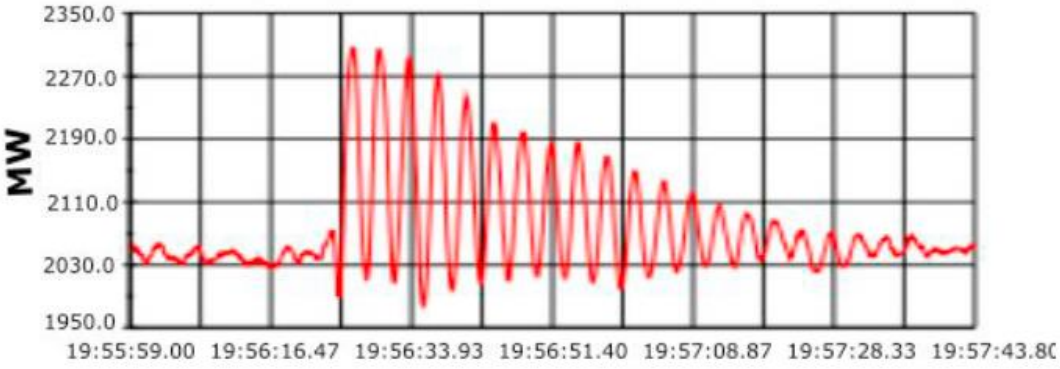

Fig.B.4 Peak condition of active power proportional to the phase angle. This condition was dumped without blackout [51]

APPENDIX (C) – The writing script (.m files) in MATLAB

C.1 The writing script (. m files) of one machine operation

```
% One_machine.m
clear all
% Calculate base quantities
we = 2*pi*Frated;
wbase = 2*pi*Frated;
wbasem = wbase*(2/Poles);
Sbase = Prated/Pfrated;
Vbase = Vrated*sqrt(2/3); % Use peak values as base quantites
Ibase = sqrt(2)*(Sbase/(sqrt(3)*Vrated));
Zbase = Vbase/Ibase;
Tbase = Sbase/wbasem;
% Calculate dq0 equivalent circuit parameters
xmq = xq - xls;
xmd = xd - xls;
xplf = xmd*(xpd - xls)/(xmd - (xpd-xls));
xplkd = xmd*xplf*(xppd-xls)/(xplf*xmd -(xppd-xls)*(xmd+xplf));
xplkq = xmq*(xppq - xls)/(xmq - (xppq-xls));
rpf = (xplf + xmd)/(wbase*Tpdo);
rpkd = (xplkd + xpd - xls)/(wbase*Tppdo);
rpkq = (xplkq + xmq)/(wbase*Tppqo);
% Convert to per unit dqo circuit parameters
H = 0.5*J_rotor*wbasem*wbasem/Sbase;
rs = rs/Zbase;
xls = xls/Zbase;
xppd = xppd/Zbase;
xppq = xppq/Zbase;
xpd = xpd/Zbase;
xpq = xpq/Zbase;
xd = xd/Zbase;
xq = xq/Zbase;
xmd = xmd/Zbase;
xmq = xmq/Zbase;
rpf = rpf/Zbase;
rpkd = rpkd/Zbase;
rpkq = rpkq/Zbase;
xplf = xplf/Zbase;
xplkd = xplkd/Zbase;
xplkq = xplkq/Zbase;
% Compute settings for variables in simulation
wb=wbase;
xMQ = (1/xls + 1/xmq + 1/xplkq)^(-1);
xMD = (1/xls + 1/xmd + 1/xplf + 1/xplkd)^(-1);
% Initial operating condition lists
P = Prated/Sbase;
Q = P*(sqrt(1-Pfrated*Pfrated)/Pfrated);
Vt = 1. + 0*j;  % infinite bus voltage, also the reference phasor
thetaeo = angle(Vt); % initial value of voltage angle
Vm = abs(Vt);
St = P+Q*j; % generated complex power
It = conj(St/Vt);
Sigma = angle(It);
Eq = Vt + (rs + j*xq)*It;
delt = angle(Eq);          % angle Eq leads Vt
% compute q-d steady-state variables
Eqo = abs(Eq);
I = It*(cos(delt) - sin(delt)*j);% same as I = (conj(Eq)/Eqo)*It;
Iqo = real(I);
Ido = -imag(I);        % when the d-axis lags the q-axis
Vto = Vt*(cos(delt) - sin(delt)*j);
```

```
Vqo = real(Vto);
Vdo = -imag(Vto);
Efo = Eqo + (xd-xq)*Ido;
Eqpo = Vqo + xpd*Ido + rs*Iqo;
Edpo = Vdo - xpq*Iqo + rs*Ido;
Ifo = Efo/xmd;
Psiado = xmd*(-Ido + Ifo);
Psiaqo = xmq*(-Iqo);
Psiqo = xls*(-Iqo) + Psiaqo;
Psido = xls*(-Ido) + Psiado;
Psifo = xplf*Ifo + Psiado;
Psikqo = Psiaqo;
Psikdo = Psiado;
Sto = Vto*conj(I);
delto = delt;% initial value of rotor angle
thetaro = delto+thetaeo;% thetar(0) in variable frequency oscillator
Pemo = real(Sto);
Qemo = imag(Sto);
Tmech = Pemo;
T2piby3 = 2*pi/3; % phase angle of bus phase voltages
```

C.2 The writing script (. m files) of two machine operation with double lines

```
%Two_machine.m
clear all
wb = 2*pi*50;
Pfrated= 0.85;
Prated=300e6;
Qrated=Prated*(sqrt(1-Pfrated*Pfrated)/Pfrated);
Sbase = Prated/Pfrated;
Vrated =15.75e3*sqrt(2/3);
P = Prated/Sbase;
Q = P*(sqrt(1-Pfrated*Pfrated)/Pfrated);
% Network parameter
Sys_Sbase = 1000e6; % System's S base in MVA % network parameters are on
system base
Vsys=230e3;
Sys_Zbase=Vsys*Vsys/Sys_Sbase;
Sys_Ybase=1/Sys_Zbase;
n_unit = 2; % number of generators
% input per unit parameters of generators
% parameters of set 1 synchronous generator
list_A = [1]; % list of buses with a machine having these parameters
if isempty(list_A)
else
for bus = list_A
Sbratio(bus) = (Sys_Sbase/Sbase);%ratio of system to machine base VA
rs(bus) = rs;
xd(bus) = xd;
xq(bus) = xq;
xls(bus) = xls;
xpd(bus) = xpd;
xpq(bus) = xpq;
Tpdo(bus) = Tpdo;
Tpqo(bus) = Tpqo;
H(bus) = H ;
Domega(bus) = Domega; % mechanical damping coeff
% Parameters of an alternator-Rectifier Excitation System
KA(bus) = KA; %nominal value
TA(bus) = TA;
VRmax(bus) = VRmax;
VRmin(bus) = VRmin;
TE(bus) = TE;
KE(bus) = KE;
```

```
TF(bus) = TF;
KF(bus) = KF;
AEx(bus) = AEx;
BEx(bus) = BEx;
end % for list_A
end % if isempty(list_A)
% parameters of set 2 synchronous generator
list_B = [2]; % list of buses with a machine having these parameters
if isempty(list_B)
else
for bus = list_B
Sbratio(bus) =(Sys_Sbase/Sbase);%ratio of system to machine base VA
rs(bus) = rs;
xd(bus) = xd;
xq(bus) = xq;
xls(bus) = xls;
xpd(bus) = xpd;
xpq(bus) = xpq;
Tpdo(bus) = Tpdo;
Tpqo(bus) = Tpqo;
H(bus) = H ;
Domega(bus) = Domega; % mechanical damping coeff
% Parameters of an alternator-Rectifier Excitation System
KA(bus) = KA; %nominal value
TA(bus) = TA;
VRmax(bus) = VRmax;
VRmin(bus) = VRmin;
TE(bus) = TE;
KE(bus) = KE;
TF(bus) = TF;
KF(bus) = KF;
AEx(bus) = AEx;
BEx(bus) = BEx;
end % for list_B
end % if isempty(list_B)
% *********Setting up machine parameters*************
 % Transformer parameters
S_trans=400e6; % VA
detaP0=0.330; %MW
detaPn=0.880; %MW
detaQ0=1.6;
Un=11;
%X_trans1=(j*0.05)*(Sys_Sbase/S_trans);
%X_trans2= (j*0.05)*(Sys_Sbase/S_trans);
X_trans1= (0.29+j*14.5)/Sys_Zbase;
X_trans2= (0.29+j*14.5)/Sys_Zbase;
% Power line parameter in SI
z=(0.045+j*0.44); %Ohm/km
y=j*3.6/1000000; %S/km
Length34=1210;
% Power line parameter in  per unit
gamma=sqrt(z*y);
Zc=sqrt(z/y);
A_=cosh(gamma*Length34);
B_=Zc*sinh(gamma*Length34);
C_=(1/Zc)*sinh(gamma*Length34);
D_=A_;
A1=A_; B1=B_/2; C1=2*C_; D1=D_;
Z_line=B1;
Y_p=(A1-1)/B1;
Z_line_pu=Z_line/Sys_Zbase;
Y_p_pu=Y_p/Sys_Ybase;
```

```
% Load parameter in  per unit
P_load1=199e6;
P_load2=399e6;
pf_load=0.8;
Q_load1= P_load1*(sqrt(1-pf_load*pf_load))/pf_load; %VAr
Q_load2= P_load2*(sqrt(1-pf_load*pf_load))/pf_load; %VAr
S_load_pu1=(P_load1 + j*Q_load1)/Sys_Sbase;
S_load_pu2=(P_load2 + j*Q_load2)/Sys_Sbase;
% Calculation starting
detaP_trans1=detaP0+detaPn*(P_load1^2+Q_load1^2)/S_trans^2;
detaP_trans2=detaP0+detaPn*(P_load2^2+Q_load2^2)/S_trans^2;
detaQ_trans1=detaQ0+Un*(P_load1^2+Q_load1^2)/(100*S_trans^2);
detaQ_trans2=detaQ0+Un*(P_load2^2+Q_load2^2)/(100*S_trans^2);
P34=(Prated-detaP_trans1*10^(6)-P_load1);
P43=(Prated-detaP_trans2*10^(6)-P_load2);
Q34=(Qrated-detaQ_trans1*10^(6)-Q_load1);
Q43=(Qrated-detaQ_trans2*10^(6)-Q_load2);
P13=(Prated-detaP_trans1*10^(6));
P24=(Prated-detaP_trans2*10^(6));
Q13=(Qrated-detaQ_trans1*10^(6));
Q24=(Qrated-detaQ_trans2*10^(6));
S13=(P13+j*Q13)/Sys_Sbase;
S24=(P24+j*Q24)/Sys_Sbase;
anpha=angle(A1); beta=angle(B1);
cos_34=abs(B1)*[(abs(D1)*Vsys^2*cos((beta-anpha))/abs(B1))-P34]/Vsys^2;
teta34=acos(cos_34)-beta; %radian
teta34_degree=(acos(cos_34)-beta)*180/pi; %degree
cos_43=abs(B1)*[(abs(A1)*Vsys^2*cos((beta-anpha))/abs(B1))+P43]/Vsys^2;
teta43=acos(cos_34)+beta; %radian
teta43_degree=(acos(cos_43)-beta)*180/pi; %degree
V3=cos(teta34)-j*sin(teta34);
V4=1;
Vt(1) = V3+X_trans1*conj((S13)/(V3));
Vt(2) = V4+X_trans2*conj((S24)/(V4));
St(1) = P + Q*j; % positive for generating
St(2) = P + Q*j;
% select voltage regulation type for each generator
% Exc_sw = 1 for ac voltage reg; Exc_sw = 0 for dc voltage reg
Exc_sw(1) = 1;
Exc_sw(2) = 1;
% Initial conditions
for nu = 1:n_unit
  It(nu) = conj(St(nu)/Vt(nu));
  Eq(nu) = Vt(nu) + (rs(nu) +j*xq(nu))*It(nu);
  delt(nu) = angle(Eq(nu));      % angle Eq leads Vt
% qd variables in generator rotor reference frame
  I(nu) = It(nu)*(cos(delt(nu)) - sin(delt(nu))*j);
  Iqo(nu) = real(I(nu));
  Ido(nu) = -imag(I(nu));        % when the d-axis lags the q-axis
  Efo(nu) = abs(Eq(nu)) + (xd(nu)-xq(nu))*Ido(nu);
  Vto(nu) = Vt(nu)*(cos(delt(nu)) - sin(delt(nu))*j);
  Vqo(nu) = real(Vto(nu));
  Vdo(nu) = -imag(Vto(nu));
  Sto(nu) = Vto(nu)*conj(I(nu));
  Eqpo(nu) = Vqo(nu) + xpd(nu)*Ido(nu) + rs(nu)*Iqo(nu);
  Edpo(nu) = Vdo(nu) - xpd(nu)*Iqo(nu) + rs(nu)*Ido(nu);
  Pemo(nu) = real(Sto(nu));
  Qemo(nu) = imag(Sto(nu));
  Tmech(nu) = Pemo(nu);
  delio(nu) = delt(nu);
  end % for nu loop
  for nu = 1:n_unit
```

```
slip(nu) = 0;
Eqp(nu) = Eqpo(nu);
Edp(nu) = Edpo(nu);
Ef(nu) = Efo(nu);
VR(nu) = KE(nu)*Efo(nu);
Vs(nu) = Efo(nu)*KF(nu)/TF(nu);
end;
% Tinh matran tong tro network
y13=1/((rs(1)+j*xpd(1))*Sbratio(1)+X_trans1);
y24=1/((rs(2)+j*xpd(2))*Sbratio(1)+X_trans2);
y34=1/Z_line_pu;
y_load1=conj(S_load_pu1)/(abs(V3)^2);
y_load2=conj(S_load_pu2)/(abs(V4)^2);
y30=y_load1;
y40=y_load2; % conj(Pload + jQload)/|Vload|^2
Y(1,1)= y13;Y(1,2)= 0;Y(1,3)= -y13;Y(1,4)= 0;
Y(2,1)= 0;Y(2,2)= y24;Y(2,3)= 0;Y(2,4)= -y24;
Y(3,1)= -y13;Y(3,2)=0;Y(3,3)= y34+y13+y30+Y_p_pu;Y(3,4)= -y34;
Y(4,1)= 0;Y(4,2)=-y24;Y(4,3)= -y34;Y(4,4)= y40+Y_p_pu+y24+y34;
gbus=[3 4]; % row 4 and column 4 to be gyrated
ix = [1 2]; % index vector
Hmod(gbus,gbus)=1./Y(gbus,gbus);
Hmod(ix,gbus)=Y(ix,gbus)/Y(gbus,gbus);
Hmod(gbus,ix)=-Y(gbus,ix)/Y(gbus,gbus);
Hmod(ix,ix) = Y(ix,ix) - (Y(ix,gbus)*Y(gbus,ix))/Y(gbus,gbus);
g=Hmod;
RZ = real(Hmod);
IZ = imag(Hmod);
% *********Determining system eigenvalues*************
% Input guesses to trim function
iqe3=0;
ide3=0;
iqe4=0;
ide4=0;
for nu = 1:n_unit
slip(nu) = 0;
Eqp(nu) = Eqpo(nu);
Edp(nu) = Edpo(nu);
Ef(nu) = Efo(nu);
VR(nu) = KE(nu)*Efo(nu);
Vs(nu) = Efo(nu)*KF(nu)/TF(nu);
end;
% If all units are dc field regulated
u = [Efo(1);Tmech(1);Efo(2);Tmech(2);iqe3;ide3;iqe4;ide4];
if(Exc_sw(1)) % Exc_sw(1) =1 unit 1 ac voltage regulated
u(1) = abs(Vto(1));
elseif(Exc_sw(2))
u(3) = abs(Vto(2)); %unit 2 ac regulated
end
% order of variables in array x has to agree with that of xstr
x
=[Eqp(1);Edp(1);delio(1);Eqp(2);Edp(2);delio(2);Ef(1);slip(1);Vs(1);VR(1
);Ef(2);slip(2);Vs(2);VR(2)];
y =[abs(Vto(1));Pemo(1);Qemo(1);abs(Vto(2));Pemo(2);Qemo(2)];
% Update steady-state value for initializing simulation
% Set reference voltage according to whether it is ac or dc
% voltage regulated
if(Exc_sw(1)) % unit 1 ac voltage regulated
vref(1) = y(1);
else
vref(1) = u(1); % unit 1 dc regulated
end;
```

```
if(Exc_sw(2)) % unit 2 ac voltage regulated
vref(2) = y(4);
else % unit 2 dc field regulated
vref(2) = u(3);
end;
% Initialize signal generators and integrators
Tmech(1) = u(2);
Tmech(2) = u(4);
Eqpo(1) = x(1);
Edpo(1) = x(2);
Eqpo(2) = x(4);
Edpo(2) = x(5);
delio(1) = x(3);
delio(2) = x(6);
Ef(1) = x(7);
Vs(1) = x(9);
VR(1) = x(10);
Ef(2) = x(11);
Vs(2) = x(13);
VR(2) = x(14);
```

C.3 The writing script (. m files) of two machine operation with the 12-bus network.

```
% Two_machine_12bus.m
% *********Setting up machine parameters*************
 % Transformer parameters
% 12 bus
clear all
wb = 2*pi*50;
tstop = 20; % stop time for simulation
Pfrated= 0.85;
Prated=300e6;
Qrated=Prated*(sqrt(1-Pfrated*Pfrated)/Pfrated);
Sbase = Prated/Pfrated;
Vrated =15.75e3*sqrt(2/3);
P = Prated/Sbase;
Q = P*(sqrt(1-Pfrated*Pfrated)/Pfrated);
% Network parameter
Sys_Sbase = 1000e6; % System's S base in MVA % network parameters are on
system base
Vsys=230e3*sqrt(2/3);
Sys_Zbase=Vsys*Vsys/Sys_Sbase;
Sys_Ybase=1/Sys_Zbase;
n_unit = 2; % number of generators
% input per unit parameters of generators
% parameters of set 1 synchronous generator
list_A = [1]; % list of buses with a machine having these parameters
if isempty(list_A)
else
for bus = list_A
Sbratio(bus) = (Sys_Sbase/Sbase);%ratio of system to machine base VA
rs(bus) = rs;
xd(bus) = xd;
xq(bus) = xq;
xls(bus) = xls;
xpd(bus) = xpd;
xpq(bus) = xpq;
Tpdo(bus) = Tpdo;
Tpqo(bus) = Tpqo;
H(bus) = H ;
Domega(bus) = Domega; % mechanical damping coeff
% Parameters of an alternator-Rectifier Excitation System
KA(bus) = KA; %nominal value
```

```
TA(bus) = TA;
VRmax(bus) = VRmax;
VRmin(bus) = VRmin;
TE(bus) = TE;
KE(bus) = KE;
TF(bus) = TF;
KF(bus) = KF;
AEx(bus) = AEx;
BEx(bus) = BEx;
end % for list_A
end % if isempty(list_A)
% parameters of set 2 synchronous generator
list_B = [2]; % list of buses with a machine having these parameters
if isempty(list_B)
else
for bus = list_B
Sbratio(bus) =(Sys_Sbase/Sbase);%ratio of system to machine base VA
rs(bus) = rs;
xd(bus) = xd;
xq(bus) = xq;
xls(bus) = xls;
xpd(bus) = xpd;
xpq(bus) = xpq;
Tpdo(bus) = Tpdo;
Tpqo(bus) = Tpqo;
H(bus) = H ;
Domega(bus) = Domega; % mechanical damping coeff
% Parameters of an alternator-Rectifier Excitation System
KA(bus) = KA; %nominal value
TA(bus) = TA;
VRmax(bus) = VRmax;
VRmin(bus) = VRmin;
TE(bus) = TE;
KE(bus) = KE;
TF(bus) = TF;
KF(bus) = KF;
AEx(bus) = AEx;
BEx(bus) = BEx;
end % for list_B
end % if isempty(list_B)
% *********Setting up machine parameters*************
 % Transformer parameters
S_trans=400e6; % VA
detaP0=0.330; %MW
detaPn=0.880; %MW
detaQ0=1.6;
Un=11;
X_trans1= (0.29+j*14.5)/Sys_Zbase;
X_trans2= (0.29+j*14.5)/Sys_Zbase;
% Power line parameter in SI
z=(0.045+j*0.44); %Ohm/km
y=j*3.6/1000000; %S/km
Length35=250;
Length512=255;
Length611=260;
% Power line parameter in  per unit
%%% 3-5 line%%%%%%%%%%
gamma=sqrt(z*y);
Zc=sqrt(z/y);
A_=cosh(gamma*Length35);
B_=Zc*sinh(gamma*Length35);
C_=(1/Zc)*sinh(gamma*Length35);
```

```
D_=A_;
A1=A_; B1=B_/1; C1=1*C_; D1=D_;
Z_line=B1;
Y_p=(A1-1)/B1;
Z_line_pu=Z_line/Sys_Zbase;
Y_p_pu=Y_p/Sys_Ybase;
%%% 5-12 line%%%%%%%%%%
A_1=cosh(gamma*Length512);
B_1=Zc*sinh(gamma*Length512);
C_1=(1/Zc)*sinh(gamma*Length512);
D_1=A_1;
A1=A_1; B1=B_1/1; C1=1*C_1; D1=D_1;
Z_line512=B1;
Y_p512=(A1-1)/B1;
Z_line_pu512=Z_line512/Sys_Zbase;
Y_p_pu512=Y_p512/Sys_Ybase;
%%% 611 line%%%%%%%%%%
A_2=cosh(gamma*Length611);
B_2=Zc*sinh(gamma*Length611);
C_2=(1/Zc)*sinh(gamma*Length611);
D_2=A_2;
A2=A_2; B2=B_2/1; C2=1*C_2; D2=D_2;
Z_line611=B2;
Y_p611=(A2-1)/B2;
Z_line_pu611=Z_line611/Sys_Zbase;
Y_p_pu611=Y_p611/Sys_Ybase;
% Load parameter in  per unit
P_load1=199e6;
P_load2=399e6;
pf_load=0.8;
Q_load1= P_load1*(sqrt(1-pf_load*pf_load))/pf_load; %VAr
Q_load2= P_load2*(sqrt(1-pf_load*pf_load))/pf_load; %VAr
S_load_pu1=(P_load1 + j*Q_load1)/Sys_Sbase;
S_load_pu2=(P_load2 + j*Q_load2)/Sys_Sbase;
% Calculation starting
detaP_trans1=detaP0+detaPn*(P_load1^2+Q_load1^2)/S_trans^2;
detaP_trans2=detaP0+detaPn*(P_load2^2+Q_load2^2)/S_trans^2;
detaQ_trans1=detaQ0+Un*(P_load1^2+Q_load1^2)/(100*S_trans^2);
detaQ_trans2=detaQ0+Un*(P_load2^2+Q_load2^2)/(100*S_trans^2);
P34=(Prated-detaP_trans1*10^(6)-P_load1);
P43=(Prated-detaP_trans2*10^(6)-P_load2);
Q34=(Qrated-detaQ_trans1*10^(6)-Q_load1);
Q43=(Qrated-detaQ_trans2*10^(6)-Q_load2);
P13=(Prated-detaP_trans1*10^(6));
P24=(Prated-detaP_trans2*10^(6));
Q13=(Qrated-detaQ_trans1*10^(6));
Q24=(Qrated-detaQ_trans2*10^(6));
S13=(P13+j*Q13)/Sys_Sbase;
S24=(P24+j*Q24)/Sys_Sbase;
anpha=angle(A1); beta=angle(B1);
cos_34=abs(B1)*[(abs(D1)*Vsys^2*cos((beta-anpha))/abs(B1))-P34]/Vsys^2;
teta34=acos(cos_34)-beta; %radian
teta34_degree=(acos(cos_34)-beta)*180/pi; %degree
cos_43=abs(B1)*[(abs(A1)*Vsys^2*cos((beta-anpha))/abs(B1))+P43]/Vsys^2;
teta43=acos(cos_34)+beta; %radian
teta43_degree=(acos(cos_43)-beta)*180/pi; %degree
V3=cos(teta34)-j*sin(teta34);
V4=1;
Vt(1) = V3+X_trans1*conj((S13)/(V3));
Vt(2) = V4+X_trans2*conj((S24)/(V4));
St(1) = P + Q*j; % positive for generating
St(2) = P + Q*j;
```

```
% select voltage regulation type for each generator
% Exc_sw = 1 for ac voltage reg; Exc_sw = 0 for dc voltage reg
Exc_sw(1) = 1;
Exc_sw(2) = 1;
% Tinh gia tri ban dau
for nu = 1:n_unit
  It(nu) = conj(St(nu)/Vt(nu));
  Eq(nu) = Vt(nu) + (rs(nu) +j*xq(nu))*It(nu);
  delt(nu) = angle(Eq(nu));      % angle Eq leads Vt
% qd variables in generator rotor reference fram
  I(nu) = It(nu)*(cos(delt(nu)) - sin(delt(nu))*j);
  Iqo(nu) = real(I(nu));
  Ido(nu) = -imag(I(nu));        % when the d-axis lags the q-axis
  Efo(nu) = abs(Eq(nu)) + (xd(nu)-xq(nu))*Ido(nu);
  Vto(nu) = Vt(nu)*(cos(delt(nu)) - sin(delt(nu))*j);
  Vqo(nu) = real(Vto(nu));
  Vdo(nu) = -imag(Vto(nu));
  Sto(nu) = Vto(nu)*conj(I(nu));
  Eqpo(nu) = Vqo(nu) + xpd(nu)*Ido(nu) + rs(nu)*Iqo(nu);
  Edpo(nu) = Vdo(nu) - xpd(nu)*Iqo(nu) + rs(nu)*Ido(nu);
  Pemo(nu) = real(Sto(nu));
  Qemo(nu) = imag(Sto(nu));
  Tmech(nu) = Pemo(nu);
  delio(nu) = delt(nu);
  end % for nu loop
  for nu = 1:n_unit
slip(nu) = 0;
Eqp(nu) = Eqpo(nu);
Edp(nu) = Edpo(nu);
Ef(nu) = Efo(nu);
VR(nu) = KE(nu)*Efo(nu);
Vs(nu) = Efo(nu)*KF(nu)/TF(nu);
end;
% *********Setting up network representation************
y13=1/((rs(1)+j*xpd(1))*Sbratio(1)+X_trans1);
y24=1/((rs(2)+j*xpd(2))*Sbratio(1)+X_trans2);
y35=1/Z_line_pu;
ypu35=Y_p_pu;
y512=1/Z_line_pu512;
ypu512=Y_p_pu512;
y611=1/Z_line_pu611;
ypu611=Y_p_pu611;
y_load1=conj(S_load_pu1)/(abs(V3)^2);
y_load2=conj(S_load_pu2)/(abs(V4)^2);
y30=y_load1;
y40=y_load2; % conj(Pload + jQload)/|Vload|^2
Y(1,1)=y13;Y(1,2)=0;Y(1,3)=-y13;Y(1,4)=0;Y(1,5)=0;Y(1,6)=0;
Y(1,7)=0;Y(1,8)=0;Y(1,9)=0;Y(1,10)=0;Y(1,11)=0;Y(1,12)=0;
Y(2,1)=0;Y(2,2)=y24;Y(2,3)=0;Y(2,4)=-y24;Y(2,5)=0;Y(2,6)=0;
Y(2,7)=0;Y(2,8)=0;Y(2,9)=0;Y(2,10)=0;Y(2,11)=0;Y(2,12)=0;
Y(3,1)=-y13;Y(3,2)=0;Y(3,3)=y13+2*y35+2*ypu35+y30;Y(3,4)=0;Y(3,5)=-y35;
Y(3,6)=0;Y(3,7)=0;Y(3,8)=0;Y(3,9)=0;Y(3,10)=0;Y(3,11)=0;Y(3,12)=-y35;
Y(4,1)=0;Y(4,2)=-y24;Y(4,3)=0;Y(4,4)=y24+2*y35+2*ypu35+y40;Y(4,5)=0;
Y(4,6)=0;Y(4,7)=0;Y(4,8)=-y35;Y(4,9)=-y35;Y(4,10)=0;Y(4,11)=0;Y(4,12)=0;
Y(5,1)=0;Y(5,2)=0;Y(5,3)=-y35;Y(5,4)=0;Y(5,5)=2*y35+2*ypu35+y512+ypu512;
Y(5,6)=-y35;Y(5,7=0;Y(5,8)=0;Y(5,9)=0;Y(5,10)=0;Y(5,11)=0;Y(5,12)=-y512;
Y(6,1=0;Y(6,2)=0;Y(6,3=0;Y(6,4)=0;Y(6,5)=-y35;
Y(6,6)=2*y35+2*ypu35+y611+ypu611;Y(6,7)=-y35;Y(6,8)=0;
Y(6,9)=0;Y(6,10)=0;Y(6,11)=-y611;Y(6,12)=0;
Y(7,1)=0;Y(7,2)=0;Y(7,3)=0;Y(7,4)=0;Y(7,5)=0;
Y(7,6)=-y35;Y(7,7)=2*y35+2*ypu35+y611+ypu611;
Y(7,8)=-y35;Y(7,9)=0;Y(7,10)=-y611;Y(7,11)=0;Y(7,12)=0;
```

```
Y(8,1)=0;Y(8,2)=0;Y(8,3)=0;Y(8,4)=-y35;Y(8,5)=0;Y(8,6)=0;
Y(8,7)=-y35;Y(8,8)=2*y35+2*ypu35+y512+ypu512;
Y(8,9)=-y512;Y(8,10)=0;Y(8,11)=0;Y(8,12)=0;
Y(9,1)=0;Y(9,2)=0;Y(9,3)=0;Y(9,4)=-y35;Y(9,5)=0;Y(9,6)=0;
Y(9,7)=0;Y(9,8)=-y512;Y(9,9)=2*y35+2*ypu35+y512+ypu512;
Y(9,10)=-y35;Y(9,11)=0;Y(9,12)=0;
Y(10,1)=0;Y(10,2)=0;Y(10,3)=0;Y(10,4)=0;Y(10,5)=0;Y(10,6)=0;
Y(10,7)=-y611;Y(10,8)=0;Y(10,9)=-y35;Y(10,10)=2*y35+2*ypu35+y611+ypu611;
Y(10,11)=-y35;Y(10,12)=0;
Y(11,1)=0;Y(11,2)=0;Y(11,3)=0;Y(11,4)=0;Y(11,5)=0;
Y(11,6)=-y611;Y(11,7)=0;Y(11,8)=0;Y(11,9)=0;
Y(11,10)=-y35;Y(11,11)=2*y35+2*ypu35+y611+ypu611;Y(11,12)=-y35;
Y(12,1)=0;Y(12,2)=0;Y(12,3)=-y35;Y(12,4)=0;Y(12,5)=-y512;Y(12,6)=0;
Y(12,7)=0;Y(12,8)=0;Y(12,9)=0;Y(12,10)=0;
Y(12,11)=-y35;Y(12,12)=2*y35+2*ypu35+y512+ypu512;
% Kron's Reduction
rmv=12; % current maxtrix size
remove=rmv; % remove=which row/column to remove
for jj=1:(rmv)
    if jj~=remove;
        j=jj;
        if jj>=remove;
            j=jj-1;
        end
        for kk=1:(rmv);
            if kk~=remove;
                k=kk;
                if kk>=remove;
                    k=kk-1;
                end
                Ynew1(j,k)=Y(jj,kk)-
Y(jj,remove)*Y(remove,kk)/Y(remove,remove);
            end;
        end
    end
end
rmv1=11; % current maxtrix size
remove1=rmv1; % remove=which row/column to remove
for jj=1:(rmv1)
    if jj~=remove1;
        j=jj;
        if jj>=remove1;
            j=jj-1;
        end
        for kk=1:(rmv1);
            if kk~=remove1;
                k=kk;
                if kk>=remove1;
                    k=kk-1;
                end
                Ynew2(j,k)=Ynew1(jj,kk)-
Ynew1(jj,remove1)*Ynew1(remove1,kk)/Ynew1(remove1,remove1);
            end;
        end
    end
end
rmv2=10; % current maxtrix size
remove2=rmv2; % remove=which row/column to remove
for jj=1:(rmv2)
    if jj~=remove2;
        j=jj;
        if jj>=remove2;
```

```
            j=jj-1;
        end
        for kk=1:(rmv2);
            if kk~=remove2;
                k=kk;
                if kk>=remove2;
                    k=kk-1;
                end
                Ynew3(j,k)=Ynew2(jj,kk)-
Ynew2(jj,remove2)*Ynew2(remove2,kk)/Ynew2(remove2,remove2);
            end;
        end
    end
end
% Kron's reduction again
rmv3=9;
remove3=rmv3;
for jj=1:(rmv3)
    if jj~=remove3;
        j=jj;
        if jj>=remove3;
            j=jj-1;
        end
        for kk=1:(rmv3);
            if kk~=remove3;
                k=kk;
                if kk>=remove3;
                    k=kk-1;
                end
                Ynew4(j,k)=Ynew3(jj,kk)-
Ynew3(jj,remove3)*Ynew3(remove3,kk)/Ynew3(remove3,remove3);
            end;
        end
    end
end
% Kron's reduction again
rmv4=8;
remove4=rmv4;
for jj=1:(rmv4)
    if jj~=remove4;
        j=jj;
        if jj>=remove4;
            j=jj-1;
        end
        for kk=1:(rmv4);
            if kk~=remove4;
                k=kk;
                if kk>=remove4;
                    k=kk-1;
                end
                Ynew5(j,k)=Ynew4(jj,kk)-
Ynew4(jj,remove4)*Ynew4(remove4,kk)/Ynew4(remove4,remove4);
            end;
        end
    end
end
% Kron's reduction again
rmv5=7;
remove5=rmv5;
for jj=1:(rmv5)
    if jj~=remove5;
        j=jj;
```

```
        if jj>=remove5;
            j=jj-1;
        end
        for kk=1:(rmv5);
            if kk~=remove5;
                k=kk;
                if kk>=remove5;
                    k=kk-1;
                end
                Ynew6(j,k)=Ynew5(jj,kk)-
Ynew5(jj,remove5)*Ynew5(remove5,kk)/Ynew5(remove5,remove5);
            end;
        end
    end
end
rmv6=6;
remove6=rmv6;
for jj=1:(rmv6)
    if jj~=remove6;
        j=jj;
        if jj>=remove6;
            j=jj-1;
        end
        for kk=1:(rmv6);
            if kk~=remove6;
                k=kk;
                if kk>=remove6;
                    k=kk-1;
                end
                Ynew7(j,k)=Ynew6(jj,kk)-
Ynew6(jj,remove6)*Ynew6(remove6,kk)/Ynew6(remove6,remove6);
            end;
        end
    end
end
rmv7=5;
remove7=rmv7;
for jj=1:(rmv7)
    if jj~=remove7;
        j=jj;
        if jj>=remove7;
            j=jj-1;
        end
        for kk=1:(rmv7);
            if kk~=remove7;
                k=kk;
                if kk>=remove7;
                    k=kk-1;
                end
                Ynew8(j,k)=Ynew7(jj,kk)-
Ynew7(jj,remove7)*Ynew7(remove7,kk)/Ynew7(remove7,remove7);
            end;
        end
    end
end
Y4=Ynew8;
gbus=4; % row 4 and column 4 to be gyrated
ix = [1 2 3]; % index vector
Hmod(gbus,gbus)=1/Y4(gbus,gbus);
Hmod(ix,gbus)=Y4(ix,gbus)/Y4(gbus,gbus);
Hmod(gbus,ix)=-Y4(gbus,ix)/Y4(gbus,gbus);
Hmod(ix,ix) = Y4(ix,ix) - (Y4(ix,gbus)*Y4(gbus,ix))/Y4(gbus,gbus);
```

```
gbus1=3; % row 3 and column 3 to be gyrated
ix1 = [1 2 4]; % index vector
Hmod1(gbus1,gbus1)=1/Hmod(gbus1,gbus1);
Hmod1(ix1,gbus1)=Hmod(ix1,gbus1)/Hmod(gbus1,gbus1);
Hmod1(gbus1,ix1)=-Hmod(gbus1,ix1)/Hmod(gbus1,gbus1);
Hmod1(ix1,ix1) = Hmod(ix1,ix1) -
(Hmod(ix1,gbus1)*Hmod(gbus1,ix1))/Hmod(gbus1,gbus1);
g=Hmod1;
RZ = real(Hmod1);
IZ = imag(Hmod1);
for nu = 1:n_unit
slip(nu) = 0;
Eqp(nu) = Eqpo(nu);
Edp(nu) = Edpo(nu);
Ef(nu) = Efo(nu);
VR(nu) = KE(nu)*Efo(nu);
Vs(nu) = Efo(nu)*KF(nu)/TF(nu);
end;
iqe3=0;
ide3=0;
iqe4=0;
ide4=0;
% If all units are dc field regulated
u = [Efo(1);Tmech(1);Efo(2);Tmech(2);iqe3;ide3;iqe4;ide4];
if(Exc_sw(1)) % Exc_sw(1) =1 unit 1 ac voltage regulated
u(1) = abs(Vto(1));
elseif(Exc_sw(2))
u(3) = abs(Vto(2)); %unit 2 ac regulated
end
% order of variables in array x
x =[Eqp(1);Edp(1);delio(1);Eqp(2);Edp(2);delio(2);Ef(1);slip(1)
;Vs(1);VR(1);Ef(2);slip(2);Vs(2);VR(2)];
y =[abs(Vto(1));Pemo(1);Qemo(1);abs(Vto(2));Pemo(2);Qemo(2)];
% Update steady-state value for initializing simulation
% voltage regulated
if(Exc_sw(1)) % unit 1 ac voltage regulated
vref(1) = y(1);
else
vref(1) = u(1); % unit 1 dc regulated
end;
if(Exc_sw(2)) % unit 2 ac voltage regulated
vref(2) = y(4);
else % unit 2 dc field regulated
vref(2) = u(3);
end;
% Initialize signal generators and integrators
Tmech(1) = u(2);
Tmech(2) = u(4);
Eqpo(1) = x(1);
Edpo(1) = x(2);
Eqpo(2) = x(4);
Edpo(2) = x(5);
delio(1) = x(3);
delio(2) = x(6);
Ef(1) = x(7);
Vs(1) = x(9);
VR(1) = x(10);
Ef(2) = x(11);
Vs(2) = x(13);
VR(2) = x(14);
```

REFERENCES

LIST OF USED EXTERNAL ACTICLES

[1] Lee C. White, John A. Carver., Lawrence 1 Connor., Charles R. Ross., Carl E. Bagge, Prevention of power failures, Volume 1- Report of the commission submitted to the President by Federal Power Commission, July 1967, http://www.blackout.gmu.edu/archive/a_1965.html- accessed August 2009, Pages 1 -197.

[2] US Department of Energy federal energy regulatory commission, The Con Edison power failure of July 13 and 14, 1977, Final staff report, June 1978, http://www.blackout.gmu.edu/archive/a_1977.html-accessed August 2009, Pages 1 _ 50.

[3] Kurita A., Sakurai T., The power system failure on July 23, 1987 in Tokyo, 27th IEEE Conference Proceedings on Decision and Control, Volume 3, 7th- 9th December 1988, Pages 2093 - 2097.

[4] Taylor C.W., Erickson D.C., Recording and analyzing the July 2 cascading outage [Western USA power system], IEEE Computer Applications in Power, Volume 10, Issue 1, January 1997, Pages 26-30.

[5] U.S. - Canada Power system Outage Task Force, Final report on the August 14, 2003 Blackout in the United States and Canada: Causes and Recommendations, April 2004, https://reports.energy.gov/ - Accessed August 2009, Pages 1 - 228.

[6] Stephen T Lee, Nick Abi-Samra, Bill Roettger, Rich Lordan, Clark W. Gellings, Factors related to the series of outages on August 14, 2003 White paper, Product ID 1009317, Published by Electric Power Research Institute, 20th November 2003, www.epri.com, Pages I - 33.

[7] Pourbeik P., Kundur P.S., Taylor C.W., The anatomy of a power grid blackout - Root causes and dynamics of recent major blackouts, IEEE Power and Energy Magazine, Volume 4, Issue 5, September – October 2006, Pages 22 - 29.

[8] Andersson G., Donalek P., Farmer R., Hatziargyriou N., Kamwa I., Kundur P., Martins N., Paserba 1., Pourbeik P., Sanchez-Gasca 1., Schulz R., Stankovic A., Taylor C., Vittal V., Causes of the 2003 major grid blackouts in North America and Europe, and recommended means to improve system dynamic performance, IEEE Transactions on Power Systems, Volume 20, Issue 4, November 2005, Pages 1922 - 1928.

[9] Department of Primary Industries, 16th January 2007 electricity supply interruptions in Victoria - What happened, why, opportunities and recommendations, July 2007, The Nous group publication, www.nousgroup.com.au - Accessed in August 2009, Pages I - 24.

[10] A. Ulbig, T. S. Borsche, and G. Andersson, Analyzing Rotational Inertia, Grid Topology and their Role for Power System Stability, IFAC-PapersOnLine, vol. 48, no. 30. Pages 541–547, 2015.

[11] P. Kundur, J. Paserba, V. Ajjarapu, G. Andersson, A. Bose, C.Canizares, N.Hatziargyriou, D.Hill, A. Stankovic, C. Taylor, T. V. Cutsem, and V. Vittal, Definition and classification of power system stability ieee/cigre joint task force on stability terms and definitions, IEEE Transactions on Power Systems, vol. 19, Pages 1387–1401, Aug 2004.

[12] F. Casella, A. Bartolini, S. Pasquini, and L. Bonuglia, Object-Oriented Modelling and Simulation of Large-Scale Electrical Power Systems using Modelica: a First Feasibility Study, Pages 0–6, 2016.

[13] R. L. Cresap and J. F. Hauer, Emergence of a new swing mode in the western power system, IEEE Trans. Power App. Syst., vol. PAS-100, no. 4, Pages 2037–2045, Apr. 1981.

[14] I. Uhlir and M. Danecek, Dynamic Grid Stability: Technology and Solutions Leading to Smart Grid Technologies. Prague, Pages 348–351, 2016.

[15] M. Mythili, and K.I. Annapoorani, Modelling of Salient Pole Synchronous Machine, International Journal of Advanced Research in Electrical, Electronics and Instrumentation Engineering, no.3, Pages 197-200, 2014.

[16] Y. Xue, S. Xiao, Generalized congestion of power system: insights from the massive blackouts in India, Journal of Modern Power Systems and Clean Energy, September 2013, Volume 1, Issue 2, Pages 91-100.

[17] C.O. Onah, J. Reuben, Dynamic Modelling and Simulation of Salient Pole Synchronous Motor Using Embedded Matlab, American Journal of Engineering Research (AJER), e-ISSN: 2320-0847, p-ISSN: 2320-0936, Volume-5, Issue-12, Pages 318-325, 2016.

[18] K. A. Hord, Modeling and validation of a synchronous machine/ Controlled rectifier system, Mater thesis, Electrical and Computer Engineering, University of Kentucky, Lexington, Kentucky, 2014.

[19] S.G. Venna, S. Vattikonda, S. Mandarapu, Mathematical modeling and simulation of permanent magnet synchronous motor, International Journal of Advanced Research in Electrical, Electronics and Instrumentation Engineering, Vol. 2, Issue 8, Pages 125-130, August 2013.

[20] M. Sattouf, Data acquisition and control system of hydroelectric power plant using internet techniques, Doctoral thesis, Brno University of Technology, Brno, Czech Republic, 2015.

[21] M. Catrinoiu, Matlab/ Simulink model of a system for determine the angle of internal synchronous generators, U.P.B. Sci. Bull, Series C, Vol. 75, Iss. 3, Pages 241-247, 2013.

[22] S.S. Kulkarni, A.G. Thosar, Mathematical modeling and simulation of permanent magnet synchronous machine, International Journal of Electronics and Electrical Engineering, Vol. 1, No 2, Pages 324-330, June 2013.

[23] Y.N. Isaev, V.A. Kolchanova, S.S. Tarasenko, O.V. Tikhomorova, Mathematical models of synchronous generators for different spatial distances of disturbance point, 2015 IEEE International conference on Mechanical Engineering, Automation and Control System (MEACS), Pages 971-978, 2015, Tomsk, Russia.

[24] Y. Yu, S. Grijalva, J. J. Thomas, L. Xiong, P. Ju, Y. Min, Oscillation energy analysis of inter-area low frequency oscillations in power system, IEEE Transaction on power system, Vol. 31, No. 2, Pages 1195 – 1203, March 2016.

[25] G. Dume, Synchronous Generator Model based on LabVIEW Software, WSES Transaction on Advances in Engineering Education, E-ISSN: 2224-3410, Issue 2, Volume 10, Pages 295 – 301, July 2013.

[26] V. Fedak, T. Balogh, P. Zaskalicky, Dynamic simulation of electrical machines and drive systems using MATLAB GUI, Chapter 14 from the book MATLAB- A Fundamental Tool for Scientific Computing and Engineering Applications- Volume 1, 2012.

[27] N. Fischer, G. Benmouyal, S. Samineni, Tutorial on the impact of the synchronous Generator model on protection studies, SEL Journal of Reliable Power, Volume 3, No. 1, Pages 79 – 86, March 2012.

[28] I. A. Yousif, A. farqad, A. Najlaa, Modeling, Simulation and Analysis of Excitation System for Synchronous Generator, Asian Journal of Engineering and Technology, ISSN: 2321-2462, Volume 02, Issue 05, Pages 252-258, October 2014.

[29] P. Bhat, H.D. Gersem, Z.Bontinck, S. Schups, J. Como, Modelling of a Permanent Magnet Synchronous Machine Using Isogeometric Analysis, 18th International Symposium on Electromagnetic Fields in Mechatronics, Electrical and Electronic Engineering, 14-16 September 2017, Pages 25-29, Lodz, Poland.

[30] A. Zaretskiy, Mathematical Models and Stability Analysis of three-phase Synchronous Machines, Doctoral thesis, University of Jyvaskyla in building Agora, Beeta Hall, 18 December 2013.

[31] K. Alicemary, B. Arundhati, P. Maridi, Modelling, Simulation and Nonlinear Control of Permanent Magnet Linear Synchronous Motor, International Journal of Advanced Research in Electrical, Electronics and Instrumentation Engineering, ISSN: 2278 -8875, Vol. 1, Issue 6, Pages 148-154, December 2012.

[32] S. Jaganathan, S. Palaniswami, R. Adithya, Synchronous Generator Modeling and Analysis for Microgrid in Autonomous and Grid Connected Mode, International Journal of Computer Application, ISSN: 0975-8887, Volume 13, No. 5, Pages 442-450, January 2011.

[33] B. Luo, S. Chi, M. Fang, M. Li, Modeling and simulation of permanent magnet synchronous motor based on neutral network control strategy, AIP conference proceedings 1820, Pages 221-228, 2017.

[34] F. Selwa, L. Djamel, Transient stability analysis of synchronous generator in electrical network, International Journal of Scientific & Engineering Research, Volume 5, Issue 8, Pages 58-65, August 2014.

[35] D. P. Rallage, A. P. Agalgaonkar, K. M. Muttaqi, Simulink model for examining dynamic interactions involving electro-mechanical oscillations in distribution systems, Power Engineering Conference (AUPEC), Australasian Universities, Australia, Pages 1-6, 2015.

[36] V. Gaikwad, S. Tripathi, Y. Wanjari, A. Thakre, D. Dakare, J. Shendre, Laboratory setup for long transmission line, International Research Journal of Engineering and Technology (IRJET), Volume 4, Issue 3, Pages 11-17, March 2017.

[37] O. R. Leanos, J. L. naredo, J. A. C. Robles, An advanced transmission line and cable model in MAtlab for the simulation of power system transient, Chapter 12 from book MALAB- A fundamental tool for scientific computing and engineering applications, Volume 1, 2012.

[38] P.G, Understanding of multi-machine simulation using Simulink model, IJSRD-International Journal for Scientific Research & Development Vol. 2, Issue 01, 2014/ ISSN (online): 2321-0613, Pages 528-531.

[39] L. S. Hunjumuhamed, A power system dynamic simulation program using MATLAB/Simulink, International Journal of Advanced Research in Electrical, Electronics and Instrumentation Engineering, Vol. 2, Issue 1, Pages 2320-2328, December 2012.

[40] S. Ekinci, H.L. Zeynelgil, A. Demiroren, A didactic procedure for transient stability simulation of a multi-machine power system utilizing SIMULINK, International Journal of Electrical Education, Vo. 53(I), Pages 54-61, 2016.

[41] R. Patel, T.S.Bhatti, D.P. Kothari, MATLAB/Simulink-based transient stability analysis of a machine power system, International Journal of Electrical Engineering Education 39/4, Volume 39 Issue 4, Pages 297-309, October 2012

[42] M. De, G. Das, K.K. mandal, A new approach for investigation of multi machine stability in a power system, Indian L.Sci.Res.14 (2): Pages 245-249, 2017, ISSN: 2250-0128 (Online).

[43] A. Kazemlou, S. Mehraeen, Stability of multi generator power system with penetration of renewable energy sources, 2012 IEEE Power and Energy Society General Meeting, Pages 1-8, 22-26 July 2012, San Diego, CA, USA.

[44] Dynamic of transmission system. Siemens.com/power-technologies. Published by and copyright © 2012: Siemens AG -Infrastructure & Cities Sector, Smart Grid Division.

[45] Prabha Kundur, Power system stability and control, Electric power research institute. ISBN 0-07-035958-X. 17-39, 699-757, Pages 89-127, 2011.

[46] J. D. Glover, M. S. Sarma, T. J. Overbye, Power system analysis and design, Fifth edition SI, Pages 222-324, 2012 Cengage learning, USA.

[47] I. Boldea, Synchronous Generators, Second Edition, IEEE Life Fellow, University Politehnica Timisoara, Romania, Pages 157-411, @ 2016 by Taylor & Francis Group, LLC.

[48] T. Weckesser, H. Jóhannsson and J. Østergaard, Impact of Model Detail of Synchronous Machines on Real-time Transient Stability Assessment, 2013 IREP Symposium-Bulk Power System Dynamics and Control –IX (IREP), ISBN: 978-1-4799-0199-9, Pages 224-230, August 25-30, 2013, Rethymnon, Greece.

[49] T. V. Cutsem, Dynamic of the synchronous machine, ELEC0047 - Power system dynamics, control and stability, Pages 115-330, October 2017.

[50] Y. I. Al. Mashhadany, F. Amir, N. Anwer, Modeling, Simulation and Analysis of Excitation System for Synchronous Generator, Asian Journal of Engineering and Technology, ISSN: 2321 – 2462, Volume 02 – Issue 05, Pages 216-222, October 2014.

[51] Balance. J. W, Bhargava. B, Rodriguez. G. D, Monitoring Power System Dynamics using Phasor Measurement Technology for Power System Dynamic Security Assessment (by Southern California Edison Co. Rosemead, CA 91770, USA) IEEE 2003, Power Tech Conference, ISBN: 0-7803-7967-5, Pages 53-59, June 23th-26th, Bologna, Italy.

[52] B.M Weedy, B.J. Cory, N.Jenkins, J.B Ekanayake, G. Strbac, Electric Power System, Fifth edition, © 2012, John Wiley & Sons Ltd. ISBN: 978-0706-8268-5, Pages 299-303.

[53] A. Uehara, A. Pratap, T. Goya, T. Senjyu, A. Yona, N. Urasaki, and T. Funabashi, “A coordinated control method to smooth wind power fluctuations of a pmsg-based wecs,” Energy Conversion, IEEE Transactions on, vol. 26, no. 2, pp. 550–558, 2011

LIST OF ACTICLES RELATED TO DISSERTATION

PI. Le Thi Minh. T, Uhlíř.I, Inter-area Power Oscillation and Potential Application Phasor Measurement Units for the Power System, Seminar on New Methods and Procedures in the Fields Instrumentation, Automatic Control and Informatics, Instrumentation and Control Department, CTU in Prague, Pages 47-51, 25.05.2015 - 27.05.2015.

PII. Le Thi Minh.T, Uhlíř.I, Analyzing of phasor oscillations in 500kV power system and using synchrophasors for control stability, Student Conference in Mechanical Engineering Faculty, CTU in Prague, Pages 4-8, 19.04.2016.

PIII. Le Thi Minh. T, Uhlíř. I, Inter-area Power Oscillation and Potential Application Phasor Measurement Units for the Vietnam 500kV Power System, IFAC and CIGRE/CIRED Workshop on Control of Transmission and Distribution Smart Grids, Prague, Pages 342-347, 11.10.2016 - 13.10.2016.

PIV. Le Thi Minh. T, Uhlíř. I, Dynamic phasor and frequency estimation with harmonic and DC offset infiltration by using weight least squared method, IEEE International Conference on Smart Grid and Smart Cities (ICSGSC), Pages 172-177, July 2017, Singapore.

PV. Le Thi Minh. T, Uhlíř.I, The frequency stability assessment of the transmission system using phasor measurement unit data, 2018 IEEE PES conference on innovative smart grid technologies, Pages 45-50, 19-22 February 2018, Washington DC, USA.

PVI. Le Thi Minh. T, H. Nouri, " Modeling Dynamic Frequency Control with Power Reserve Limitations", 53rd International Universities Power Engineering Conference (UPEC 2018), 4th – 7th September 2018, 978-1-5386-2910-9/18/$31.00 ©2018 IEEE.

PVII. Le Thi Minh. T, H. Nouri, New studies on network frequency response considering the Influence of dynamic Load, IEEE Transactions on Power Systems (submitted 2018).